Imperial College London

Broad strategies into engineering superior targeted gene therapy vectors derived from bacteriophage viruses

Effrosyni Tsafa

A dissertation submitted for the degree of

Doctor of Philosophy

at the

Imperial College London

2016

Declaration

I declare that the work presented in this thesis was undertaken in the Department of Medicine, Imperial College London during the years 2011-2015.

This thesis describes the outcome of my own work. Experiments and analysis depicted in Figures 3.6-3.7 and 4.7 were performed with the assistance of my colleagues, Keiittisak Suwan and Justyna Przystal. Experiments depicted in Figures 4.8-4.9 were performed with the assistance of Dr Nabil Hajji.

Copyright declaration

Effrosyni Tsafa

Imperial College London

2016

Acknowledgements

This work was done in the Phage Therapy group, in the Department of Medicine, Imperial College London. My sincere gratitude is owed to a number of people who participated in this project.

Firstly, I would like to thank my supervisor, Dr Amin Hajitou, for his support and guidance throughout my PhD studies. I would also like to thank the past and current members of the Phage Therapy group, in particular, Keiittisak Suwan, Justyna Przystal, Paladd Asavarut and Sajee Waramit for their friendship and advice during my PhD studies. In addition, I would like to thank Dr Nabil Hajji for his guidance and advice during my studies.

I am grateful to Onassis Foundation for awarding me this PhD scholarship and for supporting me throughout my PhD studies.

I am also grateful to my family and friends who have supported me all the way and have made this possible.

Table of contents

Chapter 2: Materials and Methods

2.1 Materials

2.2 Methods

Abbreviations

AAV	Adeno-associated virus
AAVP	Adeno-associated virus/Phage
DMEM	Dulbecco's Modified Eagle's Medium
DNA	Deoxyribonucleic acid
GCV	Ganciclovir
HSVtk	Herpes Simplex Virus thymidine kinase
GFP	Green fluorescent protein
Luc	Firefly luciferase
bp	base pair
Kb	kilobase
kDa	kilo Daltons
PCR	Polymerase chain reaction
PEG	Polyethylene glycol
DAPI	4',6-diamidino-2-phenylindole
FACS	Fluorescence-activated cell sorting
ITR	Inverted terminal repeat
PFA	Paraformaldehyde

Abstract

Chemotherapy is the most commonly used treatment for cancer. While chemotherapeutic drugs such as doxorubicin provide cure in some cases, chemotherapy is toxic and has serious side-effects. Another disadvantage is that some types of cancer develop resistance to chemotherapy. Lowering the doses of these drugs will make them safer but would decrease their efficacy. A solution to this would be to combine low doses of these anticancer drugs with a safe anticancer approach.

Cancer gene therapy is an alternative and promising approach of cancer treatment. In our group we are using the adeno-associated virus/phage, named AAVP vector, which is a hybrid vector between AAV and phage genomes. AAVP vector was engineered to display the RGD4C peptide which binds to α_v integrin receptors overexpressed in tumors. AAVP vector has been proven to be safe and efficient vector for targeted gene delivery to tumors, upon intravenous administration. The aim of my project was to combine low-dose of doxorubicin with AAVP vector in order to investigate the drug effects on the AAVP-mediated tumor cell killing. We also tested the combination of AAVP with the natural dietary genistein, an isoflavone present in soy, regarded as a phytoestrogen and proven for its anti-cancer activity. Epidemiological studies have shown that a soy-rich diet has cancer-preventive effects.

We found that combination of low doses (non-toxic) of doxorubicin or genistein with RGD4C-AAVP-guided gene therapy resulted in greater tumor cell killing than treatment with doxorubicin, genistein or the targeted vector alone. In addition, we uncovered the mechanism that doxorubicin and genistein increased the transduction efficiency of AAVP vectors.

In conclusion, our results suggest that the combined treatment of doxorubicin or genistein with targeted RGD4C-AAVP gene therapy is a novel, promising, non-invasive and, importantly, safer treatment approach. Therefore, this combined treatment should be considered for future preclinical studies to assess its efficacy in vivo in tumor-bearing animals.

Chapter 1

Introduction

1.1 Gene Therapy

Gene delivery is a process by which foreign DNA is transferred to host cells for applications such as genetic research or gene therapy. Gene delivery methods can be mechanical (e.g. microinjection, electroporation or biolistics), chemical (e.g. lipid or nanoparticle carriers) or biological (e.g. viral vectors).

Gene therapy has already been used to treat genetic diseases such as haemophilia, cystic fibrosis and muscular dystrophy. Gene therapy treatment is also being developed to treat cardiovascular (Dzau et al., 2003), neurological disease (Burton et al., 2003) and cancer by delivering genes that express necessary proteins, to alter the expression of existing genes or to produce cytotoxic proteins or prodrug activating enzymes to kill tumor cells (Pack et al., 2005).

The first gene therapy clinical trial was carried out in 1989, in patients with advanced melanoma, using tumor-infiltrating lymphocytes modified by retroviral transduction (Rosenberg et al., 2000). In the early nineties, a clinical trial was performed in children with severe combined immunodeficiency

(SCID). In this trial the gene of deaminase adenosine was transferred to lymphocytes isolated from the patients using a retrovirus (Blaese et al., 1995). Despite the initial encouraging results, the efficiency of gene therapy in clinical trials has not been very high so far. Major limitation to the development of human gene therapy is the lack of safe, efficient and targeted methods for gene delivery. Early generation vectors based on gammaretroviruses offered limited ability to transfer genes to dividing cells such as haematopoietic stem cells. Their main disadvantage is that these vectors were inserted near oncogenes causing leukemia in a fraction of patients (Naldini, 2015). The development of safer and more efficient vectors, such as lentiviral and AAV vectors, enabled the safe delivery of therapeutic genes and had remarkable therapeutic benefits for various severe inherited diseases of the blood, immune and nervous system such as immunodeficiencies, haemophilia, leukodystrophies, retinal dystrophy and cancers (Naldini, 2015).

The ideal vector should be able to achieve high efficiency and targeted gene delivery without inflammatory or cytotoxic side-effects. Gene delivery can be achieved using viral or non-viral vectors. Viral vectors can mediate high efficiency gene transfer and long-term gene expression, as they can easily enter the target cell and deliver the transgene to the nucleus. However, the

risks of immunogenicity and insertional mutagenesis pose serious safety concerns for some viral vectors (Schambach et al., 2013). Trying to address these safety issues of viral vectors, non-viral vectors have been developed. The main disadvantage of non-viral vectors is their low efficiency compared to viral vectors (Yin et al., 2014).

1.2 Viral gene delivery vectors

Most of the vectors currently used for gene therapy are derived from human pathogens, from which essential viral genes have been removed to make them non-pathogenic. The general principle to generate safe and efficient viral vectors is to separate viral genes and cis-acting sequences into distinct plasmids in order to prevent the production of replication-competent viral particles by recombination (Kay et al., 2001). Some viral vectors, such as lentiviral vectors, are able to integrate into the host genome resulting in persistent gene expression. Other vectors, such as adenoviral vectors, remain episomal in infected cells leading to transient gene expression (Ponder, 2001).

The characteristics of the most commonly used viral vectors for gene transfer are summarised in **Table 1.1.**

Virus	Size and type of genome	Physical properties	Maximum size of insert	Infects non-dividing cells	Stability of expression	Disease in Animals
Retrovirus	7-10 kb single-stranded RNA	100 nm diameter; enveloped	≤ 8Kb	No	Stable (Integrated)	induction of tumors; acquired immunodeficiency syndrome (AIDS)
Lentivirus	7-10 kb single-stranded RNA	100 nm diameter; enveloped	≤ 8Kb	Yes	Stable (Integrated)	induction of tumors; acquired immunodeficiency syndrome (AIDS)
Adenovirus	36 kb double-stranded DNA	70-100 nm in diameter; non enveloped	8Kb	Yes	Expression lost in 3-4 weeks ; No integration	Cold; conjunctivitis; gastroenteritis
Adeno-associated virus (AAV)	4.7 kb single-stranded DNA	18-26 nm in diameter; non enveloped	< 4.5 kb	Yes	Stable; DNA remains episomal but can potentially integrate	No known disease

Table 1.1. Characteristics of the most commonly used viral vectors for gene transfer

1.2.1 Retroviruses

Retroviruses contain two copies of single-stranded RNA genome of 7 to 10 kb. They are ~100 nm in diameter and contain a membrane envelope. The envelope contains a virus-encoded glycoprotein which specifies the target cells that can be infected. The envelope glycoprotein can be substituted by one from a different virus, in a process referred to as pseudotyping. Following entry into target cells, the RNA genome is retro-transcribed into double-stranded DNA by the viral enzyme reverse-transcriptase contained into the virion. The double-stranded DNA is transferred to the nucleus, where it integrates into the host genome by the virus encoded enzyme integrase (Ponder, 2001). All retroviral vectors have two long terminal repeat sequences (LTR). Between the LTR sequences there are the *gag, pol* and *env* genes that encode the structural proteins, polymerase/integrase enzymes and envelope glycoprotein, respectively. Lentiviruses contain two more regulatory genes, *tat* and *rev*, and also a set of accessory genes (Kay et al., 2001). Retroviruses have been widely used so far in clinical trials (Rosenberg et al., 2000). The main advantage of retroviruses is their ability to integrate into the target cell genome to achieve stable gene expression of the transferred gene. However, the random way their viral genome is inserted into the host cell chromosomes can cause insertional mutagenesis and induction of tumors. Another disadvantage of

retroviral vectors (exempt lentiviral vectors) is that they can infect only dividing cells as disruption of the nuclear membrane is required for the pre-integration complex to gain access to the chromatin (Kay et al., 2001).

1.2.2 Lentiviral vectors

The lentiviruses belong to the retroviruses family but they have specific biological characteristics. One of them is their ability to transduce both dividing and non-dividing cells. The *vpr* gene product and one of the matrix proteins of the lentivirus (MA) contain nuclear localisation signals that facilitate the viral DNA to the nucleus without the need of breakdown of the nuclear membrane (Ponder, 2001). Lentiviral vectors based on HIV-1 have already been used for gene delivery to non-dividing cells such as neurons and haematopoietic stem cells (An et al., 2000). VSV-G (Vesicular Stomatitis Virus- Glycoprotein) pseudotyped lentiviral vectors have already been used for *in vivo* gene delivery to the central nervous system in rodents and non-human primates (Kordower et al., 1999, Naldini et al., 1996).

1.2.3 Adenoviral vectors

Adenoviruses are 70-100 nm in diameter and do not contain a membrane. The adenoviral genome consists of 36 kb double-stranded linear DNA that replicates extrachromosomally (as episome) in the host cell nucleus. The advantage of adenoviral vectors is that they can be produced in high titers and they are able to transduce a high percentage of target cells. The major disadvantage of adenoviral vectors is their immunogenicity. This immune response can eliminate the transduced cells and can also result in severe inflammation at the site of delivery. Moreover, the pre-existing immunity against adenoviral vectors reduces the efficacy of repeat administrations. Another disadvantage of adenoviral vectors is that they are not integrating into the host cell genome which results in transient transgene expression (Ponder, 2001). Adenoviral vectors have already been used for gene delivery in preclinical animal studies to transduce the lung, liver, muscles, brain and tumors. They have been also used in clinical trials for cystic fibrosis without evidence of clinical efficiency (Kay et al., 2001). They have also been used in clinical trials for cancer treatment (Aghi et al., 2000, Heise and Kirn, 2000).

1.2.4 Adeno-associated virus vectors (AAV)

Adeno-associated virus is small (~22nm), icosahedral and non-enveloped parvoviruses whose genome is about 4.7 kb single-stranded DNA. AAV has not been associated to any human disease. AAV enters the cells by receptor-mediated endocytosis and then is transported to the nucleus. In the nucleus, the single-stranded (ss) DNA needs to be converted to double-stranded (ds)DNA from which structural and regulatory viral proteins are produced, as well as the ssDNA for packaging into the new viral particles (Coura Rdos and Nardi, 2007). AAV requires co-infection with another virus, usually adenovirus or herpes virus, for productive infection. In the absence of co-infection, AAV genome can integrate into the host cell genome remaining in a latent state. Wild-type AAV is able to integrate into the cell genome as double-stranded DNA at a specific region of chromosome 19. AAV can also remain in an extrachromosomal form (episome). The AAV DNA ends are constituted of 145 bp inverted terminal repeats (ITR). Between the ITRs there are two viral genes, *rep* and *cap*, encoding proteins for viral replication and capsid formation, respectively. The ITRs act as origin of replication, packaging and integration signal and also as a regulator element for wild-type AAV. There are many serotypes of AAV but the majority of recombinant AAV (rAAV) vectors were based on AAV serotype 2 (AAV2). However, new recombinant vectors based on

AAV serotypes 1, 5, 8 and 9 have also been developed in order to avoid immune responses in some patients (Hastie and Samulski, 2015). AAV9 serotype has been found to achieve higher transduction efficiency in vivo compared to AAV2 (Pillay et al., 2016, Zincarelli et al., 2008).

Recombinant AAV (rAAV) vectors are derived from the wild type vectors after replacing *rep* and *cap* genes by the transgene cassette of interest (Figure 1.2 B). The *rep*, *cap* genes and adenovirus helper functions are provided in other plasmids. Although wild-type AAV is able to integrate into the host cell genome in a specific site, recombinant AAV vectors are usually not able to integrate because this site-specific integration requires the Rep protein (Kotin et al., 1990, Linden et al., 1996). Therefore, most rAAV remain as episomes in the target cell although they can potentially integrate in a non-specific position (Valdmanis et al., 2012). rAAV vectors, even if they usually remain in an episomal form, they are able to achieve long-term transgene expression comparing to other vectors (Coura Rdos and Nardi, 2007). AAV vectors have already been used in preclinical studies for the treatment of genetic and acquired diseases. They have also been used in clinical trials for the treatment of cystic fibrosis, haemophilia and muscular dystrophy (Kay et al., 2001), and recently in ocular gene therapy of the retina (Feuer et al., 2015, Ku and Pennesi, 2015). A clinical trial that used AAV8 for the treatment of haemophilia

B achieved vector-dose dependent coagulation factor IX (FIX) expression at a level of 6% of the normal level after a single, intravenous dose of the vector. FIX expression was stable in most patients three years later. This low level of FIX expression turned severe haemophilia to a milder form and significantly improved patients' quality of life (Hastie and Samulski, 2015, Naldini, 2015). Another clinical trial with remarkable benefits for the patients is AAV2-mediated gene therapy in patients with type 2 Leber congenital amaurosis, an inherited retinal dystrophy causing vision loss at a young age. Three independent trials using AAV2-mediated gene therapy showed improved vision in several young patients. However, in two of the trials patients lost the benefit of the treatment 2-3 years later (Naldini, 2015).

For the production of rAAV vectors, HEK 293 cells whose genome contains the adenovirus *E1* gene are co-transfected with three plasmids: 1) vector plasmid that contains the transgene cassette, 2) a package plasmid with *rep* and *cap* genes and 3) a helper plasmid containing the adenovirus genes *E2a, E4* and *VA*. (Coura Rdos and Nardi, 2007).

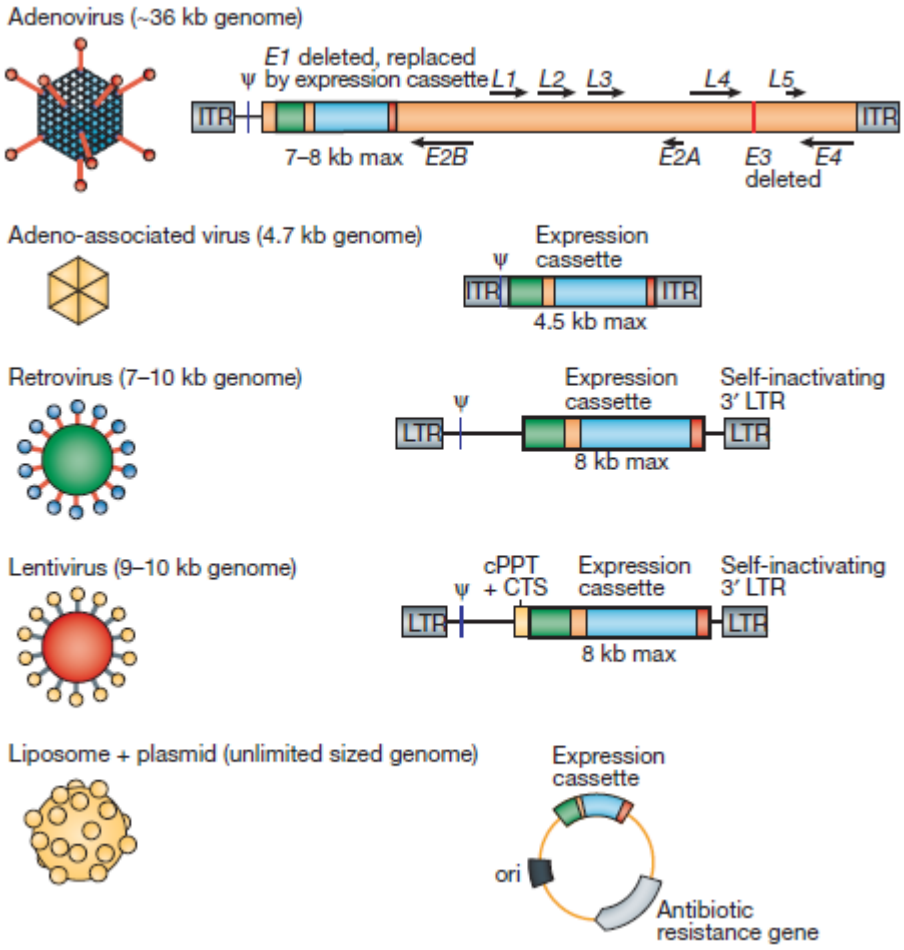

Figure 1.1 Diagram of the most commonly used viral vectors for gene delivery [from (Sheridan, 2011)]

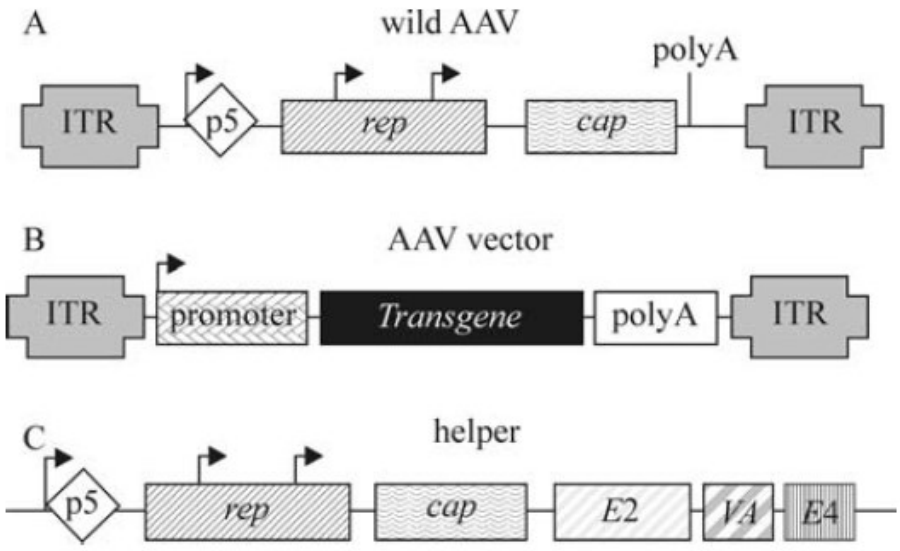

Figure 1.2 AAV genetic structure (A) wild-type AAV, (B) AAV vector containing only the ITRs from wild-type AAV and the transgene cassette, (C) helper cassette, containing the AAV rep and cap genes required for the virus packaging and the Ad virus genes E2, VA and E4, required for virus replication [from (Coura Rdos and Nardi, 2007)].

1.3 Strategies for cancer gene therapy

Strategies for cancer gene therapy can be divided in immunologic approaches and molecular approaches (**Figure 1.3**)

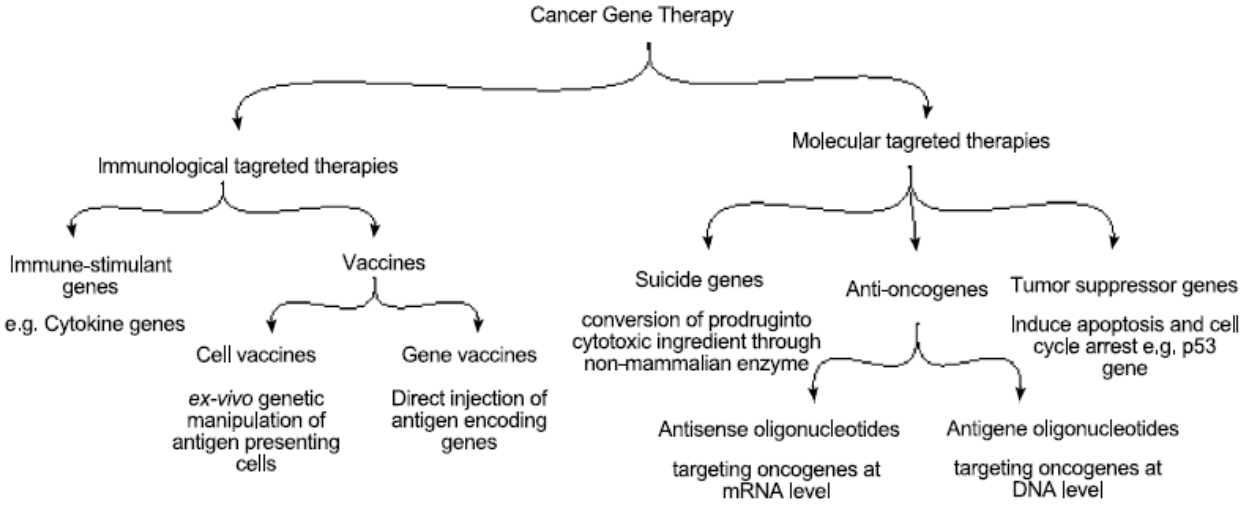

Figure 1.3 Strategies for cancer gene therapy [from(El-Aneed, 2004)]

1.3.1 Immunologic approaches

Genetic immunotherapy can be utilized to boost T-cell mediated immune response against cancer. One of the genetic immunotherapy strategies is the transfer of genes that stimulate the immune system, such as cytokines. Complete tumor regression was observed in rat models of hepatocellular carcinoma and adenocarcinoma after Interleukin-12 gene transfection into the cancer cells (Barajas et al., 2001, Shi et al., 2002). Another genetic immunotherapy approach includes the *in vitro* genetic engineering of antigen presenting cells to enable them to display tumor antigens. Dendritic cells engineered to express α-fetoprotein (AFP), a hepatocellular carcinoma antigen,

were able to trigger strong immune response against cancer cells (Vollmer et al., 1999).

1.3.2 Molecular approaches

Molecular approaches in cancer gene therapy mainly include the upregulation of tumor suppressor genes or the downregulation of oncogenes.

Tumor suppressor proteins can suppress unusual cell proliferation and induce apoptosis and/or cell cycle arrest in malignant cells. One of the most representative tumor suppressor proteins is p53. p53 protein interferes with the biochemical pathways that regulate cell growth, differentiation and apoptosis. This protein is frequently mutated in human cancers. Successful transfection of wild-type p53 into cancer cells induces apoptosis and cell cycle arrest in cultured cells (Roy et al., 2002). In addition, tumor growth inhibition and tumor regression were observed in animal models after p53 transfection (Dolivet et al., 2002).

Oncogenes encode for growth promoting proteins and are potential targets for cancer gene therapy. One of the most investigated oncogenes is *bcl-2* gene which acts as inhibitor of apoptosis. Other important oncogene families are *c-myc* and *ras*. The biological activity of oncogenes can be suppressed either on the RNA or the DNA levels. Antisense oligonucleotides bind to mRNA through

Watson-Crick base pairing inhibiting the translation step of protein synthesis. Antigen oligonucleotides bind to the DNA through Hoogsteen hydrogen bonding forming a non-functional triple helical structure (Helene et al., 1992). In this strategy, gene expression is blocked at the transcription stage (El-Aneed, 2004).

Suicide genes are also considered another molecular approach in cancer gene therapy. This strategy relies on the conversion of a non-toxic prodrug into active drug by means of non-mammalian enzymes (El-Aneed, 2004).

One of the most widely used suicide gene/prodrug systems is the herpes simplex virus thymidine kinase (HSVtk)/ganciclovir (GCV) system. HSVtk enzyme catalyzes the phosphorylation of nucleoside analogs such as GCV. The phosphorylated GCV mediates the killing of cancer cells. One of the most advantageous features of this system is the bystander effect. It is the mechanism by which the toxic metabolites are transferred from transduced cells to neighbouring cancer cells via gap junctions and/or apoptotic vesicles (El-Aneed, 2004, Trepel et al., 2009).

1.4 Bacteriophage vectors

Bacteriophages (phage) are viruses that infect bacteria. These particles consist of a protein coat containing DNA or RNA genome. The most commonly used vectors for gene delivery are the filamentous M13 and the lambda. Filamentous phage particles consist of a long cylindrical protein capsid, around 900 nm in length and 6.5 nm in diameter, enclosing a single-stranded DNA genome of about 6.4 kb (Barbas C.F., 2001). On the one end of the particle there are 3 to 5 copies of the proteins pIII and pVI and on the other end there are 3 to 5 copies of the proteins pVII and pIX. The body of the phage is composed of thousands of copies of major pVIII coat proteins (Figure 1.3).

Proteins or peptides of interest can be displayed on the surface of the phage particles by fusing the sequence encoding the foreign peptide to the sequence of a phage coat protein. Peptides are usually fused to pIII or pVIII phage coat proteins.

Bacteriophage vectors have some potential advantages over animal viral vectors. Bacteriophage has no native tropism for mammalian cells as it has evolved to infect bacteria only. In addition, bacteriophage can be modified to display tissue-specific ligands on the coat proteins without disruption of their virus structure (Hajitou et al., 2006, Larocca et al., 1998). One other important

advantage over animal viruses is that bacteriophage is safe. It has also been approved by the US Food and Drug Administration for use as safe antibacterial food additive (Lang, 2006). Other advantages of phage vectors are their large cloning capacity as well as the simple and economical large-scale production and purification (Greenstein and Besmond, 2001).

Figure 1.4 Filamentous M13 phage structure and localisation of phage coat proteins [from (Arap, 2005)]

1.5 Non-viral gene delivery vectors

Synthetic non-viral vectors have been used as an alternative method to deliver transgenes into cells to overcome the safety issues arising from the use of viral vectors. The use of non-viral method to deliver nucleic acids into cells is called transfection. The most commonly used non-viral gene delivery vectors are cationic polymers, lipid-based reagents, as well as calcium phosphate. These synthetic vectors are materials that can bind to nucleic acids, condense the genetic material into particles and facilitate cellular entry. Synthetic vectors are able to neutralize the negatively charged nucleic acids or even create positively charged complexes, thus facilitating the binding of complexes to the negatively charged membranes. The main disadvantage of synthetic vectors is their low efficiency comparing to viral gene delivery methods.

1.5.1 Lipid-based reagents

Cationic lipids are the most widely used synthetic vectors because of their relatively high efficiency. Cationic lipids interact with nucleic acids forming liposome/nucleic acid complexes (referred to as lipoplexes). Lipid-based gene delivery has been widely used in both *in vitro* and *in vivo* studies. However, it has crucial limitations, such as difficulty in reproducibly fabricating liposomes

and DNA/liposome complexes, toxicity to some cell types and colloidal stability (Pack et al., 2005).To date, a number of cationic liposomes are commercially available, such as Fugene and Lipofectamine (Faneca et al., 2002).

1.5.2 Cationic polymers

Another category of non-viral gene delivery vectors is cationic polymers. Cationic polymers are binding electrostatically to nucleic acids forming a positively charged complex (referred to as polyplex) (Pack et al., 2005). The positive charge of the polyplex facilitates the adherence of the complex to the negatively charged cell membrane. Cationic polymers that have been used to deliver nucleic acids *in vitro* are diethylaminoethyl-dextran (DEAE.DEX), polylysine and polyethylenimines (PEIs). However, *in vivo* application of cationic polymers has failed so far due to the high degree of cytotoxicity, rapid clearance and interaction between the positively charged complexes and blood components (Dash et al., 1999).

1.5.3 Calcium phosphate precipitation

The Calcium phosphate transfection method for gene delivery is based on forming a calcium-phosphate DNA precipitate that facilitates the binding of the

DNA to the cell surface. The calcium phosphate-DNA precipitates are entering the cell by endocytosis. This method has been widely used to transfect DNA into cells because it is simple and inexpensive (Graham and van der Eb, 1973). However, calcium phosphate transfection is not suitable for *in vivo* gene delivery.

1.6 Hybrid AAVP vector

Despite their advantages over eukaryotic viruses, phage-derived vectors achieve low transduction efficiency compared to eukaryotic viral vectors. The reason is that bacteriophage has evolved to infect bacteria only so it has no intrinsic strategies for gene delivery to mammalian cells (Przystal et al., 2013, Stoneham et al., 2012). Bacteriophage contains single-stranded DNA (ssDNA) which has to be converted to double-stranded DNA (dsDNA) for transgene expression. Another limiting step is related to the post-targeting fate of the ssDNA of the phage genome (Hajitou et al., 2006). To address these limitations the mammalian transgene cassette flanked by full length ITRs from the recombinant adeno-associated virus (rAAV) -which is mammalian ssDNA virus- was genetically incorporated into the phage genome (Hajitou et al., 2007). The hybrid vector between AAV and phage is called adeno-associated virus phage

or AAV/phage, AAVP (Figure 1.5). This vector was engineered to display the RGD4C peptide, derived from *in vivo* phage display screening, which binds to α_v integrins overexpressed in tumors, but absent or barely detectable in the healthy tissues (Hajitou et al., 2007). The targeted RGD4C AAVP vector was reported to achieve improved mammalian transduction efficiency over the conventional phage-based vectors (Hajitou et al., 2007, Hajitou et al., 2006).

The specificity and efficacy of RGD4C AAVP vector was evaluated in preclinical models *in vivo* (Hajitou et al., 2006). Targeted vectors carrying reporter genes, green fluorescent protein gene (*GFP*) or firefly luciferase gene (*Luc*) were systemically administered in immunocompromised tumor-bearing mice. Immunofluorescence showed GFP expression largely in tumor cells and tumor blood vessels in mice that received RGD4C AAVP-GFP while no GFP staining was observed in tumors from control mice that received non-targeted AAVP-GFP. Bioluminescence (BLI) imaging of *Luc* expression confirmed tumor-specific expression of Luc in mice receiving RGD4C AAVP-Luc while tumor-associated bioluminescence was not observed in control mice receiving the non-targeted AAVP-Luc. The therapeutic efficacy of RGD4C AAVP was evaluated in immunocompetent and immunocompromised tumor-bearing mice models after systemic administration of RGD4C AAVP vector carrying the *HSVtk* (*Herpes Simplex Virus thymidine kinase*) gene. HSVtk gene can serve both as a ‘’

suicide'' gene (when combined with ganciclovir [GCV]) and a reporter gene for clinically applicable PET imaging with HSVtk-specific radiolabeled nucleoside analogs (Hajitou et al., 2006). Tumor growth was significantly suppressed in immunodeficient mice bearing human Kaposi's sarcoma (KS1767) as well as in immunocompetent mice bearing subcutaneous EF43-FGF4 tumors after a single systemic administration of RGD4C AAVP-HSVtk followed by GCV treatment (Hajitou et al., 2006).

RGD4C AAVP vector was also used to selectively deliver therapeutic genes to pet dogs after intravenous administration (Hajitou et al., 2007, Paoloni et al., 2009). In this study, systemic administration of the vector carrying the gene encoding the tumor necrosis factor- α (TNF-α) resulted in significant reduction of the tumor volumes without any evidence of cytotoxicity.

In 2012 our group developed a novel AAVP vector by substituting the viral CMV (cytomegalovirus) promoter with the Grp78 tumor-specific mammalian promoter in the AAV transgene cassette (Kia et al., 2012). Grp78 gene encodes a 78 kDa endogenous macromolecule which is overexpressed in many different tumor cell types. This tumor double-targeted AAVP vector displaying the RGD4C peptide and carrying the Grp78 promoter should be able to target both tumor cells and tumor vasculature. The other advantage of this novel AAVP vector is the long-term transgene expression under the Grp78 promoter

compared to the viral CMV promoter which gets inactive over time. *In vitro* studies showed significantly higher GFP expression over time in 9L cells transduced with RGD4C AAVP carrying the Grp78 promoter compared to cells transduced with RGD4C AAVP carrying the CMV promoter. Moreover, significantly increased tumor cell killing over time was observed by *HSVtk*/GCV therapy under Grp78 promoter compared to CMV, both *in vitro* and *in vivo* (Pranjol and Hajitou, 2015).

Although targeted AAVP vectors are very promising, they have to be improved in order to be used for clinical gene therapy. One significant barrier to the efficacy of targeted AAVP vectors is proteasomal degradation. Proteasome has been shown to be a barrier to gene delivery even for animal viruses such as lentiviral vectors and adeno-associated virus (AAV) (Jennings et al., 2005, Santoni de Sio et al., 2008). Phage is more susceptible to proteasomal degradation compared to animal viruses, as it has been evolved to infect bacteria and has not developed strategies to escape from proteasomal degradation.

Other barriers that AAVP vectors have to overcome can be extracellular or intracellular barriers. Extracellular barriers, such as the extracellular matrix or the cell surface negative charge causing repulsion of the negatively charged phage capsid, can obstruct the vectors to enter the target cells (Yata et al.,

2014, Yata et al., 2015). Intracellular barriers faced by AAVP include the mechanism of entry to the target cell, endosomal escape and nuclear transport of AAVP genome.

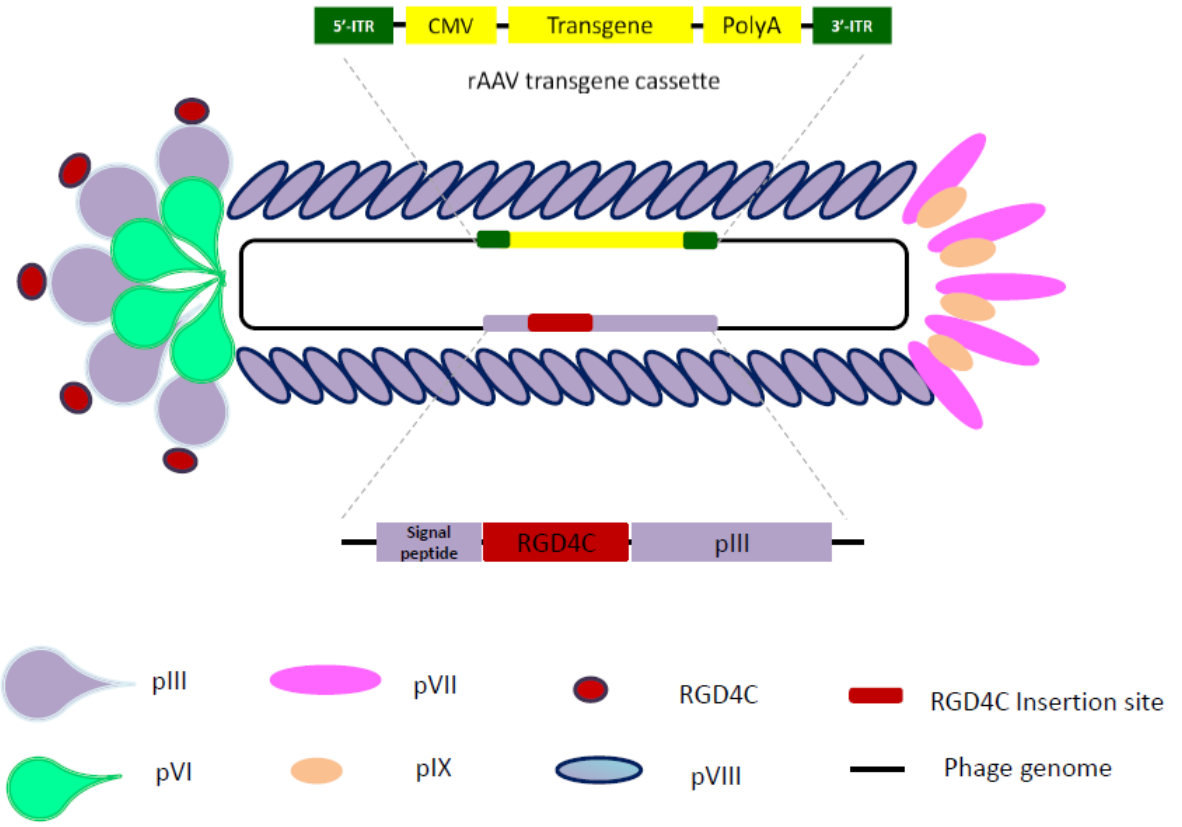

Figure 1.5 Structure of the hybrid vector AAV/Phage (AAVP) designed by Hajitou et al. (Hajitou et al., 2007, Hajitou et al., 2006)**.** The particle contains a chimeric genome of a cytomegalovirus CMV-transgene cassette flanked by inverted terminal repeats (ITR) from AAV2 and the genome of M13 filamentous bacteriophage. RGD4C, the α_v-integrin binding ligand, is displayed on the pIII coat protein of AAVP in order to achieve ligand-directed targeting of tumor cells and tumor vasculature.

1.7 Genistein

Genistein is an isoflavone present in soy (Conklin et al., 2007) and is regarded as a phytoestrogen because it is structurally similar to hormones and can bind to hormone receptors (Kuiper et al., 1998). Genistein has been shown to inhibit the growth and development of several malignancies (Li et al., 2015, Spagnuolo et al., 2015, Xiao et al., 2015). Epidemiological studies have shown that a soy-rich diet is associated with low risk of breast and prostate cancer (Banerjee et al., 2008). Several experimental and clinical investigations suggest a therapeutic role of genistein on different types of cancer. Moreover, genistein has shown synergistic behaviour when combined with well-known anti-cancer drugs such as adriamycin, docetaxel, and tamoxifen (Spagnuolo et al., 2015). Genistein has already been used in clinical trials to investigate combined therapy of genistein and gemcitabine for the treatment of breast cancer patients and also to evaluate the use of genistein together with gemcitabine and erlotinib for the treatment of pancreatic cancer patients (Shen et al., 2012, Yang et al., 2009).

Moreover, genistein has already been shown to increase AAV2-mediated transduction efficiency (Mah et al., 1998, Qing et al., 1997). Importantly, genistein has been reported for its ability to interfere with and inhibit cellular

pathways, a characteristic that can be used to enhance the gene transfer efficacy of RGD4C-AAVP. For instance, the ability of genistein to inhibit the chymotrypsin-like activity of proteasome (Kazi et al., 2003), can be used to prevent phage degradation by the proteasome. Moreover, the ability of genistein to induce G2/M cell cycle arrest could result in increased nuclear transport of gene therapy vectors (Cui et al., 2014, Han et al., 2013, Ouyang et al., 2009). Consequently, taking into account the safety of genistein, its anticancer activity and interference with cellular pathways, we hypothesized that combination of genistein with our tumor-targeted RGD4C-AAVP biotherapeutic particle would lead to enhanced tumor cell killing along with reduced toxicity.

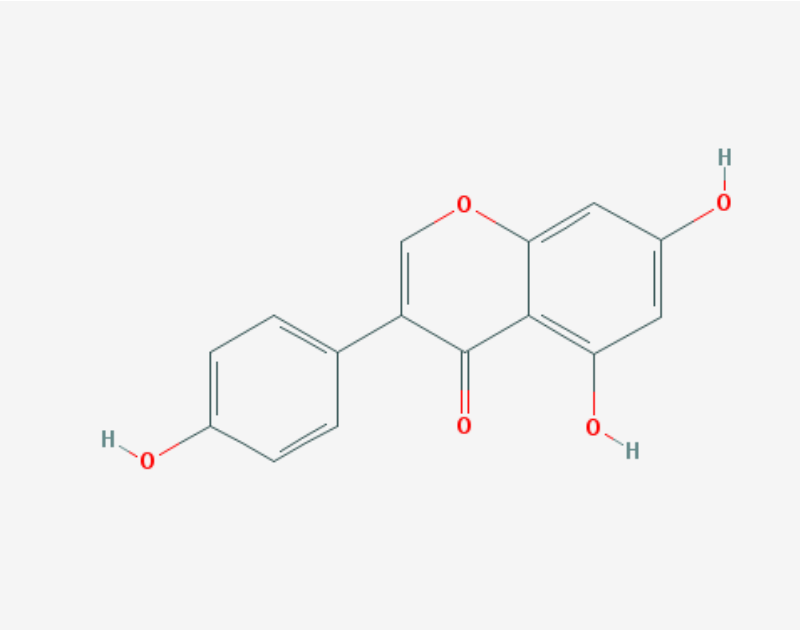

Figure 1.6 Genistein molecular structure (from PubChem)

1.8 Doxorubicin

Doxorubicin is a chemotherapeutic drug that interacts with DNA by intercalation. This inhibits the progression of the enzyme topoisomerase II, which relaxes supercoils in DNA for transcription. Doxorubicin has been used for cancer treatment for over 30 years. While it provides cure in some cases, doxorubicin is very toxic on non-cancerous cells and can cause serious side-effects. This toxicity poses serious risks and forces the treatment to become

dose-limiting (Tacar et al., 2013). Another disadvantage is that some types of cancer develop resistance to chemotherapy.

AAV second-strand synthesis has been shown to be one of the rate-limiting steps that significantly impacts upon transduction efficiency by AAV (Ferrari et al., 1996, Qing et al., 1997). It has also been shown that genotoxic stress can increase AAV-mediated transduction efficiency (Ferrari et al., 1996). Doxorubicin has already been published to improve AAV transduction in airway cell lines (Yan et al., 2004). It has also been shown that doxorubicin can enhance rAAV-2 transduction in rat neuronal cell lines by facilitating nuclear translocation of rAAV-2 (Zhang et al., 2009). Doxorubicin has already been reported to delay proper chromosome condensation and nuclear envelope formation during mitosis (Fasulo et al., 2012). In addition, it has been shown that DNA damage caused by doxorubicin can activate DNA repair enzymes, such as PARP-1(poly(ADP-ribose) polymerase-1) or Bcl-2/Bax apoptosis pathway (Tacar et al., 2013) .

So, we hypothesized that combining low-dose doxorubicin with our targeted RGD4C AAVP vector can increase the AAVP-mediated transduction efficiency resulting in increased AAVP-mediated cancer cell killing. We also hypothesized that one possible mechanism could be that treatment with low-dose doxorubicin can cause moderate DNA damage and trigger DNA repair

mechanisms. DNA repair enzymes can facilitate the conversion from single-stranded DNA to double-stranded DNA which is one of the rate-limiting steps for AAVP mediated transduction. Another possible mechanism could be that doxorubicin facilitates the nuclear translocation of vector's genome by delaying the chromosome condensation and proper envelope formation during mitosis.

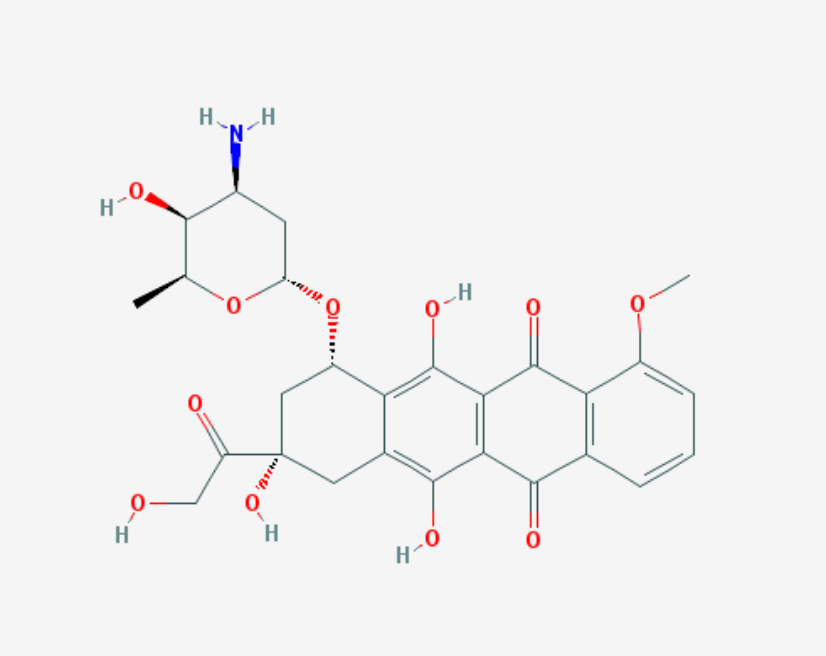

Figure 1.7 Doxorubicin molecular structure (from PubChem)

1.9 Hypotheses of thesis

Hypothesis 1: Combination of genistein with our targeted AAVP vector could increase the AAVP-mediated transduction efficiency resulting in higher AAVP-guided cancer cell killing by delivering therapeutic genes.

Hypothesis 2: Treatment with genistein can inhibit proteasome-mediated degradation of AAVP particles resulting in increased gene expression from AAVP.

Hypothesis 3: Combination of low-dose doxorubicin with our targeted AAVP vector could increase the AAVP-mediated transduction efficiency resulting in higher AAVP-mediated cancer cell killing.

Hypothesis 4: Treatment with low-dose doxorubicin can cause moderate DNA damage and trigger DNA repair mechanisms. DNA repair enzymes can facilitate the conversion from single-stranded DNA to double-stranded DNA necessary for gene expression to occur from AAVP.

Hypothesis 5: Doxorubicin facilitates the nuclear translocation of vector's genome by delaying the chromosome condensation and proper envelope formation during mitosis. Therefore, combination of doxorubicin with our targeted AAVP vector could result in increased nuclear accumulation of vector and subsequently in enhanced AAVP-mediated gene expression efficiency.

1.10 Aims of thesis

Aim 1: The aim of this study was to investigate if genistein can increase the transduction efficiency of AAVP vectors in cancer cell lines and tumor spheroids. This aim also investigated possible mechanisms of genistein effect on AAVP efficacy.

Aim 2: The aim of this study was to investigate if doxorubicin can increase the transduction efficiency of AAVP vectors in cancer cell lines and tumor spheroids. This aim also investigated possible mechanisms of doxorubicin effect on AAVP efficacy.

Chapter 2

Materials and Methods

2.1 Materials

2.1.1. Chemical reagents

Name	Source
Genistein	Sigma
Doxorubicin	Sigma
Dulbecco's Modified Eagle's Medium (DMEM)	Sigma
Phosphate buffer saline (PBS)	Sigma
Fetal bovine serum (FBS)	Sigma
Penicillin/Streptomycin	Sigma
L-glutamine	Sigma
Kanamycin	Sigma
Tetracycline	Sigma
Polyethyleneglycol (PEG)	Sigma
Sodium Chloride (NaCl)	Sigma
Glo Lysis Buffer	Promega
MTT Reagent	Sigma
Ganciclovir	Sigma
Phenol:Chloroform:Isoamyl alcohol 25:24:1, Saturated with 10mM Tris pH 8.0, 1mM EDTA	Sigma

Chloroform: Isoamyl alcohol 24:1	Biochemica
Glycogen	Acros Organics
Bradford Reagent	Sigma
Trypan Blue	Sigma
Dimethyl Sulfoxide (DMSO)	Sigma
Paraformaldehyde (PFA)	Sigma
Bovine Serum Albumin (BSA)	Sigma
Saponin	Sigma
Ammonium Chloride	Sigma
Triton X-100	Sigma
DAPI	Sigma
Prolong Gold antifade reagent	Invitrogen
Q5 Polymerase	New England Biolabs
RIPA buffer	Sigma
Protease inhibitors tablets	Roche
Laemmli buffer (2x)	Biorad
Bradford reagent	Sigma
40% Acrylamide	Biorad
Tris-HCl	Sigma
Ammonium persulfate	Sigma
Sodium Dodecyl Sulphate (SDS)	Sigma
N,N,N',N'-tetramethylethylenediamine (TEMED)	Sigma

Tris/Glycine/SDS 10x concentrate (Running buffer)	Sigma
Tris/Glycine 10x concentrate (Transfer buffer)	Sigma
methanol	Sigma
Non-fat milk powder	Marvel
Tween 20	Sigma
Pierce ECL Western Blotting Substrate	Thermoscientific
Agarose	Sigma
Low melting agarose	Sigma
N- lauroylsarcosine	Sigma
EDTA disodium salt	Sigma

Table 2.1: Chemical reagents used during the investigation

2.1.2. Kits

Name	Source
Steady-Glo luciferase assay kit	Promega
CellTiter-Glo cell viability assay kit	Promega

Table 2.2: Kits used during the investigation

2.1.3. Antibodies

Primary antibodies			
Name	**Conjugation**	**Species raised**	**Source**
anti-M13-bacteriophage	-	rabbit	Sigma
anti-ubiquitin	-	mouse	Invitrogen
anti-PARP antibody	-	rabbit	Cell Signalling,9532
anti-GAPDH antibody	-	mouse	Santa Cruz
Secondary antibodies			
Name	**Conjugation**	**Species raised**	**Source**
anti-rabbit	AlexaFluor-647	goat	Invitrogen
anti-mouse	AlexaFluor-488	goat	Invitrogen
anti-rabbit	HRP	goat	Jackson Immunoresearch
anti-mouse	HRP	goat	Jackson Immunoresearch

Table 2.3: Antibodies used during the investigation

2.1.4. Cell lines

Name	Tissue origin	Source
9L	Rat glioma	Dr Hrvoje Miletic (University of Bergen, Norway)
M21	Human Melanoma	Dr David Cheresh (American Type Culture Collection)

Table 2.4: Cell lines used during the investigation

2.1.5. Oligonucleotides

Oligonucleotides (Primers)	Sequence
Forward	5'-ATGAATACGGCTACAGCAACAGG-3'
Reverse	5'-CTCTTGCTCAGTGTCCTTGCTG-3'

Table 2.5: Primer sequences used in PCR on the ITR domain of AAVP genome.

2.2 Methods

2.2.1. AAVP preparation

AAVP preparation

A loopfull of K91 from Luria-Bertani (LB) plate containing 50 μg/ml kanamycin was used to inoculate 7 ml of TB (Terrific broth) without antibiotic, which was then grown at 37 ^{o}C with shaking at 250 rpm until optical density reaches mid-log phase (OD_{600} between 1.5-2.0). 1ml starter culture was incubated with AAVPs for 1 hour at room temperature. Then the mixture was added to 1000 ml LB broth containing 50 μg/ml kanamycin and 40 μg/ml tetracycline. The culture was grown overnight (preferably 16-20 hours) in two 2L flasks at 37 ^{o}C with shaking at 250 rpm.

AAVP purification

The overnight cultures were centrifuged at 6,000 x g for 20 min at 4 ^{o}C. The supernatant was collected and the bacteria pellet was discarded. Cold Polyethylene-glycol/ Sodium chloride (PEG/Nacl) was added to the supernatant (15% of supernatant volume) and incubated on ice after mixing very well. After 2-3 hours incubation on ice the mixture was centrifuged for 30 minutes at

10,000 x g and the supernatant was then discarded. The pellet, containing the AAVP particles, was resuspended in Phosphate buffer saline (PBS) by shaking for 30 minutes in a 37 ^{o}C shaker incubator at 250rpm. After the pellet was dissolved, PEG/Nacl was added (15% of solution volume) and the mixture was incubated on ice for 30min-1hour. Following incubation, the mixture was centrifuged at 14,000 x g for 30 minutes at 4^{o}C. The supernatant was discarded and the pellet was resuspended in 1 ml PBS by shaking for 30 minutes in a 37 ^{o}C shaker incubator at 250rpm. To remove the remaining bacterial debris, the AAVP solution was centrifuged at 13,000 x g for 10 minutes at room temperature. The supernatant containing the AAVP particles was then filtered through a 0.45µm filter. The resulting phage solution was then titrated according to the following protocol.

AAVP titration

The titration was carried out by preparing serial dilutions of the AAVP in PBS (10^{-6}-10^{-9}) and infecting K91 host bacteria. A loopfull of K91 from Luria-Bertani (LB) plate containing 50 µg/ml kanamycin was used to inoculate 7 ml TB (Terrific broth) without antibiotic, which was then grown at 37 ^{o}C with shaking at 250 rpm until optical density reaches mid-log phase (OD_{600} between 1.6-

2.0). 1ml starter culture was incubated with 5 µl of the diluted AAVP for 20 min at room temperature without shaking to allow infection. 200 µl of the mixture were plated on LB agar plates containing 50 µg/ml kanamycin and 40 µg/ml tetracycline. The plates were incubated in a 37 ^{o}C incubator for 16 hours and colonies were formed. The titer of AAVP is calculated by counting the number of colonies multiplied by the dilution of the AAVP and is expressed as bacterial transducing units per µl (TU/µl) as previously described (Hajitou et al., 2007).

2.2.2. Cell culture

2.2.2.1 Maintenance of cell stocks

Human M21 melanoma cells were purchased from the ATCC while the rat 9L glioblastoma cells were a gift from Dr Hrvoje Miletic (University of Bergen, Norway). We investigated our hypotheses in these two cell lines from different histopathological types and species. Another reason for choosing these two cell lines is that 9L cells exhibit a bystander effect (described in the Introduction) while M21 do not.

Both cell lines were maintained in a humidified incubator at 37 ^{o}C in 5% CO_2 and cultured in Dulbecco's Modified Eagle's Medium supplemented with 10% fetal bovine serum (FBS), penicillin (100 units/ml), streptomycin (100 µg/ml),

and L-glutamine (2 mmol/l). The FBS was heat-inactivated for 1 hour at 56 ^{o}C to destroy complement before use. Genistein stock solution of 150 mM in dimethyl sulfoxide (DMSO) was prepared. Doxorubicin stock solution of 500 µM in PBS was prepared.

2.2.2.2 Storage of cell stocks

Monolayer cultures grown in 175 cm^2 flasks, were trypsinized and the cell suspension was transferred to a 50 ml tube and centrifuged at 1000 rpm for 5 minutes. The pellet was resuspended in 10 ml of freezing medium containing 95% (v/v) FBS and 5% (v/v) dimethyl sulfoxide (DMSO). Aliquots of 1 ml cell suspension were added to cryotubes. The vials were then placed in cryofreezing containers with isopropanol and then placed at -80 ^{o}C overnight. Subsequently the vials were transferred to liquid nitrogen for long term storage.

2.2.3. Mammalian cell transduction by AAVP in monolayer cell cultures

9L and M21 cells were trypsinized and counted by a haemocytometer. A suspension of 30,000 cells in total volume of 500 µl of complete DMEM were seeded on 48-well flat-based plates (corning) and grown in CO_2 incubator at 37^{o}C for 48 hours until they reach 70-80% confluence. Subsequently, cells were

transduced with targeted or control non-targeted AAVP vectors (10^6 TU/cell for HSVtk carrying vectors, 2.5 x 10^5 TU/cell for GFP carrying vectors, and 10^4 TU/cell for Luc carrying vectors) in serum-free medium (150 µl total volume per well). The plate was then incubated at 37 ^oC in the CO_2 incubator for 4 hours and manually rotated every 30 min during incubation. After 4 hours, 350 µl of complete medium were added to make up a total volume of 500 µl per well. The plate was then incubated in the CO_2 incubator at 37^oC. The medium was renewed every two days. Depending on the experiment, transduction efficiency was assessed by the expression of reporter genes at various indicated time points. The different amount of TU/cell between vectors carrying different transgenes is related to the sensitivity of the reporter gene assay. For example, luciferase assay is very sensitive and we had to use 10^4 TU/cell in order to avoid saturation of signal.

2.2.3.1 Genistein treatment in monolayer cell cultures

Genistein stock solution of 150 mM in dimethyl sulfoxide (DMSO) was prepared. Genistein was diluted in complete medium and added to the cells at a final concentration of 150 µM (Qing et al., 1997). After 2 hrs treatment, genistein-containing medium was removed and cells were washed with serum-

free medium. Following treatment with genistein, cells were transduced with targeted or control non-targeted AAVP vectors in serum-free medium as described above.

2.2.3.2 Doxorubicin treatment in monolayer cell cultures

Doxorubicin stock solution of 500 µM in PBS was prepared. Doxorubicin was diluted in 150 µl serum-free medium per well of 48-well plate containing AAVP vectors at a final concentration of 0.5 µM for 9L cells and 0.6 µM for M21 cells and was added to the cells at the same time with AAVP vectors. After 4 hours, 350 µl of complete medium containing doxorubicin were added to make up a total volume of 500 µl per well. 24 hours after doxorubicin treatment, medium was removed, cells were washed with PBS and fresh complete medium without doxorubicin was added.

2.2.4. Cytotoxicity assay

Cytotoxicity of genistein and doxorubicin were assessed using the MTT assay. MTT is colorimetric assay to measure cell viability based on mitochondrial activity. NAD(P)H-dependent cellular oxidoreductase enzymes are capable of reducing the tetrazolium dye MTT 3-(4,5-dimethylthiazol-2-yl)-2,5-

diphenyltetrazolium bromide to its insoluble formazan, which has a purple color, indicating the number of viable cells present. 9L and M21 cells were plated in 96-well plates at a density of 4 x 10^3cells/well. Next day, complete medium (100 µl) containing different concentrations of drug was added to cells in triplicates. After 2 hours treatment with genistein or 24 hours treatment with doxorubicin, the drug-containing medium was removed and replaced with 100 µl fresh medium. MTT assay was carried out 48 hrs later. 20 µl MTT solution was added on the top of the growth medium in each well of 96-well plate. The plate was then placed on a shaker for 5 minutes to thoroughly mix the MTT into the media. Subsequently, the plate was incubated for 4 hours at 37 ^oC in CO_2 incubator. Following incubation, the media was removed carefully without disturbing the MTT product. MTT product was then solubilised in 100 µl DMSO and the plate was incubated for 1 hour at room temperature on a plate shaker. Optical density was read at 570 nm using a plate reader.

2.2.5. Examination of reporter gene expression

Quantification of luciferase expression was carried out using Steady-Glo luciferase assay. Medium was removed and 110 µl of Glo Lysis buffer, was added per well of 48 well plate. After 10 min incubation, 50 µl of the cell lysate was transferred to a 96-well white opaque microplate (BD Falcon) and mixed

with an equal volume of Steady-Glo® luciferase substrate. After 10 min the plate was read using a Promega Glomax plate reader. Luciferase expression was normalized to 100 µg protein levels from cell lysate as determined by the Bradford assay. Results are shown as Relative Luminescence Units (RLU) per 100 µg of protein. GFP expression was visualized using a Nikon Eclipse TE2000-U fluorescence microscope.

2.2.6. Determination of tumor cell killing *in vitro*

9L and M21 cells were seeded in 48 well-plates for 48 hours until they reach 70-80% confluence. Then, cells were transduced with RGD4C-AAVP-HSVtk (RGD-HSVtk) targeted vector or control non-targeted vector carrying the *Herpes simplex virus thymidine kinase (HSVtk)* gene with or without genistein/doxorubicin treatment. Ganciclovir (GCV) was added to the cells at a concentration of 20 µM at day 3 post vector transduction and renewed daily. Cancer cell killing was quantified at 0, 24, 48, 72, 96 hours post GCV treatment. Cells were counted by using the trypan blue exclusion methodology. Results were normalized to non-targeted vector (fd-HSVtk).

2.2.7. 3D model of multicellular tumor spheroid culture and treatment

9L and M21 multicellular tumor spheroids were prepared by seeding 5 x 10^3 cells into a 96-well ultra-low attachment surface plate (Corning, Nottingham, UK) in 200 µl complete medium. After 48 hours of incubation, a spheroid was formed in each well. Then, after removing 100 µl of media, spheroids were transduced with targeted AAVP vectors or control non-targeted vectors in 100 µl complete medium with or without 2 hours pretreatment with genistein (150 µM). Doxorubicin treatment was carried out by co-administration of doxorubicin with AAVP vectors in final concentration of 0.5 µM for 9L and 0.6 µM for M21 spheroids. After 24 hours, the medium was replaced with 200 µl complete medium and renewed every 3 days by fresh complete medium. GFP gene expression was evaluated using fluorescent microscopy at day 10 post-transduction. When spheroids were transduced with vectors carrying the HSVtk gene, GCV (20 µM) was added on day 5 post-transduction and renewed every 2-3 days. Cell viability was evaluated on day 5 and day 7 post-GCV treatment on 9L and M21 spheroids respectively using CellTiter-Glo assay. First, medium was removed and then 100 µl of Glo Lysis buffer were added in each well. After 30 min incubation, M21 spheroids were dissolved by pipetting in the Lysis Buffer while 9L spheroids were dissolved using sonicator. 50 µl of the lysate was then transferred to a 96-well white opaque microplate (BD

Falcon), mixed with an equal volume of CellTiter-Glo substrate and read with a Promega Glomax plate reader.

2.2.8. Nuclei extraction

9L cells were plated on 48-well plates (70-80% confluent) and transduced with RGD-Luc targeted or fd-Luc control non-targeted vectors in serum-free medium for 4 hours with or without 2 hours pretreatment with genistein. The same experiment was carried out with doxorubicin by co-administration of doxorubicin and AAVP vectors in serum-free medium. On day 4 after transduction, cells were harvested and nuclei were extracted as previously reported (Cervelli et al., 2008). Cells were washed with PBS, trypsinized and then pelleted by centrifugation at 1,500 x g for 5 min. The pellet was washed with PBS and pelleted again by centrifugation at 1,500 x g for 5min. Subsequently, the pellet was resuspended in hypotonic buffer (20mM Hepes-KOH [pH 8.0], 5mM KCl, 1.5mM $MgCl_2$, 5mM Na butyrate, 0.1mM dithiothreitol [DTT]) and lysed by Dounce homogenization. Nuclei were collected by centrifugation (10 min, 16,000 x g, 4^oC) and resuspended in 200 µl nuclear extraction buffer (15mM Tris-HCl [pH 7.5], 1mM EDTA, 0.4 M NaCl, 10% sucrose, 1mM DTT). DNA was extracted using Phenol/Chloroform and precipitated by ethanol.

2.2.9. DNA extraction using Phenol-Chloroform

In the 200 µl of nuclei sample equal volume of the phenol/chloroform/isoamyl solution was added. The solution was mixed vigorously by vortex for 1 minute and then it was spun at 13,000 x g for 5 minutes. The top aqueous phase (~ 180 µl) was removed carefully and placed into a new tube (TUBE 2) without picking up any of the phenol/chloroform/isoamyl phase. 200 µl of Elution Buffer (EB) were added to the first tube (TUBE 1). The solution was mixed vigorously by vortex for 1 minute and then it was spun at 13,000 x g for 5 minutes. The top aqueous phase (~ 180 µl) was removed carefully and placed into TUBE 2. In TUBE 2 equal volume (~ 360 µl) of chloroform/isoamyl alcohol was added. The solution was mixed vigorously by vortex for 1 minute and then it was spun at 13,000 x g for 5 minutes. The top aqueous phase (~ 300-320 µl) was removed carefully and placed into a new tube (TUBE 3) without picking up any of the chloroform/isoamyl phase.

2.2.10. Ethanol precipitation

In TUBE 3, 1/10 volume of 3M sodium acetate (NH_4OAc), pH 5.2 was added. In addition, 1 µl of glycogen (20 µg) was added and the solution was mixed well. Subsequently, 2.5x volume of 100% ethanol was added, the solution was

mixed and incubated at -20 ^{o}C overnight. Next day the solution was spun for 20 minutes in a 4^{o}C centrifuge at top speed. The supernatant was carefully discarded without disturbing the pellet. The pellet was washed by adding 500 µl of 70% ethanol and mixing by vortex three times. The solution was spun for 15 minutes in a 4^{o}C centrifuge at top speed. The supernatant was carefully discarded without disturbing the pellet. The pellet was washed again by adding 500 µl of 70% ethanol, mixing by vortex three times and spun for 15 minutes in a 4^{o}C centrifuge at top speed. The supernatant was carefully discarded without disturbing the pellet. Residual ethanol was removed with a P20 pipette after a quick spin on a table top centrifuge. The pellet was air-dried for 2 minutes and then resuspended in 20 µl EB.

2.2.11. Semi-quantitative PCR analysis

After extraction and ethanol precipitation, DNA was used as template for PCR targeting the ITR domain of the vector in order to semi-quantify the amount of vector in the nucleus with or without treatment with genistein or doxorubicin. The same amount of DNA was used as template for PCR in the *GAPDH* gene. PCRs were performed in a 25- µl volume containing 2 mM MgCl2, 0.4 mM dNTP mixture, 0.2 µM forward ITR primer (fwd ITR primer, 5'-

GGAACCCCTAGTGATGGAGTT-3'), 0.2 µM reverse ITR primer (rev ITR primer, 5'-CGGCCTCAGTGAGCGA-3'), 10 ng DNA template and 1 Unit of Q5 polymerase . The PCR program contained an initial denaturation step at 98 ^{o}C for 10 min followed by 35 cycles of denaturation at 98 ^{o}C for 15 sec, annealing at 61.5 ^{o}C for 30 sec, and extension at 72 ^{o}C for 1 min, with a final extension after the last cycle at 72 ^{o}C for 5 min (Aurnhammer et al., 2012).The 62-bp PCR product was analysed on a 4% agarose gel. The band intensity of the pcr product was quantified using ImageJ software and normalised to *GAPDH* pcr product (Fwd gapdh primer: 5'-ATGAATACGGCTACAGCAACAGG-3', Rev gapdh primer: 5'-CTCTTGCTCAGTGTCCTTGCTG-3').

2.2.12. Internalization assay

Internalization assay was performed as previously described (Yata et al., 2014). After 2 hours pre-treatment with medium containing genistein, cells were transduced with targeted and control non-targeted vectors (10^{6} TU per cell) in serum-free medium for 1, 2 and 4 hours at 37^{o}C incubator. The same experiment was carried out with doxorubicin by co-administration of doxorubicin and AAVP vectors in serum-free medium. Subsequently, cells were cooled on ice to stop endocytosis and washed three times with PBS to remove

unbound vectors. Cells were trypsinized for 5 min at 37 °C (to remove surface-bound phage) and pelleted by centrifugation at 2000 rpm for 5 min. Subsequently, cells were fixed in 4% paraformaldehyde (PFA, pH 7.2) for 10 minutes at room temperature. Untreated cells were used as negative controls. Cells were blocked with 0.1% saponin in 2% bovine serum albumin in PBS (BSA-PBS) for 30 minutes. To detect internalised phage-derived vectors, cells were stained with rabbit anti-M13-bacteriophage antibody (diluted 1:1000) in 0.1% saponin in 1% BSA-PBS for 1 hour at room temperature. Cells were washed three times (pelleted and resuspended) in 0.1% saponin in 1% BSA-PBS. Subsequently, cells were incubated with the secondary antibody, goat anti-rabbit AlexaFluor-647 (diluted 1:500) for 1 hour at room temperature. Finally, cells were washed twice with 0.1% saponin-PBS and resuspended in PBS before analysis.

Fluorescence-activated cell sorting (FACS) analysis was carried out using a FACscalibur Flow cytometer (BD Biosciences). The mean fluorescence intensity was measured for at least 10,000 gated cells per triplicate well. Results were analysed using Flowjo (TreeStar) software.

2.2.13. Attachment assay

9L cells were seeded in 48-well plates and grown for 48 hours until they reach 70-80% confluence. Genistein was diluted in complete medium and added to the cells at a final concentration of 150 µM (Qing et al., 1997). After 2 hours, genistein-containing medium was removed and cells and cells were treated with targeted or control non-targeted AAVP vectors (10^6 TU per cell) in serum-free medium (150 µl total volume per well). The same experiment was carried out with doxorubicin by co-administration of doxorubicin and AAVP vectors in serum-free medium. The 48-well plates were placed on ice for 1 hour to prevent internalisation of AAVP. After 1 hour, supernatants were collected and serially diluted in PBS. The amount of AAVP particles in the supernatant was quantified using the K91 bacterial infection method, as previously described (Hajitou et al., 2007).

2.2.14. Immunofluorescence staining

9L cells were seeded on 18 mm^2 coverslips in 12-well plates. After 48 hours, cells were approximately 80% confluent and were infected by targeted phage (10^6 TU per cell) in serum-free medium with or without 2 hours pretreatment with Genistein (150 µM). After 4 hours, 350 µl of complete medium were

added to make up a total volume of 500 µl per well. After 2 hours (6 hours post-transduction), cells were washed with PBS and fixed in 4% paraformaldehyde (PFA). Cells were then incubated in 50 mM Ammonium Chloride for 5 min, permeabilized with 0.2 % Triton X-100, washed, and blocked with PBS containing 2% BSA. Subsequently, cells were incubated with rabbit anti-M13 bacteriophage (diluted 1:1000) and mouse anti-ubiquitin (diluted 1:200) diluted in 1% BSA at 4^{o}C overnight. Next day, cells were washed with PBS and incubated for 1 hour at room temperature with 1% BSA containing goat anti-rabbit AlexaFluor-647 and goat anti-mouse AlexaFluor-488 secondary antibodies (diluted 1:750) and also DAPI (diluted 1:2000). Cells were washed three times in PBS and twice in distilled water, allowed to air-dry and mounted in Prolong Gold antifade reagent. Images were acquired with a Leica laser confocal microscope. Semi-quantification of the ubiquitin staining was carried out calculating the corrected total cell fluorescence (CTCF = Integrated Density – (Area of selected cell X Mean fluorescence of background readings)) using ImageJ software.

2.2.15. Sample preparation for Western blotting

The cell culture dish was placed on ice and the cells were washed with cold PBS. RIPA buffer (containing protease inhibitors) was added and the cells were kept on ice for 15 minutes. The cells were scraped off the dish using a plastic cell scraper and the cell lysate was transferred to a microcentrifuge tube. The tubes were spun at 16,000 x g for 20 minutes in a 4^{o}C pre-cooled centrifuge. The supernatant was transferred to a fresh tube, also kept on ice, and the pellet was discarded. A small volume of the lysate (1-5 µl) was used to determine the protein concentration (described in 2.2.16) and the samples were stored at -20 ^{o}C. 50 µg from each sample were mixed with equal volume of 2x Laemmli buffer and the samples were boiled at 95 ^{o}C for 5 minutes.

2.2.16 Protein concentration determination (Bradford assay)

Bradford assay is a colorimetric protein assay. It is based on a shift in the absorption maximum of the Coomassie Brilliant Blue dye from 465nm to 595nm when it binds to proteins. The bound form of the dye (blue) has an absorption spectrum maximum at 595 nm. The unbound forms are green or red. The binding of the dye to the protein stabilizes the blue form. The increase

in absorbance at 595 nm is proportional to the amount of bound dye (blue), and thus to the amount (concentration) of protein present in the sample.

The sample protein concentrations were calculated by linear regression from the standard curve. Standard samples ranging from 0-1 mg/ml BSA were prepared. The lysed cell samples were diluted to ensure they fall within the linear part of the standard curve. The samples and the standards were added in duplicate into a 96-well plate (5 µl/well) followed by addition of 250µl of Bradford assay reagent. After 5 minutes colour equilibration at room temperature the plate was read on Promega Glomax plate reader at 595 nm.

2.2.17. Protein separation by gel electrophoresis

Proteins were separated by sodium dodecyl sulphate polyacrylamide gel electrophoresis (SDS-PAGE) using acrylamide gels [8% v/v acrylamide, 375 mM Tris-HCl, 1mg/ml sodium dodecyl sulphate (SDS), 0.775 mg/ml N,N,N',N'-tetramethylethylenediamine (TEMED) and 1 mg/ml ammonium persulfate, pH 8.8]. The stacking gel consisted of 6% v/v acrylamide, 78 mM Tris-HCl, 1mg/ml SDS, 0.775 mg/ml TEMED and 1mg/ml ammonium persulfate at pH 6.8. Equal amounts of protein samples were loaded in individual wells along with

molecular weight marker. The gel was run at 100V for around 60-90 minutes (Running buffer: 25 mM Tris, 192 mM glycine, 0.1% SDS at pH 8.3).

2.2.18 Transferring protein from the gel to membrane

The PVDF membrane (Millipore) was activated by emerging in methanol for 1 minute and washed in transfer buffer (25mM Tris, 192 mM glycine and 20% methanol at pH 8.3). The gel containing the separated proteins was placed in the transfer buffer for 10min. The transfer sandwich was prepared without air bubbles trapped in it, and then it was placed in the tank containing the transfer buffer and an ice block. The proteins were transferred to PVDF membrane by electrophoresis at 400mA for 1 hour at room temperature (or 10mA overnight transfer at 4^{o}C).

2.2.19 Western blot with chemiluminescent detection

The PVDF membrane was washed for 10 minutes in Tris-buffered saline with Tween 20 (TBST; 20mM Tris pH 7.5, 150mM NaCl, 0.1% Tween 20), and incubated in 5% non-fat milk powder in TBST for 1 hour at room temperature on a rocking platform. The membrane was then incubated at 4^{o}C overnight under agitation with rabbit monoclonal anti-PARP antibody diluted 1:1000 in

5% non-fat milk in TBST. Next day, the membrane was washed 3 times (15 minutes each wash) with TBST and incubated with horseradish peroxidase (HRP) conjugated anti-rabbit IgG antibody at 1:3000 in TBST for 1 hour at room temperature under agitation. The membrane was washed 4 times (15 minutes each) and antibody binding was visualised by enzymatic chemiluminescence (ECL) according to manufacturer's instructions.

To ensure equal amounts of protein were loaded, the membrane was then washed with TBST and incubated in 5% non-fat milk in TBST for 1 hour at room temperature on a rocking platform. The membrane was then incubated with mouse monoclonal anti-GAPDH antibody at 1:1000 in TBST for 1 hour at room temperature. The membrane was washed (3 times, 15 minutes per wash) and incubated with HRP-conjugated anti-mouse IgG antibody at 1:3000 in TBST for 1 hour at room temperature on a rocking platform. The membrane was washed (4 times, 15 minutes per wash) and the bands were visualised by ECL detection.

The proteins were visualised by exposure of the membrane to X-ray film for up to 5 minutes following development using automated machine.

2.2.20. Comet Assay

Comet assay is a single cell based technique that allows to detect and quantify DNA damage. Comet assay essentially measures the degree of relaxation as well as fragmentation of DNA within the cell.

The standard slides were immersed vertically in 1% normal melting agarose in dH_20 at 55 ^oC and left vertically to allow the agarose to solidify. The slides were stored at 4^oC until use. Approximately 10,000 cells were counted and mixed with 85 µl of 0.7% low melting agarose in PBS at 37 ^oC. The cell suspension was pipetted and spread onto the first agarose layer using a coverslip. The slides were kept at 4^oC for 10 minutes for the second layer to solidify. The coverslips were then removed. A third layer of 100 µl 0.7% low melting agarose was added, covered with a coverslip and again allowed to solidify at 4^oC for 10 minutes. The coverslips were again removed. After the top layer of agarose was solidified, the slides were immersed in cold lysis buffer (2.5M NaCl, 0.1 M Na_2EDTA, 0.01 M Tris-HCl, 1% N- lauroylsarcosine sodium salt, pH adjusted at 10, then 1% Triton X-100 and 10% DMSO were added just before use). The slides were kept at 4^oC in the dark for at least 1 hour to lyse the cells and to allow DNA unfolding. The slides were removed from the lysis buffer, drained and placed in a gel electrophoresis machine, side by side. The tank was filled with fresh cold electrophoresis solution (1mM Na_2EDTA, 0.3M NaOH) at 4^oC

and pH 12.8. Before electrophoresis, the slides were left in the solution for 20 minutes to allow the unwinding of DNA. The electrophoresis was carried out at 300mA for 20 minutes at 4^{o}C in the dark. During electrophoresis, DNA fragments (damaged DNA) migrates away from the nucleus forming the ‘’tail’’ of the comet. The size of the ‘’tail’’ is proportional to the damaged DNA. After electrophoresis, slides were gently washed with neutralization buffer (0.3M Tris-HCl, pH 7.5) to remove alkali and detergent, and stained with DAPI (5 µg/ml) in mounting medium.

Individual nuclei were viewed using a fluorescent microscope. Images of 50 randomly selected nuclei were captured and analysed using ImageJ software.

2.2.21 Statistical analysis

Statistical analysis was performed using GraphPad Prism software (version 5.0). Data are expressed as mean ± standard error of the mean (s.e.m.) P values were generated by one-way ANOVA and Tukey tests. P values were considered significant when <0.05 and denoted as follows: *p<0.05, **p<0.01, ***p<0.001.

Chapter 3

The natural dietary genistein boosts bacteriophage-mediated cancer cell killing by improving phage-targeted tumor cell transduction

3.1. Introduction

The concentration of genistein that was previously reported to enhance gene delivery by AAV vectors is 150 µM (Qing et al., 1997). First, we set out to investigate if this concentration is toxic, therefore we performed MTT assay in 9L and M21 cancer cell lines. We found that this concentration is not toxic, so we used it for further experiments. The next step was to investigate our hypothesis in 9L and M21 cell lines (2D model) using RGD4C-AAVP carrying reporter genes (*GFP*, firefly *luciferase* reporter genes) or RGD4C-AAVP carrying the Herpes simplex virus thymidine kinase (*HSVtk*) which kills cells in the presence of ganciclovir. The same experiments were carried out in 3D 9L and M21 tumor spheroid models. Finally, we investigated potential mechanisms that genistein increased RGD4C-AAVP mediated transduction efficiency.

3.2. Cytotoxicity of genistein on 9L and M21 cells

First, we sought to assess the cytotoxicity of genistein *in vitro* on 9L and M21 cancer cell lines. Tumor cells were treated with increasing concentrations of genistein ranging from 100 to 800 µM for 2 hours and compared to non-treated cells. Subsequently, cell survival was assessed at 48 hours post drug treatment. The data show that tumor cell death raised as the concentration of the drug increased (Figure 3.1) for both 9L and M21 cancer cells with a more pronounced effect on the 9L glioblastoma cells than M21 melanoma cells. Cytotoxic doses expressed as IC_{50} values, corresponding to inhibitory concentration required to induce the cell death by 50%, are shown by the lines on the graphs to approximate the IC_{50} value (Figure 3.1). We found that 50% of cell death in the presence of genistein was induced by ~650µM in 9L cells (Figure 3.1A), while in M21 cells, 50% of cell death was achieved at a dose of over 800 µM (Figure 3.1B). Next, to assess the effect on tumor cell killing by RGD4C-AAVP, we selected genistein concentration of 150 µM for both 9L and M21 cancer cells, as this dose is below the IC_{50} and cause little toxicity, and was previously reported to enhance gene delivery by human-derived viral vectors (Qing et al., 1997).

A

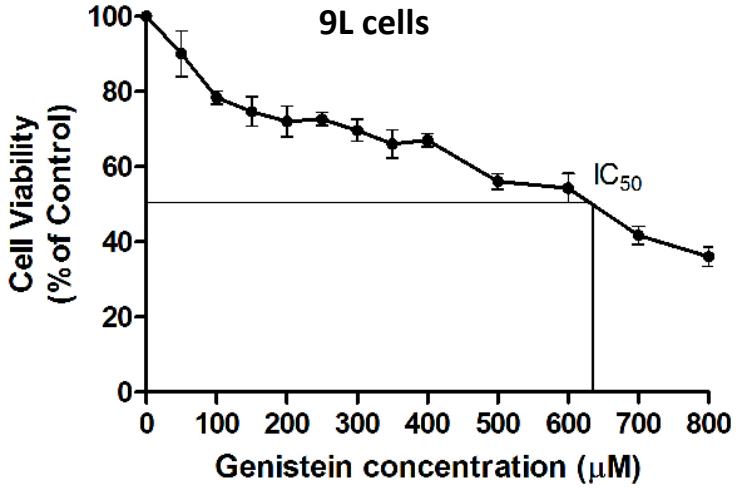

B

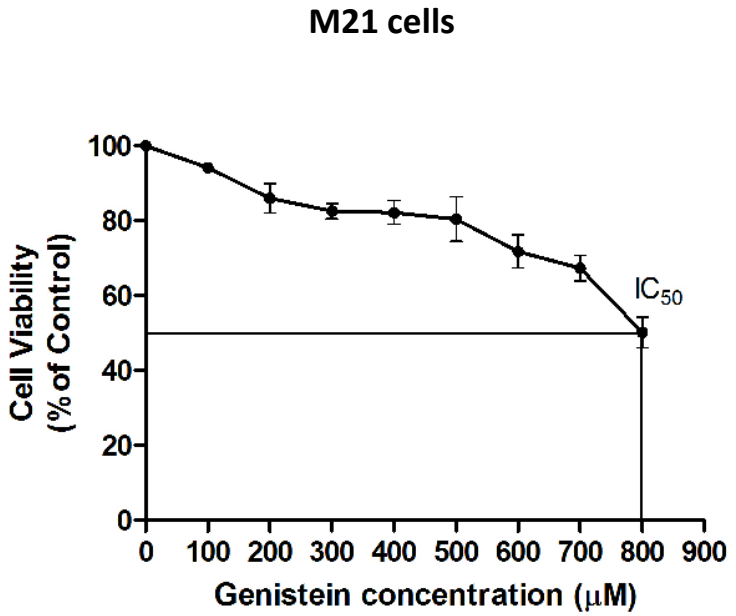

Figure 3.1 Cytotoxicity of genistein on 9L and M21 cells. 9L **(A)** and M21 **(B)** cells were cultured in 96-well plates, then treated with increasing concentrations of genistein ranging from 100 to 800 µM for 2 hours. Subsequently, cells were grown for further 48 hours without the drug. Cell survival was determined by using the MTT assay and expressed as percentage of cells counted in parallel cultures without drug. The assay was repeated twice in triplicate and the results shown are representative of one experiment. Data represent the mean ± standard error of the mean (s.e.m.) of triplicate samples from one representative experiment.

3.3 Genistein drug treatment boosts cancer cell death by phage-mediated suicide gene killing

To test tumor cell killing efficacy, we used the RGD4C-*HSVtk* vectors encoding the gene for the Herpes simplex virus thymidine kinase (*HSV1tk*) mutant SR39 (Black et al., 2001) which kills cells in the presence of ganciclovir, GCV (Figure 3.2). 9L and M21 cells were transduced with RGD-HSVtk or control non-targeted vector fd-HSVtk (without RGD) carrying the *HSVtk* gene with or without 2 hours pretreatment with genistein. The cells were then treated with GCV (20 μM) at day 3 post vector transduction. Cancer cell killing was quantified at 0, 24, 48, 72, 96 hours post GCV treatment. Results were normalized to non-targeted vector which didn't show any tumor cell death (data not shown). In both cancer cell lines, the combination treatment with genistein and RGD-HSVtk therapy resulted in greater cell killing compared to cells treated cells with RGD-HSVtk or genistein drug alone (Figure 3.2). For instance, at 72 hours post GCV treatment, combination treatment induced 91.6% and 70.5% killing of 9L and M21 cancer cells, respectively (Figure 3.2), compared to 79.5% and 44.7% death induced by vector alone in 9L and M21 cells, respectively, and 69.8% death and 49.6% death induced by genistein alone in 9L and M21 cells, respectively. These data show that drug treatment of

cancer cells with an isoflavone is a promising approach to enhance targeted gene therapy by RGD4C-AAVP.

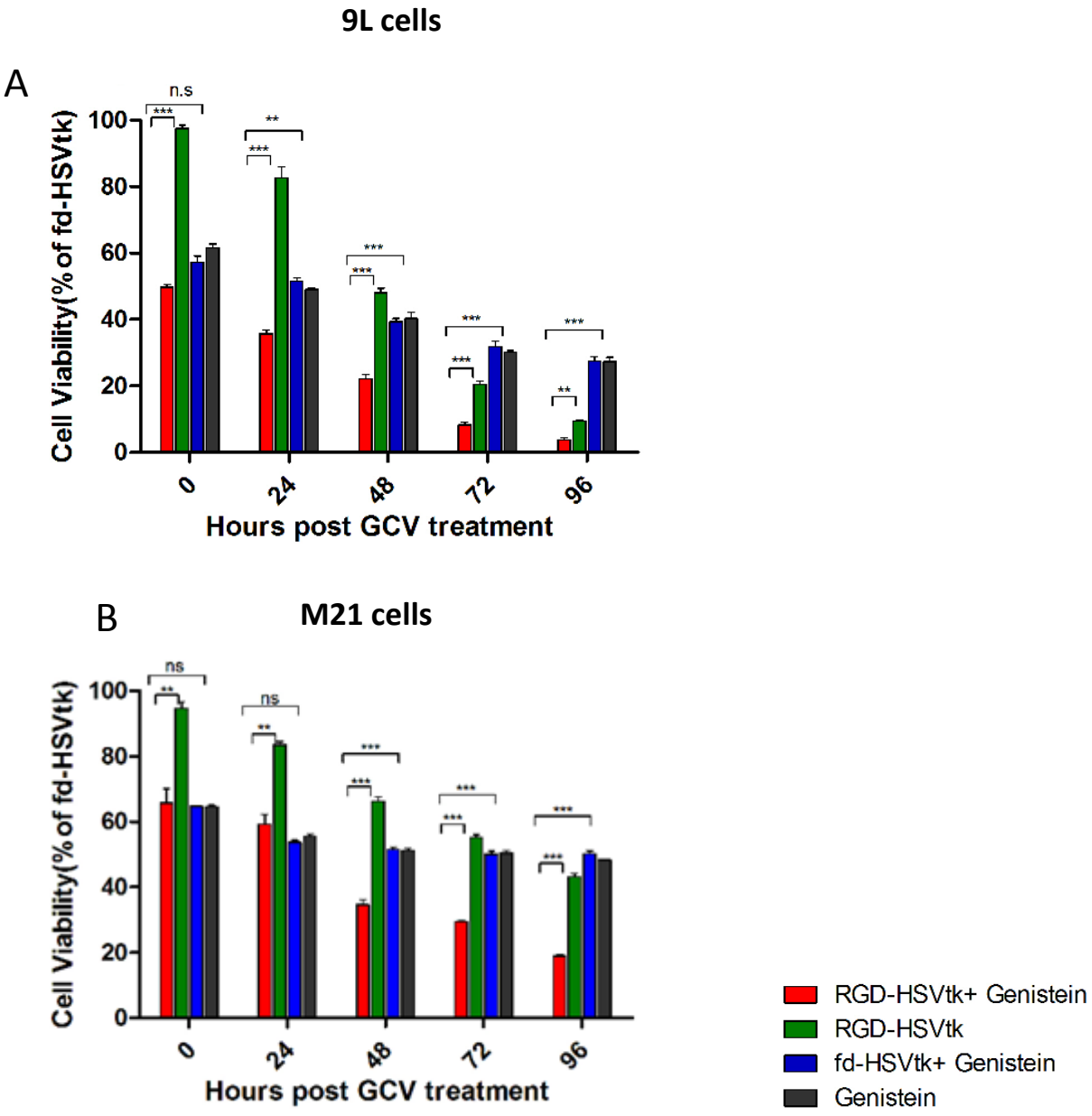

Figure 3.2 Genistein increased the cell death after transduction with RGD-HSVtk (+GCV) in 9L and M21 cells. 9L **(A)** and M21 cells **(B)** grown in 48 well-plates (60-80% confluent) were transduced with RGD-HSVtk targeted vector or control non-targeted vector with or without 2 hours pretreatment with genistein (150µM). The cells were treated with GCV (20 µM) at day 3 post vector transduction and renewed daily. Cancer cell killing was quantified at 0, 24, 48, 72, 96 hours post GCV treatment. Cells were counted by using the trypan blue exclusion methodology. Results were normalized to non-targeted vector. The experiment was repeated twice in triplicate and the results shown are representative of one experiment. Data represent the mean ± standard error of the mean (s.e.m.) of triplicate samples. P values were generated by one-way ANOVA and tukey's post hoc tests. P values were considered significant when <0.05 and denoted as follows: n.s.-not significant, *p<0.05, **p<0.01, ***p<0.001.

3.4 Genistein increases targeted reporter gene transfer by the RGD4C-AAVP in 9L and M21 cancer cells *in vitro*

To gain insight into the improved tumor cell killing by RGD4C-HSVtk following combination with genistein, we investigated the effect of genistein on gene delivery by RGD4C-AAVP. We first conducted qualitative analyses of transgene expression by using vectors carrying the reporter gene of the *green fluorescent protein* (*GFP*) and combined with 2 hours pretreatment with 150 µM of genistein (Figure 3.3). Fluorescent microscopic analysis of GFP expression at day 4 post vector transduction showed that in both cell lines the combination treatment of RGD-GFP and genistein, resulted in significantly higher GFP expression, compared to RGD-GFP vector alone in both 9L and M21 tumor cells (Figure 3.3). Next, to confirm the increased gene delivery by RGD4C-AAVP in combination with genistein, we carried out a quantitative analysis of transgene expression over a time course of 4 days post vector transduction by using RGD4C-*Luc* vectors expressing the firefly *Luc* reporter gene (Figure 3.4). Consistently with GFP reporter transgene expression experiments, we observed a significant increase in RGD4C-mediated *Luc* expression at various time points post vector transduction by genistein treatment in both 9L and M21 cancer cells compared to cells treated with the vector alone. For instance, at day 4 post-transduction, quantitative analysis of *Luc* transgene expression

showed that the combination treatment (RGD-Luc + Genistein) resulted in ~ 4.7 fold and ~3.8 fold increase in luciferase expression in 9L and M21 cells, respectively, compared to RGD-Luc treatment alone. Moreover, in 9L cells, initiation of the luciferase expression occurred as early as day 2 post vector transduction, in the presence of genistein (Figure 3.4). Importantly, no luciferase expression was detected in cells transduced with non-targeted fd-Luc vector alone or in combination with genistein, which shows that genistein does not affect the specificity and targeting of the RGD4C-AAVP vector.

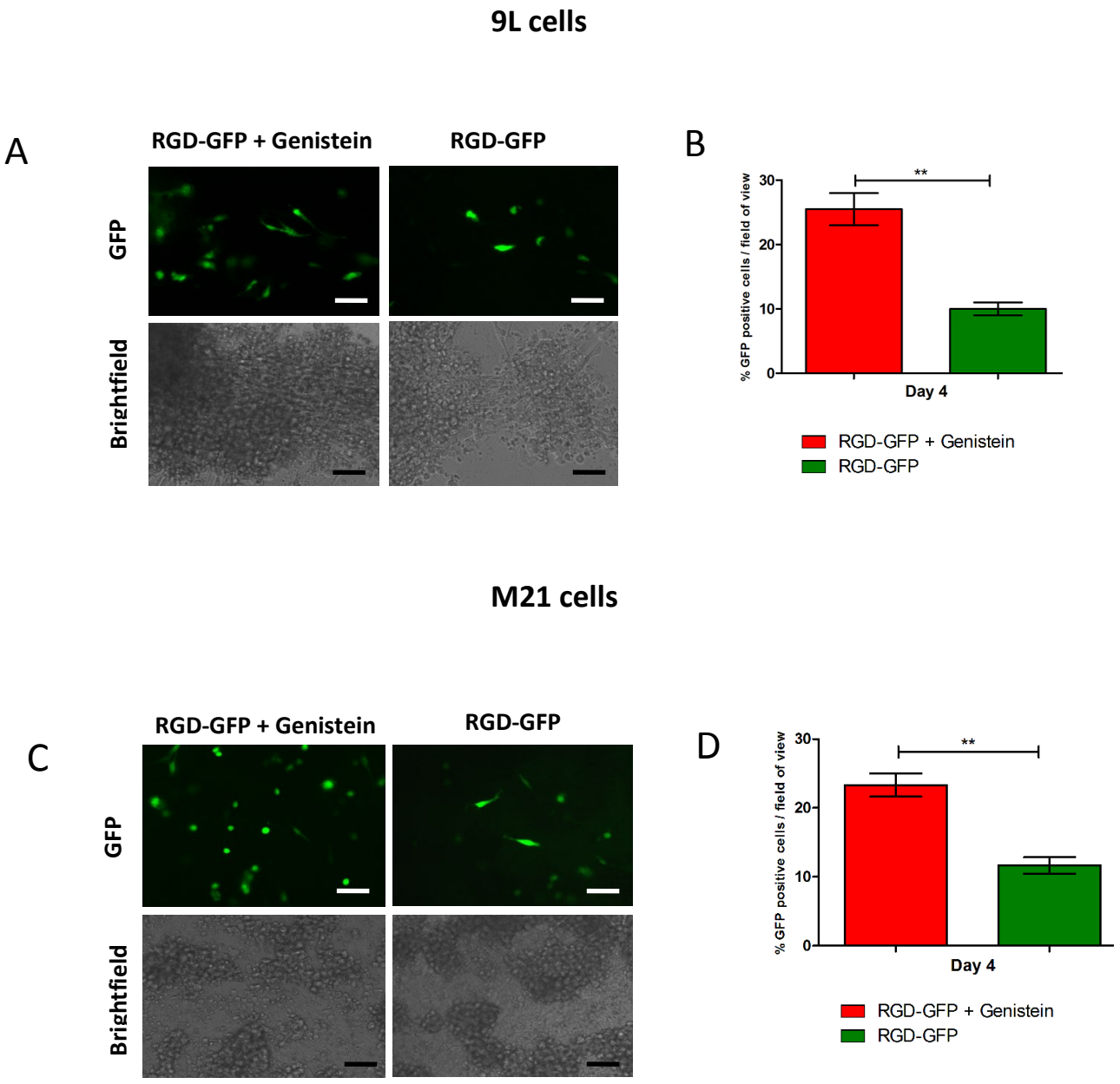

Figure 3.3 Genistein increased the transduction efficiency in 9L and M21 cells. 9L **(A,B)** and M21 cells **(C,D)** were plated on 48-well plates (70-80% confluent) and transduced with RGD-GFP targeted or control non-targeted vectors in serum free medium for 4 hours with or without 2 hours pretreatment with genistein (150µM). GFP expression was evaluated by fluorescent microscopy on day 4 post vector transduction. The experiment was repeated twice in triplicate and the results shown are representative of one experiment. Data represent the mean ± standard error of the mean (s.e.m.) of %GFP positive cells in five independent fields of view. P values were generated by Student's t-test. P values were considered significant when <0.05 and denoted as follows: *p<0.05, **p<0.01, ***p<0.001.Scale bar= 100 µM

A

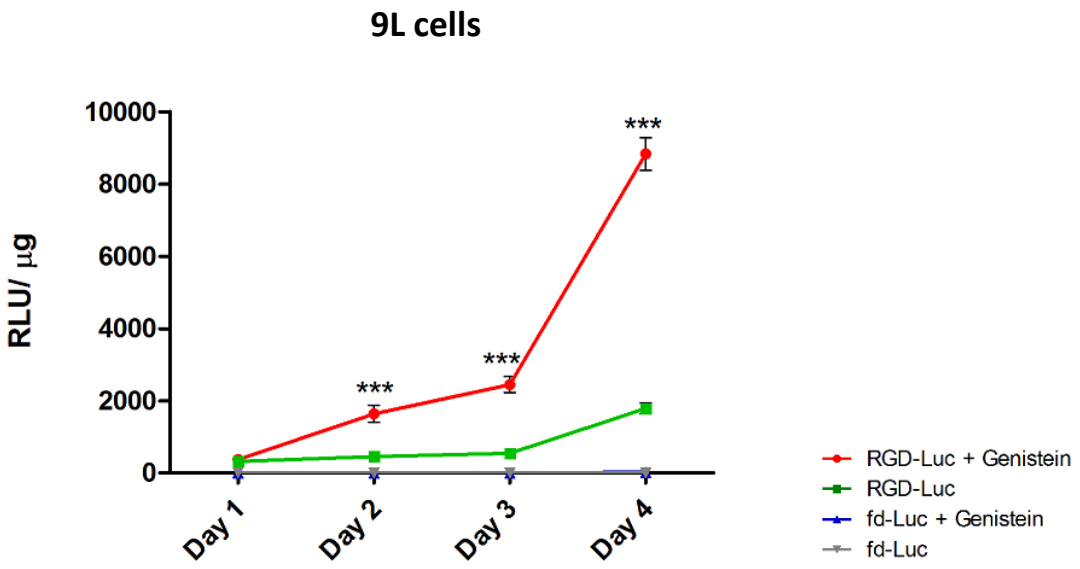

B

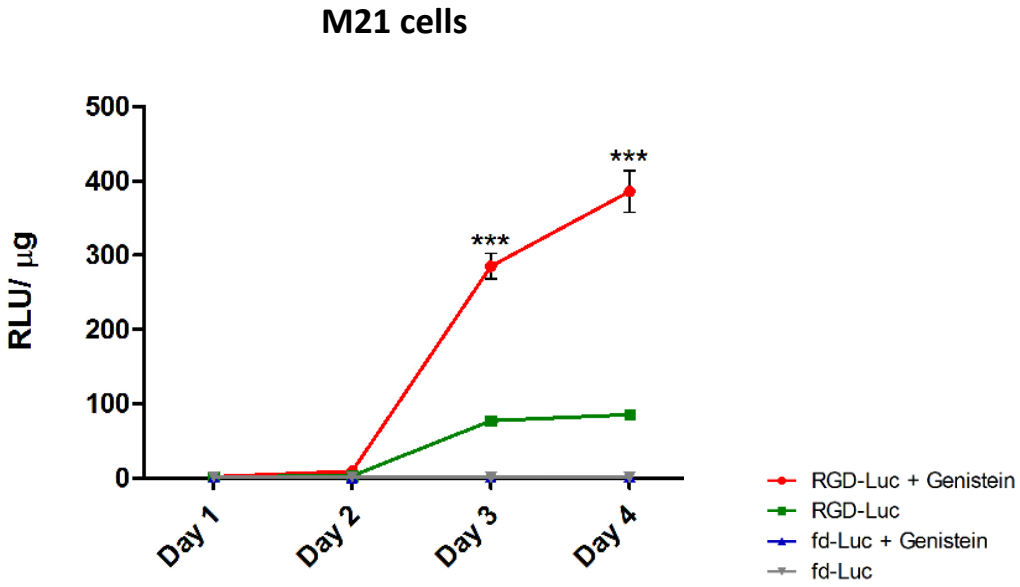

Figure 3.4 Genistein increased the transduction efficiency in 9L and M21 cells. 9L **(A)** and M21 cells **(B)** were plated on 48-well plates (70-80% confluent) and transduced with RGD-Luc targeted or fd-Luc control non-targeted vectors in serum free medium for 4 hours with or without 2 hour pretreatment with genistein (150µM). Luciferase measurement assays were performed at days 1-4 post-transduction and normalized to protein concentration as determined by the bradford assay. Results are shown as RLU (Relative Luminescence Units) per 1µg of protein and represent the average from triplicate wells. The experiment was repeated twice in triplicate and the results shown are representative of one experiment. Data represent the mean ± standard error of the mean (s.e.m.) of triplicate samples. P values were generated by one-way ANOVA and tukey's post hoc tests. P values were considered significant when <0.05 and denoted as follows: n.s.-not significant, *p<0.05, **p<0.01, ***p<0.001.

3.5 Evaluation of vector cellular entry following genistein pretreatment.

After demonstrating that the increased tumor cell killing by RGD4C-AAVP observed in combination with genistein was associated with enhanced RGD4C AAVP-mediated gene expression, we set out to gain further understanding into the mechanism of enhanced gene transfer by RGD4C-AAVP in combination with genistein. Therefore, we sought to investigate the effect of genistein on steps involved in gene transfer. It is well established that vector-mediated gene delivery depends on several steps where the vector needs to access the cell surface to bind to its receptor, followed by cell internalization and intracellular trafficking, then transport to the nucleus for gene expression to occur (Nishikawa and Huang, 2001, Wiethoff and Middaugh, 2003). We first examined the effect of genistein on vector attachment to the surface of cells, as we previously reported that gene transfer by RGD4C-AAVP is hindered by its weak accessibility to the surface of tumor cells (Yata et al., 2014). Hence, we quantified the free cell-unbound phage in the supernatant above the adherent cells by infection of host bacteria followed by colony counting (Figure 3.5). An amount of 52%, of input phage particles, was recovered from the supernatant of cells treated with the RGD4C-phage vector showing that a fraction of 48% of input phage was bound to the surface of tumor cells. However, pretreatment with genistein had no effect on vector attachment to the cell surface (Figure

3.5). The non-targeted vector showed no attachment to surface of tumor cells with 100% recovery. Finally, internalization assays revealed that combination of vector with genistein does not increase entry of the RGD4C-AAVP into cancer cells (Figure 3.6). These data prove that genistein has no effect on cell attachment and internalisation of the RGD4C-AAVP viral particles.

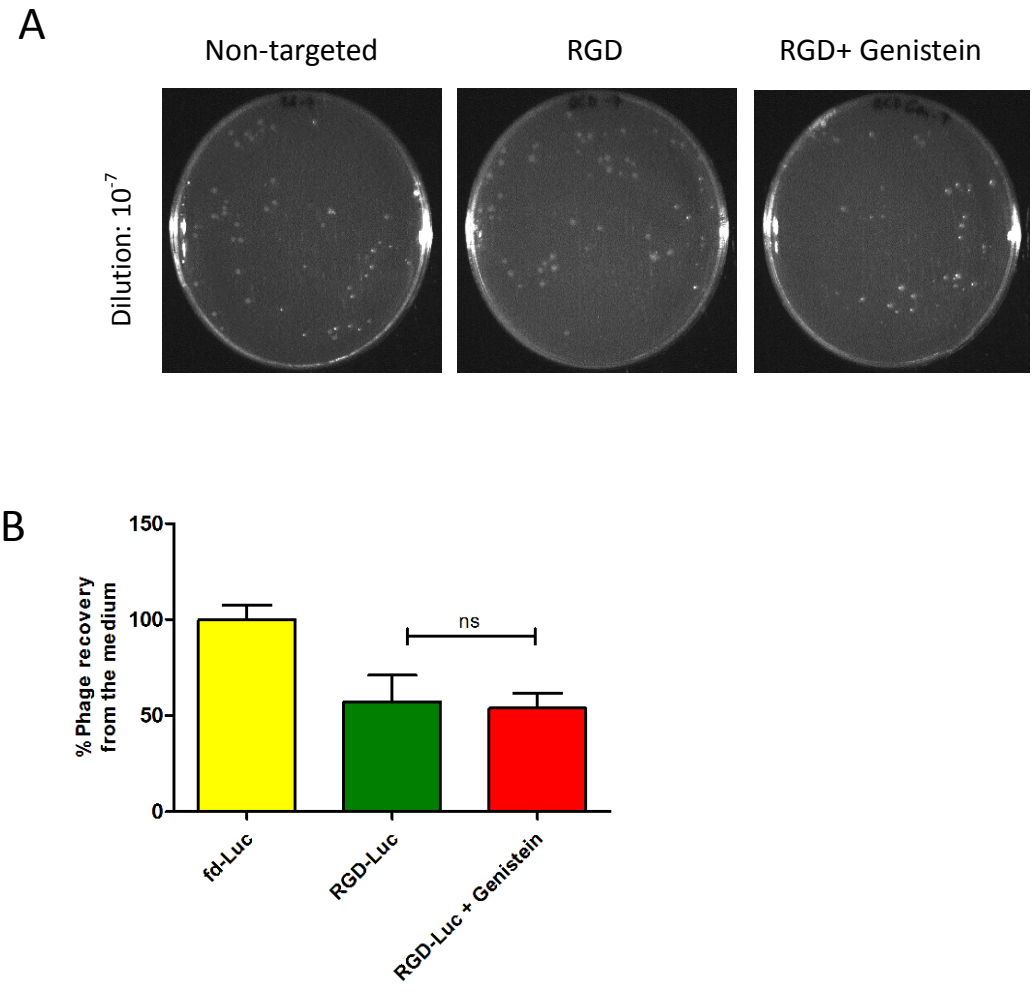

Figure 3.5 Attachment assay. Evaluation of the phage/genistein attachment by titrating the unbound phage in the supernatant of 9L cells. **(A)** Representative plates showing bacterial colonies generated by infection of K91 batceria by the phage recovered from the media of transduced cells. **(B)** Quantitative analysis of recovered phage following bacterial colony counting. Data represent the mean ± standard error of the mean (s.e.m.) of triplicate samples. P values were generated by one-way ANOVA and tukey's post hoc tests. P values were considered significant when <0.05 and denoted as follows: n.s.-not significant, *p<0.05, **p<0.01, ***p<0.001.

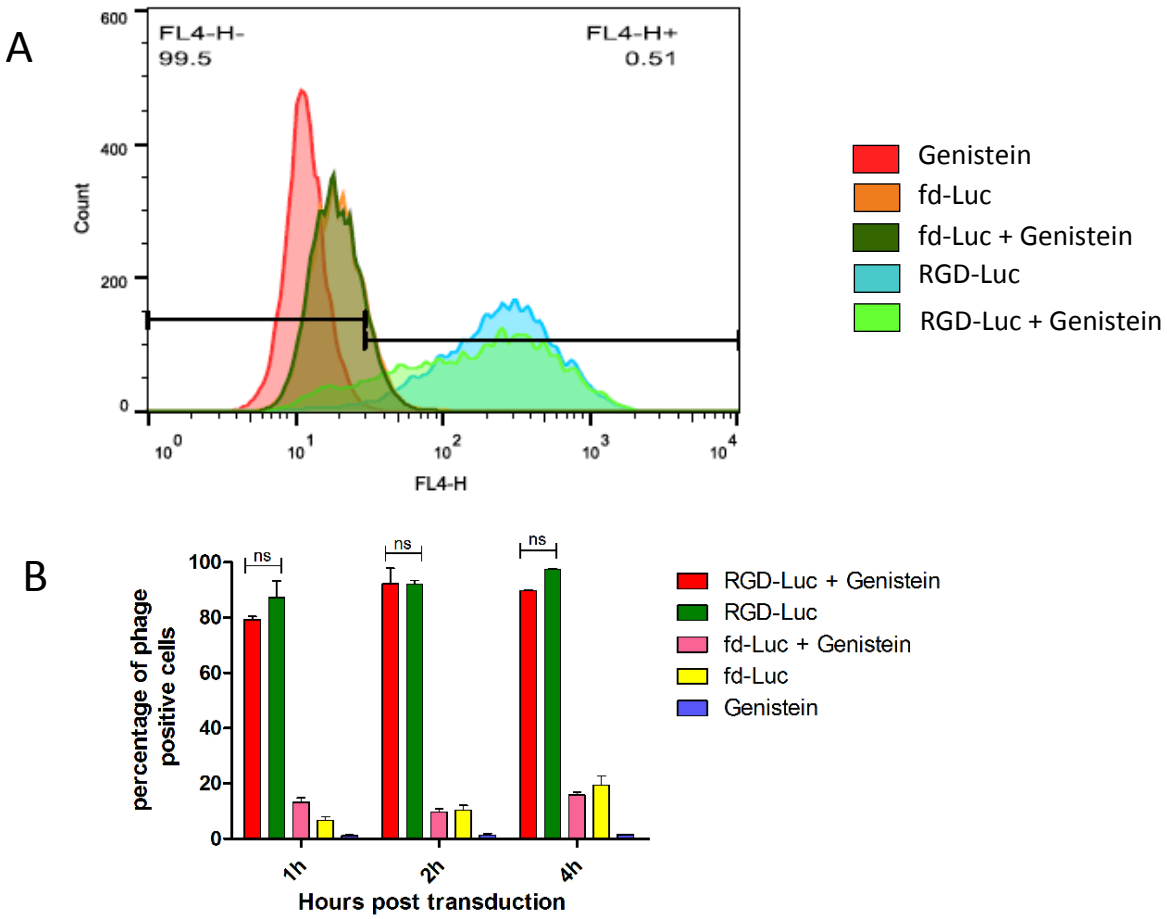

Figure 3.6 Internalization assay. Evaluation of the phage internalization in the presence or absence of genistein. **(A)** Graph showing FACS results after immunostaining of 9L cells treated with phage with or without pretreatment with genistein. **(B)** Graph showing the percentage of phage positive cells according to FACS data at three different time points (1hour, 2 hours, 4 hours). The experiment was carried out in triplicates. Data represent the mean ± standard error of the mean (s.e.m.) of triplicate samples. P values were generated by one-way ANOVA and tukey's post hoc tests. P values were considered significant when <0.05 and denoted as follows: n.s.-not significant, *p<0.05, **p<0.01, ***p<0.001.

3.6 Genistein protects RGD4C-AAVP from proteasome degradation.

After ruling out the effect of genistein on vector cell entry, we sought to determine whether genistein improves intracellular persistence of the RGD4C-AAVP. As we previously reported the proteasome is a barrier to gene transfer by RGD4C-AAVP vectors (Przystal et al., 2013). Genistein was found to possess proteasome-inhibitory activity (Kazi et al., 2003). Thus, we investigated the effect of genistein pretreatment of tumor cells on vector protection against proteasome degradation. 26S proteasome targets the degradation of polyubiquitinated protein substrates; thus inhibition of proteasome degradation by genistein would lead to accumulation of AAVP ubiquitination (Zhu et al., 2005). So, we searched whether genistein increases polyubiquitination of AAVP phage coat proteins. 9L tumor cells were transduced with RGD-AAVP vector alone or following pretreatment with genistein. Next, the cells were analyzed for co-localization of AAVP coat proteins and ubiquitin by immunofluorescence as reported (Neumann et al., 2007), by using antibodies against ubiquitin and phage coat proteins (Figure 3.7). Confocal microscopic analyses showed strong co-localization of ubiquitin and AAVP coat proteins in cells treated with combination of vector and genistein (Figure 3.7). These data prove that the combination treatment results in accumulation of polyubiquitinated AAVP particles compared to the

treatment with the targeted vector alone, indicating that genistein can increase the transduction efficiency by inhibiting proteasome-mediated degradation of AAVP particles.

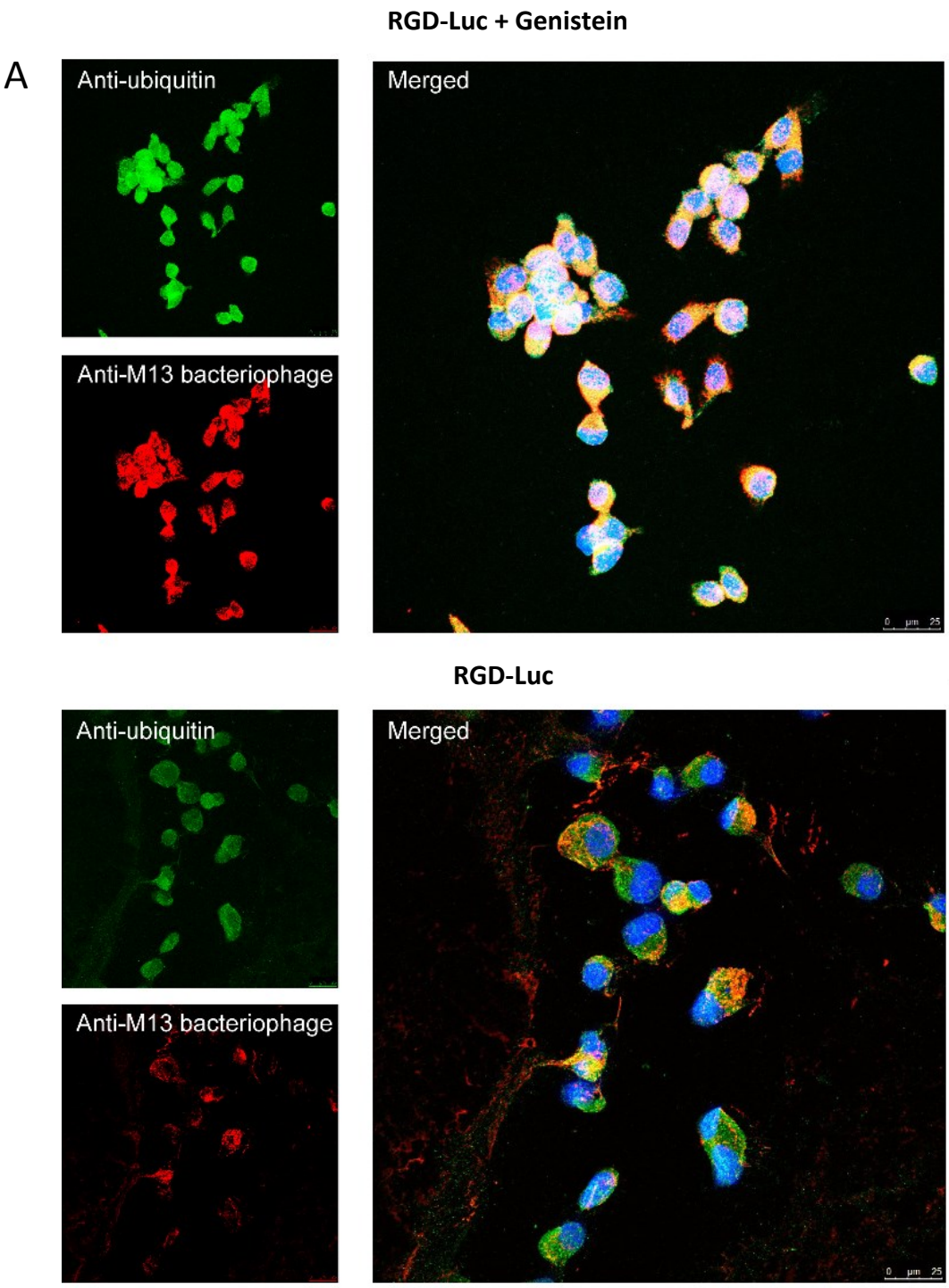

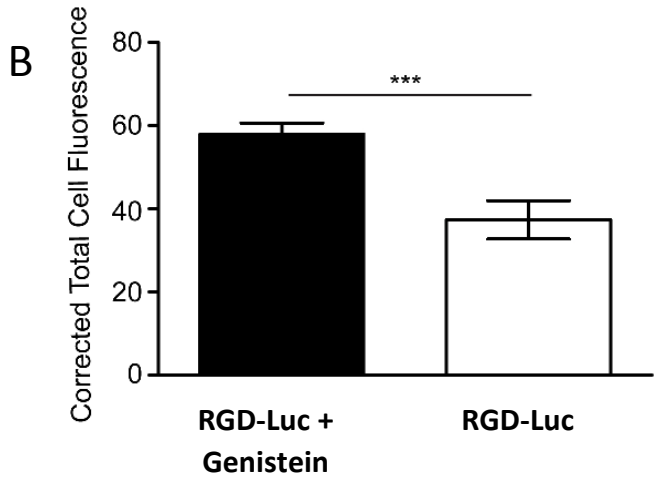

Figure 3.7 Ubiquitination of RGD-Luc AAVP particle increased upon treatment with genistein. (A) 9L cells were transduced by targeted phage (RGD-Luc) in serum-free medium with or without pretreatment with genistein. 6 hours post-transduction, RGD-Luc was detected using rabbit anti-M13-phage primary antibody and goat anti-rabbit AlexaFluor-647 secondary antibody (shown in red) and ubiquitin was stained using mouse anti-ubiquitin primary and AlexaFluor-488 secondary antibody (shown in green). Samples were analysed by confocal microscopy and representative sections are shown. Scale bar=25 μM

(B) Corrective total cell fluorescence analysis of ubiquitination in single optical sections using ImageJ. Data represent the mean ± standard error of the mean (s.e.m.) of five independent optical sections. P values were generated by Student's t-test. P values were considered significant when <0.05 and denoted as follows: n.s.-not significant, *p<0.05, **p<0.01, ***p<0.001.

3.7 Genistein enhances nuclear localisation of the RGD4C-AAVP vector genome.

Finally, we examined vector's genome accumulation in the nucleus to check whether enhanced resistance of vector to proteasome degradation would result in enhanced nuclear localisation of vector's genome. Genistein was reported for its ability to induce G2/M cell cycle arrest (Cui et al., 2014, Han et al., 2013, Ouyang et al., 2009), which results in pronounced opening of the nuclear pores allowing better nuclear transport of vector's genome. Thus, we evaluated the nuclear accumulation of the AAV2 transgene cassette of AAVP, since gene expression by RGD4C-AAVP is mediated through its AAV2 transgene cassette. 9L cells were transduced with RGD-Luc or fd-Luc non-targeted vector with or without 2 hours pretreatment with genistein (150µM), and harvested at day 4 post transduction. Next, the nuclei were extracted from the cells, followed by PCR using primers reading within the AAV2 ITR domain, as previously described (Aurnhammer et al., 2012), in order to semi-quantify the amount of vector genome in the nucleus (Figure 3.8). The data revealed a PCR product at the expected size, and electrophoresis gel analysis showed increased intensity of the ITR-derived PCR product when RGD4C-AAVP vector was used in combination with genistein (Figure 3.8). Then product quantification of the band intensities using ImageJ software confirmed that combination of genistein

with the targeted vector results in significant increase of vector DNA in the nucleus (Figure 3.8B).

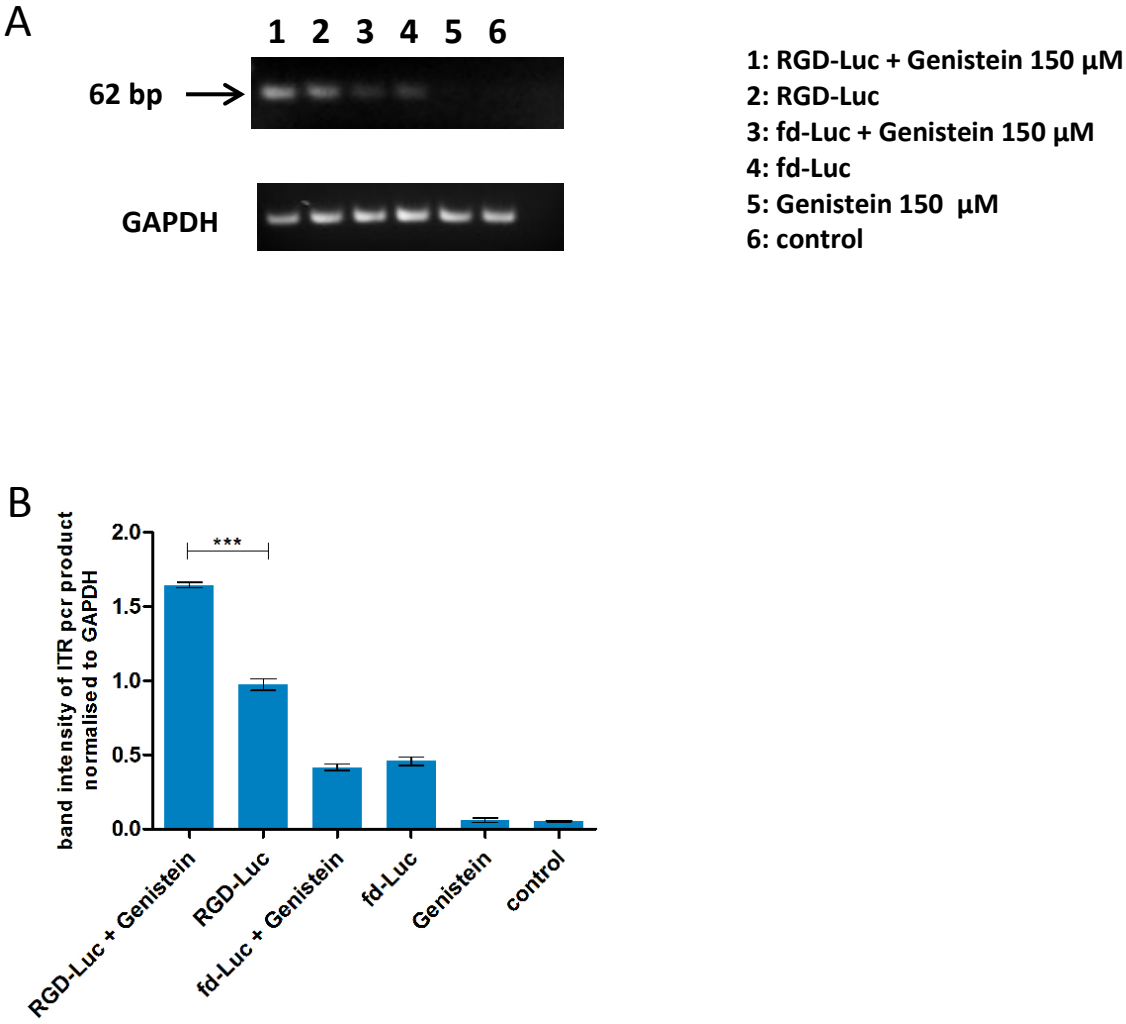

Figure 3.8 Mechanism of genistein. (A) 9L cells were plated on 48-well plates (70-80% confluent) and transduced with RGD-Luc targeted or fd-Luc control non-targeted vectors in serum free medium for 4 hours with or without 2 hours pretreatment with genistein (150µM). On day 4 after transduction, cells were harvested and nuclei were extracted. Subsequently, DNA was extracted and used as template (10 ng of DNA) for PCR on the ITR domain of the vector in order to semi-quantify the amount of vector in the nucleus with or without pretreatment with genistein. The same amount of DNA (10 ng) was used as template for PCR in the *GAPDH* gene. **(B)** The band intensity of the ITR pcr product was quantified using ImageJ software and normalised to GAPDH. PCR of the ITR domain was repeated three times and shown is the mean ± standard error of the mean (s.e.m.) of triplicate samples. P values were generated by one-way ANOVA and tukey's post hoc tests. P values were considered significant when <0.05 and denoted as follows: *p<0.05, **p<0.01, ***p<0.001.

3.8 Evaluation of efficacy of genistein and RGD4C-AAVP combination in a three-dimensional (3D) multicellular tumor spheroid

After showing that genistein dramatically increases the RGD4C-AAVP mediated targeted gene therapy in tumor cells *in vitro*, we set up to assess the efficacy of this combination in a 3D tumor spheroids that simulate the 3D tumors more accurately. The 3D tumor spheroids are considered valid models to recapitulate features of solid tumors *and* were used in this study to evaluate and confirm the efficacy of gene therapy by the targeted RGD4C-AAVP gene therapy in combination with genistein. Since the increased tumor cell killing *in vitro* of the combination genistein and RGD4C-AAVP was associated with the enhancing effect of genistein on RGD4C-AAVP-mediated gene transfer, we first assessed efficacy of gene transfer using phage carrying the *GFP* reporter gene to allow microscopic imaging of GFP expression within the 3D model of 9L and M21 tumor spheroids (Figure 3.9). The 9L and M21 tumor spheroids were transduced with RGD4C-AAVP GFP or control non-targeted fd-GFP non-targeted vector with or without pretreatment with genistein (150µM). GFP expression was monitored with fluorescent microscopy over a period of 20 days to allow detectable gene expression by the RGD4C-AAVP in the spheroids. While the targeted RGD4C-AAVP showed minimal GFP expression in the spheroids at day 10 post-transduction, combination treatment (RGD-GFP + Genistein) yielded

dramatic increase in GFP expression compared to RGD-GFP treatment alone in both 9L and M21 spheroids (Figure 3.9).

Next, application of *HSVtk*/GCV suicide gene therapy on rat 9L and human M21 tumors *in vitro* resulted in pronounced regression of the 9L and M21 spheroid volumes by combination of genistein with the targeted RGD4C-AAVP HSVtk upon GCV treatment, compared to individual treatments with RGD4C-AAVP HSVtk or genistein alone (Figure 3.10, 3.11)**.** Subsequently, in 9L spheroids measurement of cell viability showed that the combination of genistein plus RGD4C-AAVP achieved higher tumor cell killing ~93%, than the targeted RGD4C-AAVP alone or genistein alone that induced ~81% and ~33% cancer cell killing, respectively (Figure 3.10). In M21 spheroids measurement of cell viability showed that the combination of genistein plus RGD4C-AAVP achieved higher tumor cell killing ~65%, than the targeted RGD4C-AAVP alone or genistein alone that induced ~33% and ~24% cancer cell killing, respectively (Figure 3.11). These findings clearly establish that combination of genistein with RGD4C-AAVP-mediated gene therapy greatly increases its potential as a gene therapy vector.

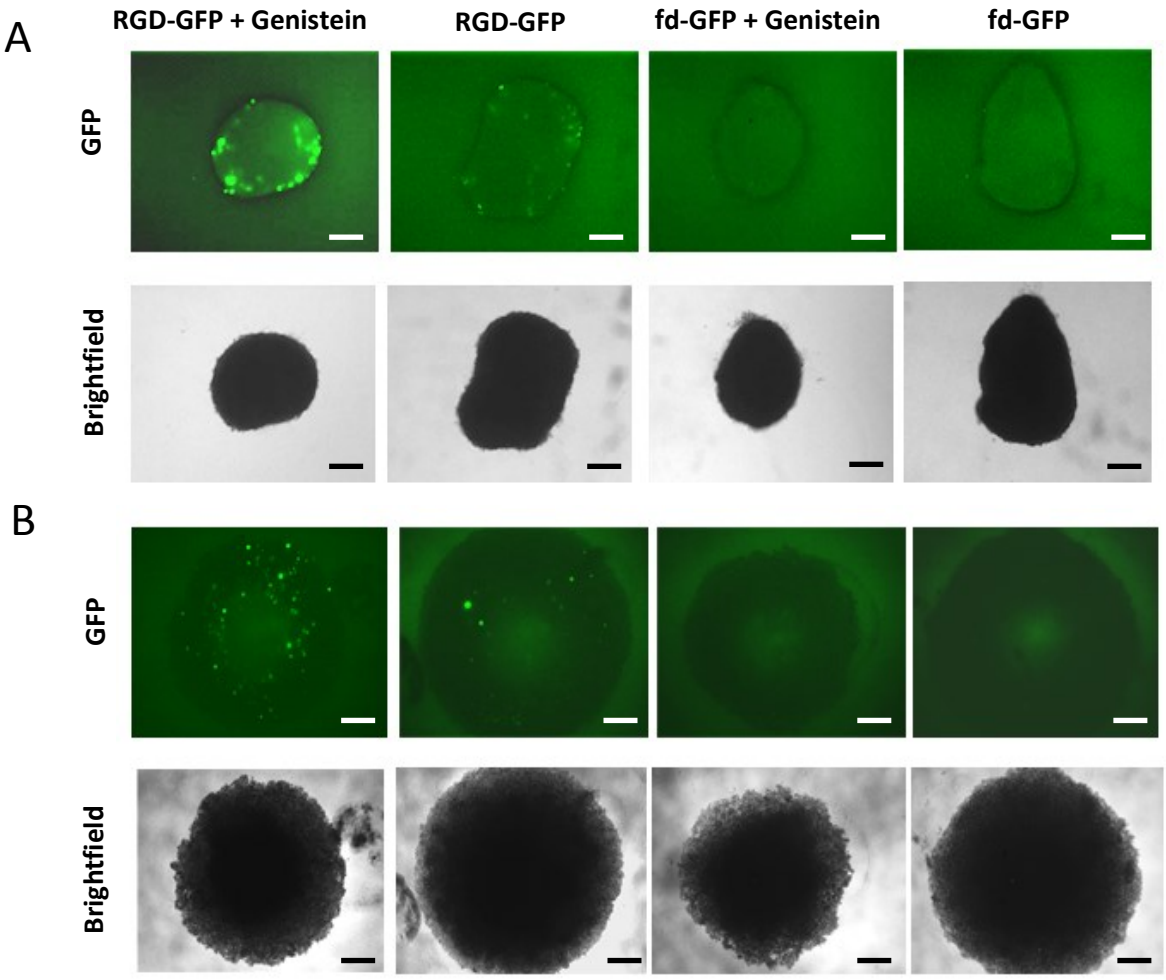

Figure 3.9 Genistein increased the transduction efficiency in 9L and M21 spheroids. 9L **(A)** and M21 **(B)** cells (5 x 10^3) were seeded into a 96-well ultra-low attachment surface plate in 200µL complete medium. After 48 hours of incubation, a spheroid was formed in each well. Spheroids were then transduced with RGD-GFP targeted vector or fd-GFP control non-targeted vector with or without pretreatment with genistein (150µM). GFP expression was evaluated with fluorescent microscopy at day 10 post-transduction. Scale bar= 0.5 mm

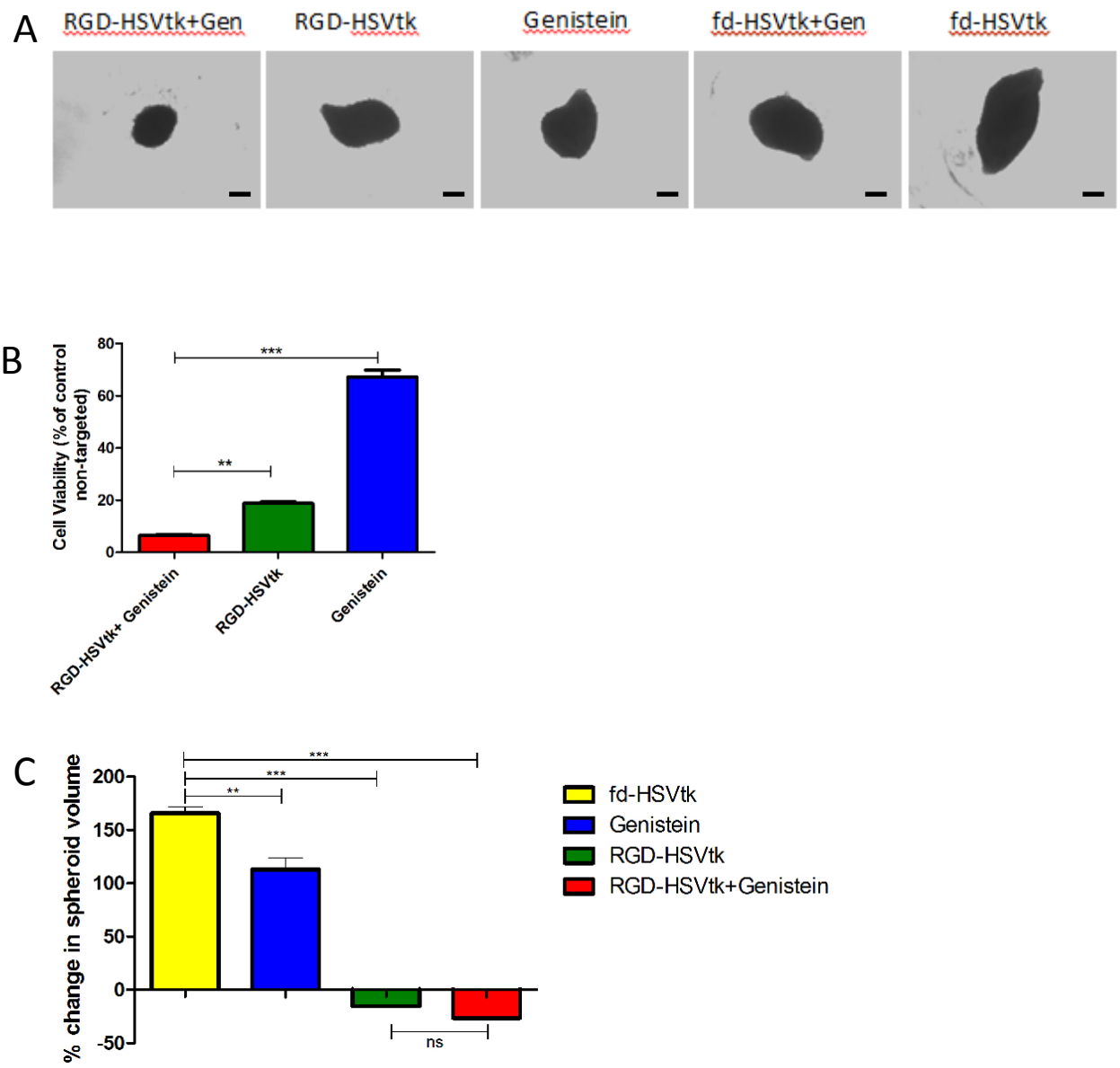

Figure 3.10 Genistein increased the cell death after transduction with RGD-HSVtk (+GCV) in 9L spheroids.

(A) Brightfield images showing the size of 9L tumor spheroids following transduction with RGD-HSVtk targeted phage or fd-HSVtk non-targeted phage with or without pretreatment with genistein (150µM). GCV was added to the spheroids at day 5 post vector transduction and renewed every 2 days. Images were taken at day 5 post GCV treatment. Scale bar= 0.5 mm

(B) Evaluation of cell viability in 9L spheroids at day 5 post GCV treatment by using the CellTiter-Glo cell viability assay.

(C) Measurement of 9L spheroid volumes at days 0 and 5 post GCV treatment. The graph shows the % change of the average spheroid volumes. Data represent the mean ± standard error of the mean (s.e.m.) of triplicate samples. P values were generated by one-way ANOVA and tukey's post hoc tests. P values were considered significant when <0.05 and denoted as follows: n.s.-not significant, *p<0.05, **p<0.01, ***p<0.001.

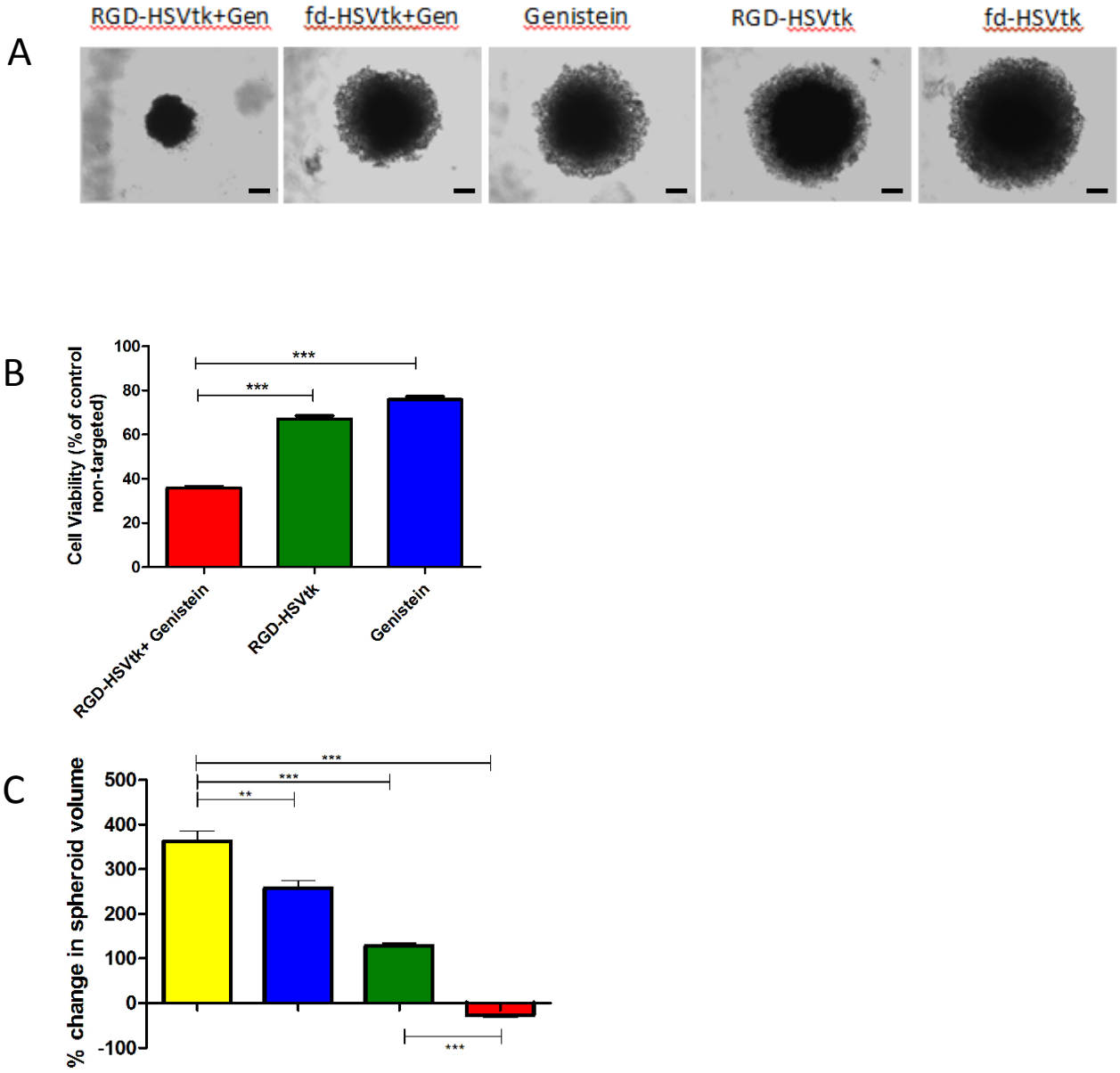

Figure 3.11 Genistein increased the cell death after transduction with RGD-HSVtk (+GCV) in M21 spheroids.

(A) Brightfield images showing the size of M21 tumor spheroids following transduction with RGD-HSVtk targeted phage or fd-HSVtk non-targeted phage with or without pretreatment with genistein (150µM). GCV was added to the spheroids at day 5 post vector transduction and renewed every 2 days. Images were taken at day 7 post GCV treatment. Scale bar= 0.5 mm

(B) Evaluation of cell viability in M21 spheroids at day 7 post GCV treatment by using the CellTiter-Glo cell viability assay.

(C) Measurement of M21 spheroid volumes at days 0 and 7 post GCV treatment. The graph shows the % change of the average spheroid volumes. Data represent the mean ± standard error of the mean (s.e.m.) of triplicate samples. P values were generated by one-way ANOVA and tukey's post hoc tests. P values were considered significant when <0.05 and denoted as follows: n.s.-not significant, *p<0.05, **p<0.01, ***p<0.001.

3.9 Discussion

We have demonstrated that genistein pretreatment of tumor cells from different histopathological types and species resulted in enhanced targeted tumor cell killing by RGD4C-AAVP-mediated HSVtk and GCV suicide gene therapy in 2D tissue culture and 3D tumor spheroid settings. Then, we found that treatment with genistein of 9L and M21 cancer cells increased GFP and Luc reporter gene expression, which demonstrates that the enhanced tumor cell killing of RGD4C-AAVP by genistein is probably associated with increased HSVtk gene expression. Moreover, we have investigated the mechanisms linked with this increased reporter gene expression and tumor cell killing. Importantly gene transfer by RGD4C-AAVP remains targeted in the presence of genistein, indicating that the tumor specificity of RGD4C-AAVP is not affected by genistein. We also found that genistein increases polyubiquitination of AAVP particles and accumulation of vector genome in the nucleus. These data suggest that genistein may bestow an advantage in gene expression from RGD4C-AAVP by means of increased vector accumulation in the nucleus and vector protection from proteasome degradation, or perhaps a combination of these two non-mutually exclusive mechanisms.

Our findings of increased RGD4C-AAVP-mediated cancer gene therapy are in agreement with a previous report showing enhanced cancer cell killing by a

mutant oncolytic adenovirus in combination with genistein (Adam et al., 2012). The observed difference in cell viability between 9L and M21 cell lines can be attributed partially to the fact that 9L cells can get transduced more easily compared to M21 cells and also to the bystander effect of the HSVtk/GCV in 9L cells (Trepel et al., 2009). The enhanced RGD4C-AAVP-mediated GFP and Luc gene expression by genistein is also consistent with previous reports that genistein increased AAV2-mediated gene transfer in the human HeLa cervical carcinoma cells (Mah et al., 1998). Moreover, the authors reported that genistein enhanced accumulation of the dephosphorylated form of single-stranded D-sequence-binding protein (ssD-BP), which facilitates the conversion of single to double stranded DNA resulting in improved AAV gene expression (Mah et al., 1998). Importantly, our findings that genistein increased AAV2 PCR product in the nuclear fraction of cells treated with RGD4C-AAVP are consistent with that study, as gene expression by RGD4C-AAVP is mediated by the AAV2 transgene cassette, incorporated within the phage genome. The increased nuclear accumulation of AAVP genome, upon genistein pre-treatment, provides an additional mechanism that could further explain the improved AAVP-mediated gene expression by genistein. One explanation is that pretreatment with genistein enhances the size of the nuclear pores, as genistein was reported to induce G2/M cell cycle arrest, during which nuclear

localisation of gene therapy vectors can be enhanced(Cui et al., 2014, Han et al., 2013, Ouyang et al., 2009).

Moreover, resistance to proteasome degradation upon genistein pretreatment should result in better intracellular persistence and availability of the RGD4C-AAVP particles to be transported to the nucleus. These data also suggest that genistein increases the RGD4C-AAVP-targeted gene expression, at least in part, through inhibition of proteasome-mediated degradation of the RGD4C-AAVP particles. Indeed, genistein was reported to inhibit the chymotrypsin-like activity of proteasome in purified 20S proteasome and 26S proteasome (Kazi et al., 2003). Taking into account that genistein doesn't affect vector attachment on the surface of cancer cells nor its internalisation, our data indicate that genistein affects the intracellular fate of AAVP.

It is important to note that other mechanisms of action of genistein might also account for its enhancing effect on transduction efficiency of RGD4C-AAVP. For instance, genistein was reported to modulate the lysosomal metabolism (Moskot et al., 2014). Given that the endosomal-lysosomal pathway has been identified as an intracellular barrier to efficient transduction by RGD4C-AAVP (Stoneham et al., 2012), lysosomal alteration by genistein might facilitate RGD4C-AAVP escape from the lysosomes and subsequently higher nuclear accumulation of AAVP genome and enhanced gene expression. One possible

way to investigate this is to perform immunofluorescence experiments to investigate RGD4C-AAVP trafficking to the endosomal-lysosomal degradative pathway. RGD4C-AAVP can be labeled with anti-fd-phage antibody, early endosomes with anti-EEA-1 while late endosomes/lysosomes with anti-LAMP-1 antibody. Confocal microscopic analysis can show if there is less phage accumulation in the early or late endosomes over time in cells treated with genistein/RGD4C-AAVP compared to cells treated with RGD4C-AAVP vector only (Stoneham et al., 2012).

In conclusion, despite their advantageous natural characteristics, bacteriophage viruses are still considered poor vectors for gene delivery due to their low gene transfer efficiency compared to eukaryotic vectors. The AAVP vector was reported as an improved version of phage-based gene therapy vectors to achieve enhanced gene delivery compared to conventional phage-derived vectors. Although promising, AAVP still has limitations inherent to bacteriophage. In this study we have shown that combining targeted RGD4C-AAVP with genistein significantly improves AVVP-guided gene transfer efficacy and consequently its cancer cell killing as a gene therapy vector. In addition, we elucidated possible mechanisms of increased AAVP-mediated gene expression by genistein. The next preclinical step will be taken to assess efficacy of this combination treatment in tumor-bearing mice. Given that

genistein and AAVP have been demonstrated to cross the blood-brain barrier (Malinowska et al., 2010, Staquicini et al., 2011) this combination treatment has potential applications for brain tumors. Our study indicates that combination of RGD4C-AAVP and genistein, is a promising strategy that can be considered for future clinical applications of targeted systemic gene therapy with RGD4C-AAVP in cancer patients.

Chapter 4

Dual attack of cancer using synergistic combination of phage-guided gene therapy and doxorubicin

4.1 Introduction

First, we had to determine the concentration of doxorubicin that gives the optimal transduction efficiency by RGD4C-AAVP in 9L and M21 cells. We found that the optimal doxorubicin concentration is 0.5 μM for 9L and 0.6 μM for M21 cells. Then, we investigated if these concentrations are toxic, therefore we performed MTT assay in 9L and M21 cancer cell lines. We found that these concentrations are not toxic so we used them for further experiments. The next step was to investigate our hypothesis in 9L and M21 cell lines (2D model) using RGD4C-AAVP carrying reporter genes (*GFP*, firefly *luciferase* reporter genes) or RGD4C-AAVP carrying the *HSVtk* gene which kills cells in the presence of ganciclovir. The same experiments were carried out in 3D 9L and M21 tumor spheroid models. Finally, we investigated potential mechanisms that doxorubicin increased RGD4C-AAVP mediated transduction efficiency.

4.2 Determination of doxorubicin concentration that results in optimal RGD4C-AAVP transduction efficiency in 9L and M21 cells

First, we had to determine the concentration of doxorubicin that gives the optimal transduction efficiency by RGD4C-AAVP in 9L and M21 cells. 9L and M21 cells were transduced with the targeted vector carrying the firefly *luciferase* reporter gene (RGD-Luc) in combination with increasing concentrations of doxorubicin ranging from 0.5 to 8 μM for 24 hours. On day 3 after transduction, luciferase assay was performed. The results were normalised to the amount of protein and presented as RLU (Relative Luminescence Units)/100 μg protein (Figure 4.1). We found that the optimal doxorubicin concentration is 0.5 μM for 9L and 0.6 μM for M21 cells.

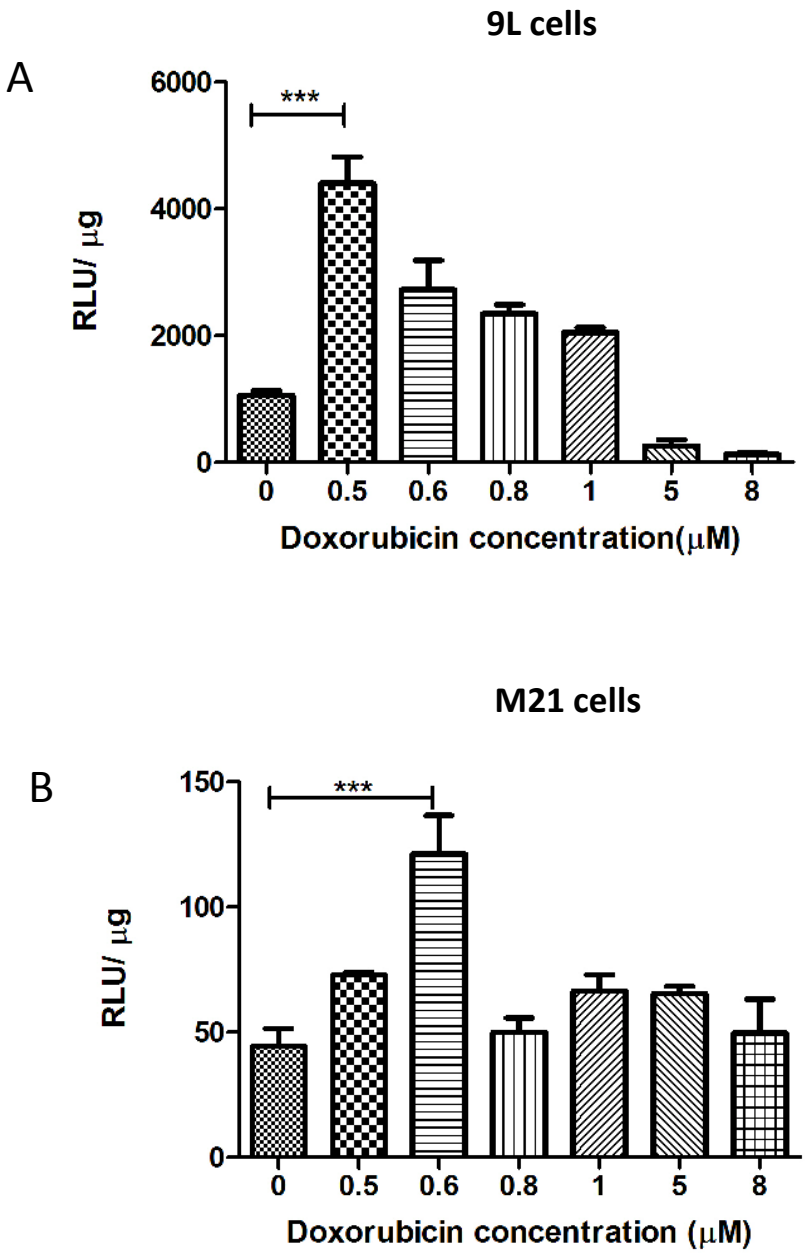

Figure 4.1 Determination of optimal doxorubicin dose in 9L and M21 cells using luciferase assay. 9L **(A)** and M21 **(B)** cells were transduced with RGD-Luc targeted vector in combination with increasing concentrations of doxorubicin ranging from 0.5 to 8 µM for 24 hours. On day 3 after transduction, luciferase assay was performed. The results were normalised to the amount of protein and presented as RLU (Relative Luminescence Units)/ µg of protein. Data represent the mean ± standard error of the mean (s.e.m.) of triplicate samples. P values were generated by one-way ANOVA and tukey's post hoc tests. P values were considered significant when <0.05 and denoted as follows: n.s.-not significant, *p<0.05, **p<0.01, ***p<0.001.

4.3 Cytotoxicity of doxorubicin on 9L and M21 cells

Then we sought to assess the cytotoxicity of doxorubicin *in vitro* on 9L and M21 cancer cell lines. Tumor cells were treated with increasing concentrations of doxorubicin ranging from 0.5 µM to 8 µM for 24 hours and compared to non-treated cells. Subsequently, cell survival was assessed at 48 hours post drug treatment. The data show that tumor cell death raised as the concentration of the drug increased (Figure 4.2) for both 9L and M21 cancer cells with a more pronounced effect on the 9L glioblastoma cells than M21 melanoma cells. Cytotoxic doses expressed as IC_{50} values, corresponding to inhibitory concentration required to induce the cell death by 50%, are shown by the lines on the graphs to approximate the IC_{50} value (Figure 4.2). We found that 50% of cell death in the presence of doxorubicin was induced by ~ 1µM in 9L cells (Figure 4.2A), while in M21 cells, 50% of cell death was achieved at a dose of over 4.5 µM (Figure 4.2B). Next, to assess the effect on tumor cell killing by RGD4C-AAVP, we selected doxorubicin concentration of 0.5 µM for 9L and 0.6 µM for M21 cancer cells, as these doses are below the IC_{50} and cause little toxicity.

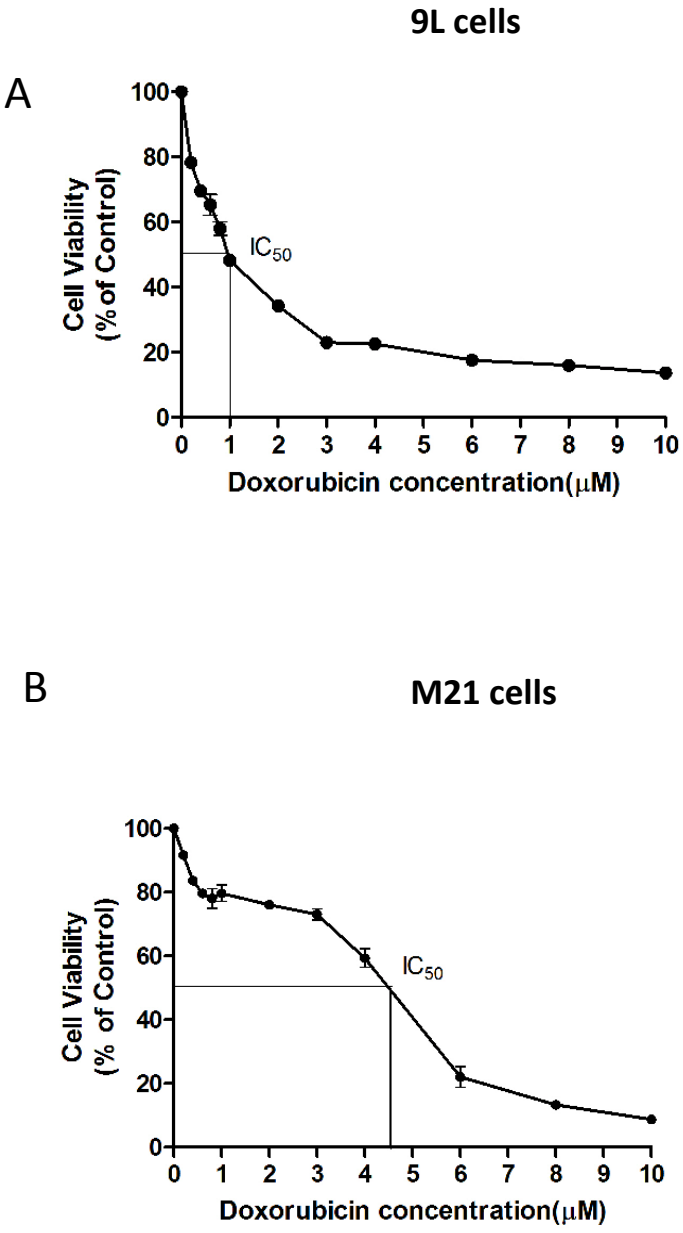

Figure 4.2 Cytotoxicity of doxorubicin on 9L and M21 cells. 9L **(A)** and M21 **(B)** cells were cultured in 96-well plates, then treated with increasing concentrations of doxorubicin ranging from 0.5 to 8 µM for 24 hours. Subsequently, cells were grown for further 48 hours without the drug. Cell survival was determined by using the MTT assay and expressed as percentage of cells counted in parallel cultures without drug. The assay was repeated twice in triplicate and the results shown are representative of one experiment. Data represent the mean ± standard error of the mean (s.e.m.) of triplicate samples from one representative experiment.

4.4 Doxorubicin drug treatment boosts cancer cell death by phage-mediated suicide gene killing

To test tumor cell killing efficacy, we used the RGD4C-*HSVtk* vectors encoding the gene for the Herpes simplex virus type I thymidine kinase (*HSVtk*) mutant SR39 (Black et al., 2001) which kills cells in the presence of ganciclovir, GCV . Thus, 9L and M21 cells were transduced with RGD-HSVtk or control non-targeted vector fd-HSVtk (without RGD) carrying the *HSVtk* gene in the presence or absence of doxorubicin. The cells were then treated with GCV (20 μM) at day 3 post vector transduction. Cancer cell killing was quantified at 0, 24, 48, 72, 96 hours post GCV treatment. Results were normalized to non-targeted vector which didn't show any tumor cell death (data not shown). In both cancer cell lines, the combination treatment with doxorubicin and RGD-HSVtk therapy resulted in greater cell killing compared to cells treated with RGD-HSVtk or doxorubicin drug alone (Figure 4.3). For instance, at 92 hours post GCV treatment, combination treatment induced 99.7% and 96.4% killing of 9L and M21 cancer cells, respectively (Figure 4.3), compared to 87% and 58.3% death induced by vector alone in 9L and M21 cells, respectively, and 82.4 % death and 90.9% death induced by doxorubicin alone in 9L and M21 cells, respectively. These data show that drug treatment of cancer cells with

doxorubicin is a promising approach to enhance targeted gene therapy by RGD4C-AAVP.

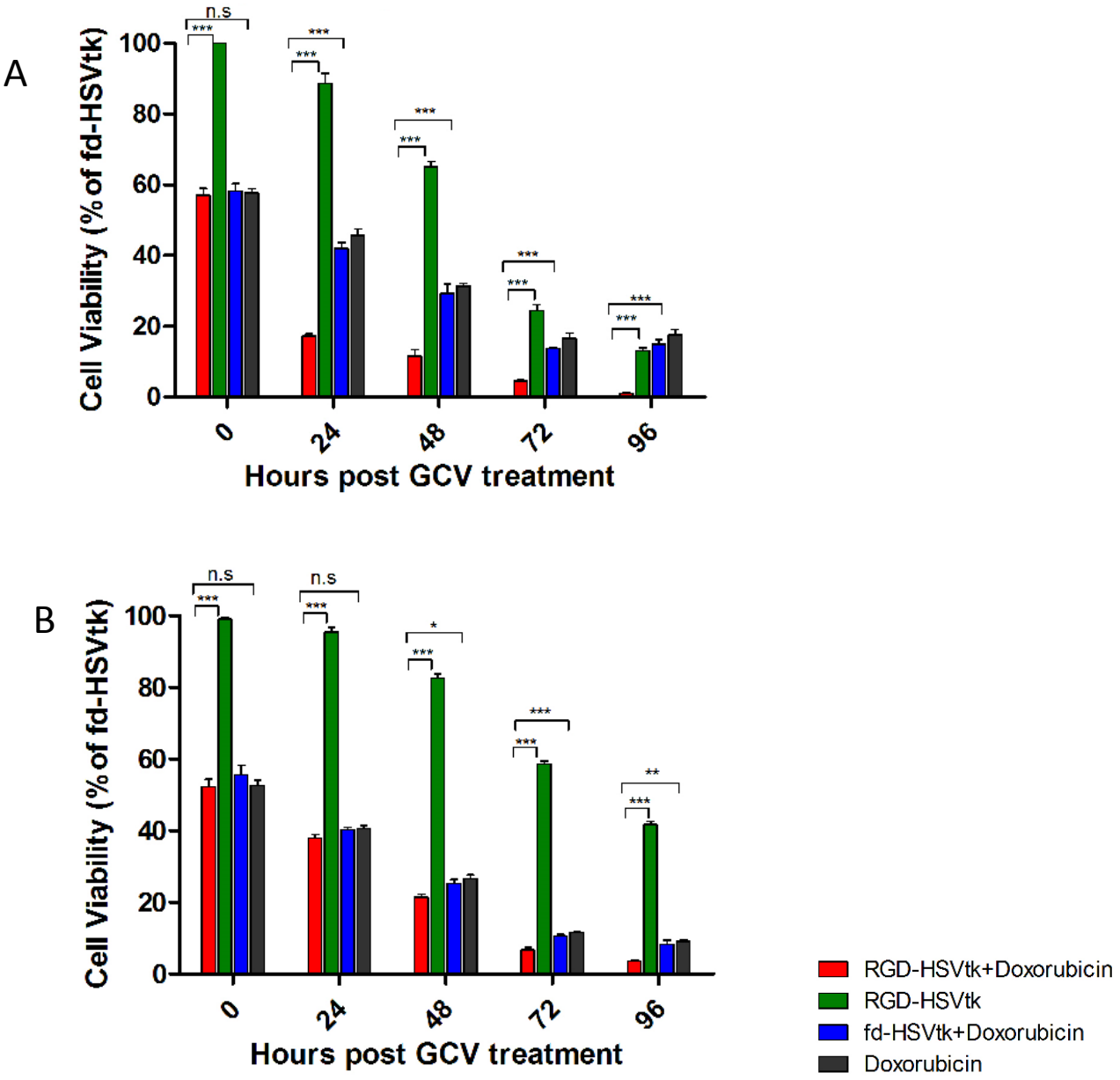

Figure 4.3 Doxorubicin increased cancer cell death after transduction of 9L and M21 cells with RGD-HSVtk (+GCV). 9L **(A)** and M21 cells **(B)** grown in 48 well-plates (60-80% confluent) were transduced with RGD-HSVtk targeted vector or control non-targeted vector in the presence or absence of doxorubicin. The cells were treated with GCV (20 µM) at day 3 post vector transduction and renewed daily. Cancer cell killing was quantified at 0, 24, 48, 72, 96 hours post GCV treatment. Cells were counted by using the trypan blue exclusion methodology. Results were normalized to non-targeted vector. The experiment was repeated twice in triplicates and the results shown are representative of one experiment. Data represent the mean ± standard error of the mean (s.e.m.) of triplicate samples. P values were generated by one-way ANOVA and tukey's post hoc tests. P values were considered significant when <0.05 and denoted as follows: n.s.-not significant, *p<0.05, **p<0.01, ***p<0.001.

4.5 Doxorubicin increases targeted reporter gene transfer by the RGD4C-AAVP in 9L and M21 cancer cells *in vitro*

To gain insight into the improved tumor cell killing by RGD4C-HSVtk following combination with doxorubicin, we investigated the effect of doxorubicin on gene delivery by RGD4C-AAVP. We first conducted qualitative analysis of transgene expression by using vectors carrying the reporter gene of the *green fluorescent protein* (*GFP*) and combined with doxorubicin (Figure 4.4). Fluorescent microscopic analysis of GFP expression at day 4 post vector transduction showed that in both cell lines the combination treatment of RGD-GFP and doxorubicin, resulted in significantly higher GFP expression, compared to RGD-GFP vector alone in both 9L and M21 tumor cells (Figure 4.4). Next, to confirm the increased gene delivery by RGD4C-AAVP in combination with doxorubicin, we carried out a quantitative analysis of transgene expression over a time course of 4 days post vector transduction by using RGD4C-*Luc* vectors expressing the firefly *Luc* reporter gene (Figure 4.5). Consistently with GFP reporter transgene expression experiments, we observed a significant increase in RGD4C-AAVP-mediated *Luc* expression at various time points post vector transduction by doxorubicin treatment in both 9L and M21 cancer cells compared to cells treated with vector alone. For instance, at day 4 post-transduction, quantitative analysis of *Luc* transgene expression showed that the

combination treatment (RGD-Luc + doxorubicin) resulted in ~ 5.3 fold and ~12 fold increase in luciferase expression in 9L and M21 cells, respectively, compared to RGD-Luc vector alone. Moreover, in 9L cells, initiation of the luciferase expression occurred as early as day 2 post vector transduction, in the presence of doxorubicin (Figure 4.5). Importantly, no luciferase expression was detected in cells transduced with non-targeted fd-Luc vector alone or in combination with doxorubicin, which shows that doxorubicin does not affect the specificity and targeting of the RGD4C-AAVP vector.

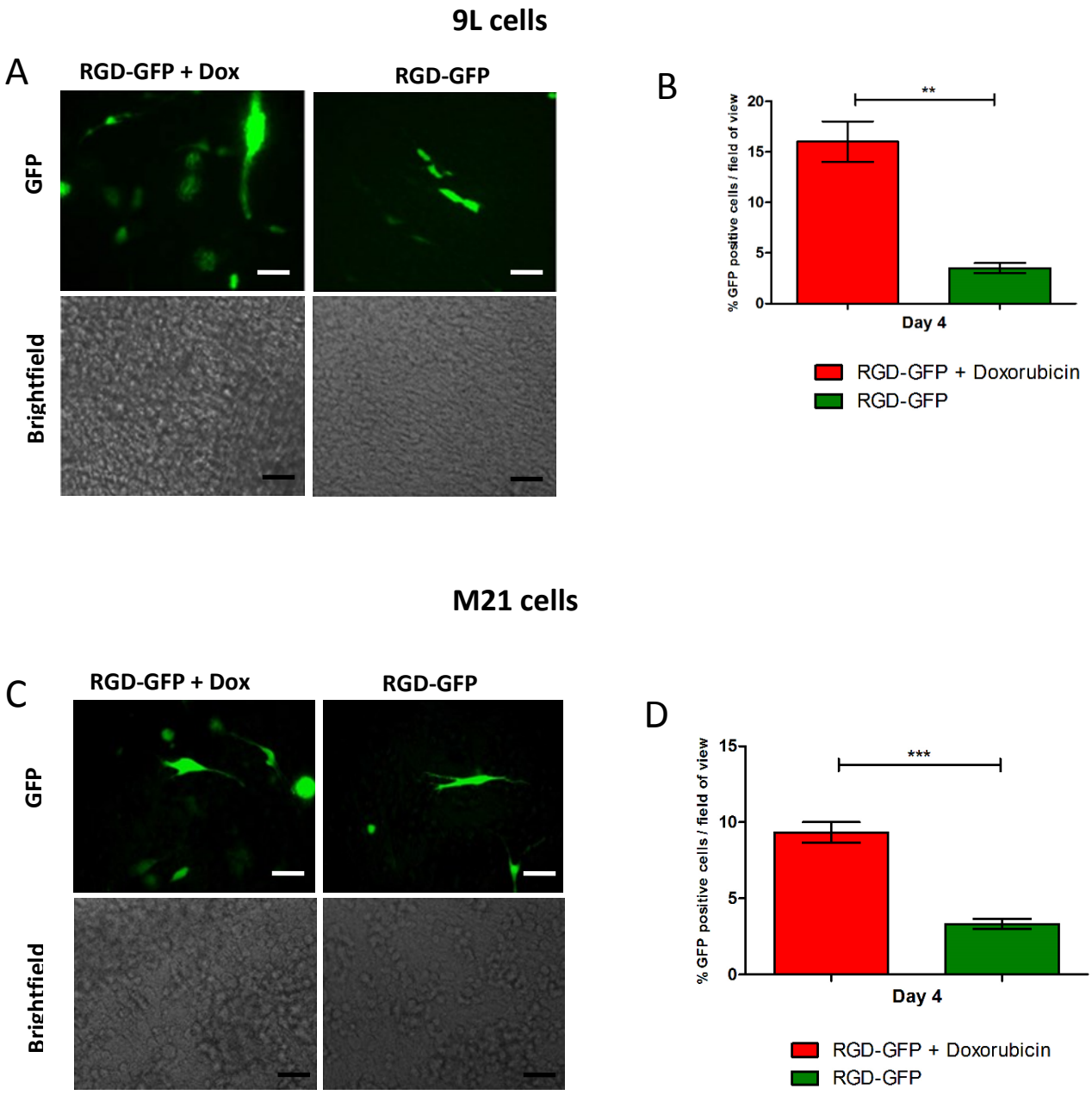

Figure 4.4 Doxorubicin increased the transduction efficiency in 9L and M21 cells. 9L **(A,B)** and M21 cells **(C,D)** were plated on 48-well plates (70-80% confluent) and transduced with RGD-GFP targeted or control non-targeted vectors in the presence or absence of doxorubicin. GFP expression was evaluated by fluorescent microscopy on day 4 post vector transduction. The experiment was repeated twice in triplicate and the results shown are representative of one experiment. Data represent the mean ± standard error of the mean (s.e.m.) of %GFP positive cells in five independent fields of view. P values were generated by Student's t-test. P values were considered significant when <0.05 and denoted as follows: *p<0.05, **p<0.01, ***p<0.001. Scale bar= 100 µM

A

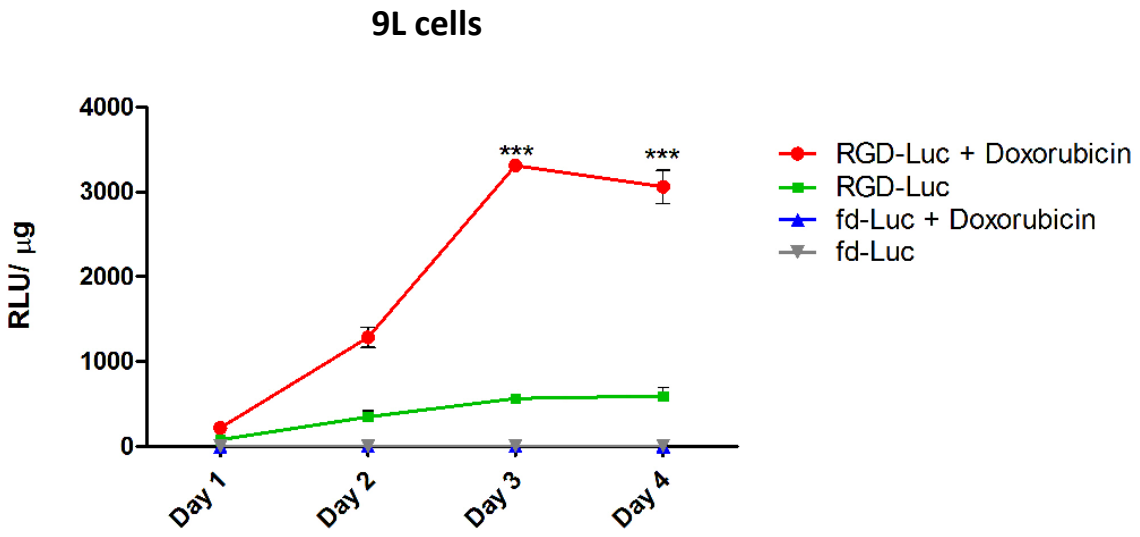

B

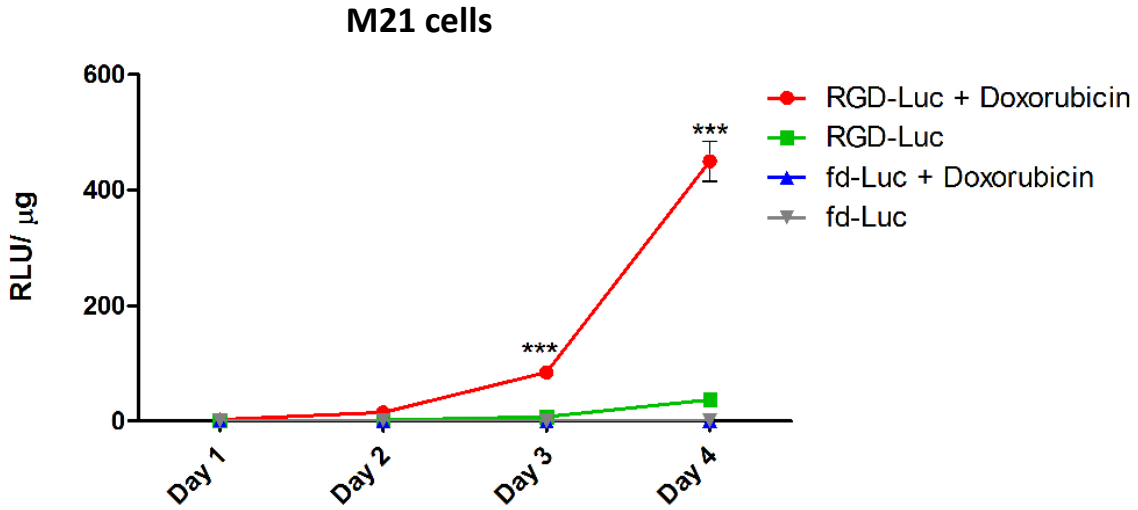

Figure 4.5 Doxorubicin increased the transduction efficiency in 9L and M21 cells. 9L **(A)** and M21 cells **(B)** were plated on 48-well plates (70-80% confluent) and transduced with RGD-Luc targeted or fd-Luc control non-targeted vectors in the presence or absence of doxorubicin. Luciferase measurement assays were performed at days 1-4 post-transduction and normalized to protein concentration as determined by the bradford assay. Results are shown as RLU (Relative Luminescence Units) per 1µg of protein and represent the average from triplicate wells. The experiment was repeated twice in triplicates and the results shown are representative of one experiment. Data represent the mean ± standard error of the mean (s.e.m.) of triplicate samples. P values were generated by one-way ANOVA and tukey's post hoc tests. P values were considered significant when <0.05 and denoted as follows: n.s.-not significant, *p<0.05, **p<0.01, ***p<0.001.

4.6 Evaluation of the effect of doxorubicin treatment on vector cellular entry

After demonstrating that the increased tumor cell killing by RGD4C-AAVP observed in combination with doxorubicin was associated with enhanced RGD4C-AAVP-mediated gene expression, we set out to gain further understanding into the mechanism of this effect. Therefore, we sought to investigate the effect of doxorubicin on steps involved in gene transfer. It is well established that vector-mediated gene delivery depends on several steps where the vector needs to access the cell surface to bind to its receptor, followed by cell internalization and intracellular trafficking, then transport to the nucleus for gene expression to occur (Nishikawa and Huang, 2001, Wiethoff and Middaugh, 2003). We first examined the effect of doxorubicin on vector attachment to the surface of cells. Hence, we quantified the free cell-unbound phage in the medium above the adherent cells by infection of host bacteria followed by colony counting (Figure 4.6). An amount of 37%, of input phage particles, was recovered from the medium of cells treated with the RGD4C-AAVP vector showing that a fraction (63% of input phage) was bound to the surface of tumor cells. However, doxorubicin treatment had no effect on RGD4C-AAVP vector attachment to the cell surface (Figure 4.6). The non-targeted vector showed no attachment tumor cell surface with 100% recovery. Finally, internalization assays revealed that combination of vector with

doxorubicin does not increase entry of the RGD4C-AAVP into cancer cells (Figure 4.7). These data prove that doxorubicin does not affect cell attachment and internalisation of the RGD4C-AAVP viral particles.

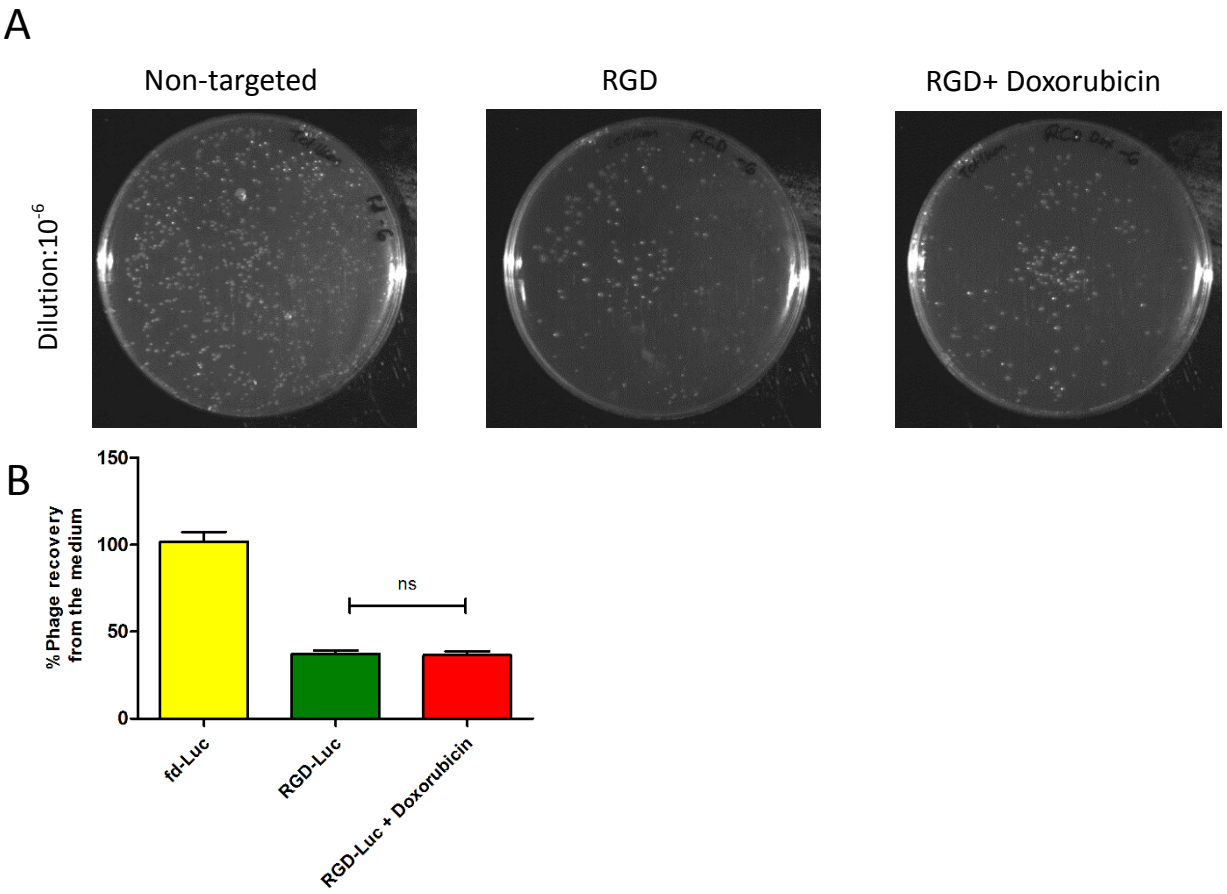

Figure 4.6 Attachment assay. Evaluation of the AAVP attachment by titrating the unbound phage in the medium of 9L cells. (**A**) Representative plates showing bacterial colonies generated by infection of K91 batceria by the phage recovered from the medium of transduced cells. **(B)** Quantitative analysis of recovered phage following bacterial colony counting. Data represent the mean ± standard error of the mean (s.e.m.) of triplicate samples. P values were generated by one-way ANOVA and tukey's post hoc tests. P values were considered significant when <0.05 and denoted as follows: n.s.-not significant, *p<0.05, **p<0.01, ***p<0.001.

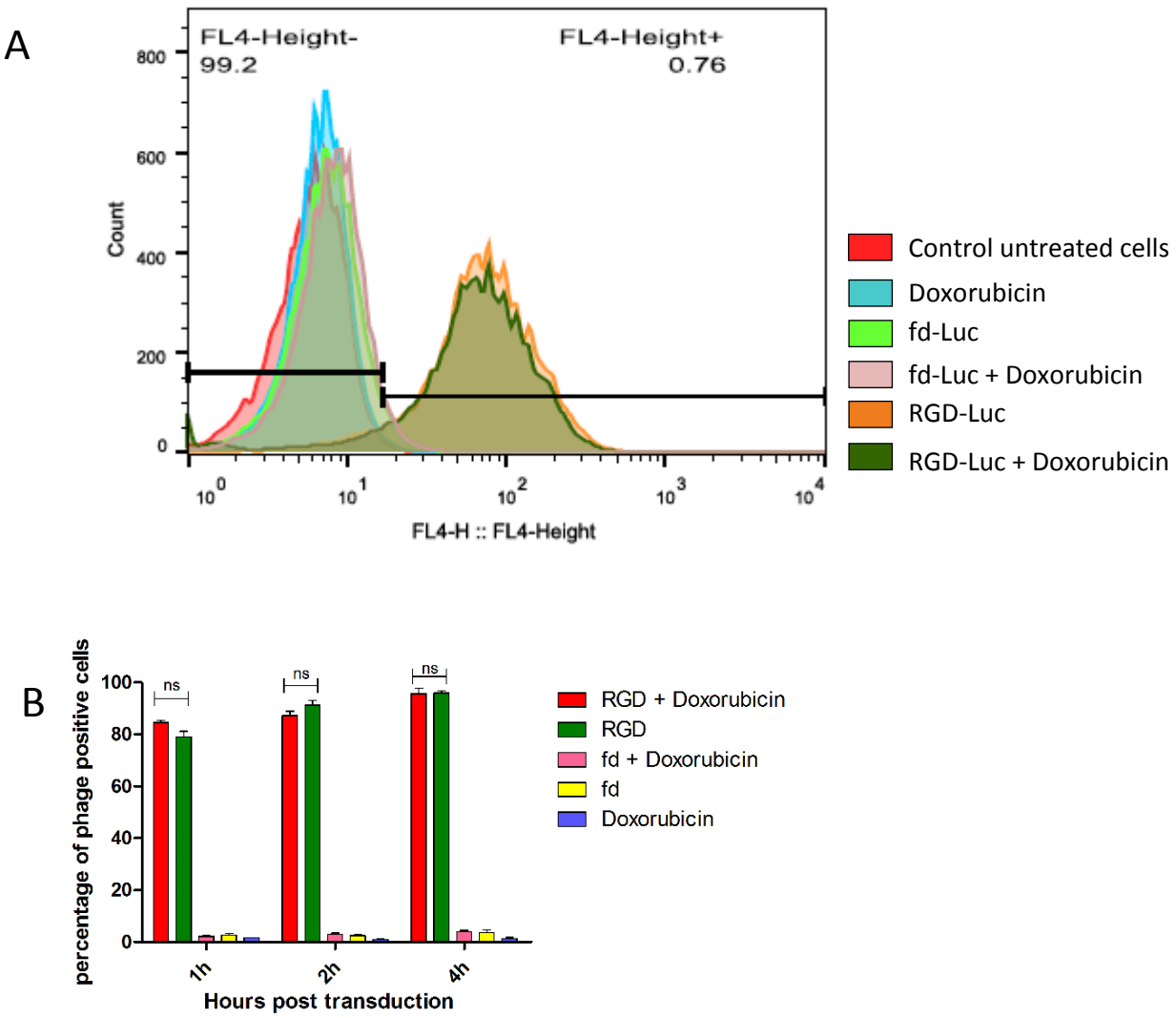

Figure 4.7 Internalization assay. Evaluation of phage internalization in the presence or absence of doxorubicin. **(A)** Graph showing FACS results after immunostaining of 9L cells treated with AAVP in the presence or absence of doxorubicin. **(B)** Graph showing the percentage of positive cells according to FACS data at three different time points (1 hour, 2 hours, 4 hours). The experiment was carried out in triplicates. Data represent the mean ± standard error of the mean (s.e.m.) of triplicate samples. P values were generated by one-way ANOVA and tukey's post hoc tests. P values were considered significant when <0.05 and denoted as follows: n.s.-not significant, *p<0.05, **p<0.01, ***p<0.001.

4.7 Evaluation of DNA damage caused by doxorubicin and activation of DNA repair mechanisms

Another possible mechanism of doxorubicin-increased transduction efficiency of AAVP vector could be that low dose of doxorubicin caused a moderate DNA damage (Tacar et al., 2013) that enabled activation of DNA repair enzymes such as PARP-1. According to our hypothesis, DNA repair enzymes can facilitate the conversion of single-stranded vector DNA to double-stranded thus increasing the transgene expression and the transduction efficiency of AAVP vector. In order to investigate our hypothesis first we performed a comet assay to assess the DNA damage caused by the low-dose of doxorubicin that increased the transduction efficiency of our vector. DNA damage was assessed by counting the number of cells that create a ‘’comet’’ as well as the length of the comet ‘’tail’’ (Figure 4.8). Our comet assay results in 9L cells indicate that the low-dose doxorubicin that increased transduction efficiency of our vector causes moderate DNA damage. Then, we performed western blot analysis in order to investigate the expression of PARP-1 repair enzyme in 9L and M21 cells after treatment with low-dose and high-dose doxorubicin (Figure 4.9). PARP-1 expression was upregulated in M21 cells treated with the low-dose doxorubicin compared to control untreated cells which indicates that the DNA repair mechanism has been activated. In 9L cells, PARP-1 expression was

slightly down-regulated after low-dose doxorubicin treatment compared to control untreated cells but still indicates that there is DNA repair. This difference between the two cell lines can be attributed to the increased sensitivity of 9L cells to doxorubicin compared to M21 cells (as was shown in MTT assay, Figure 4.2).

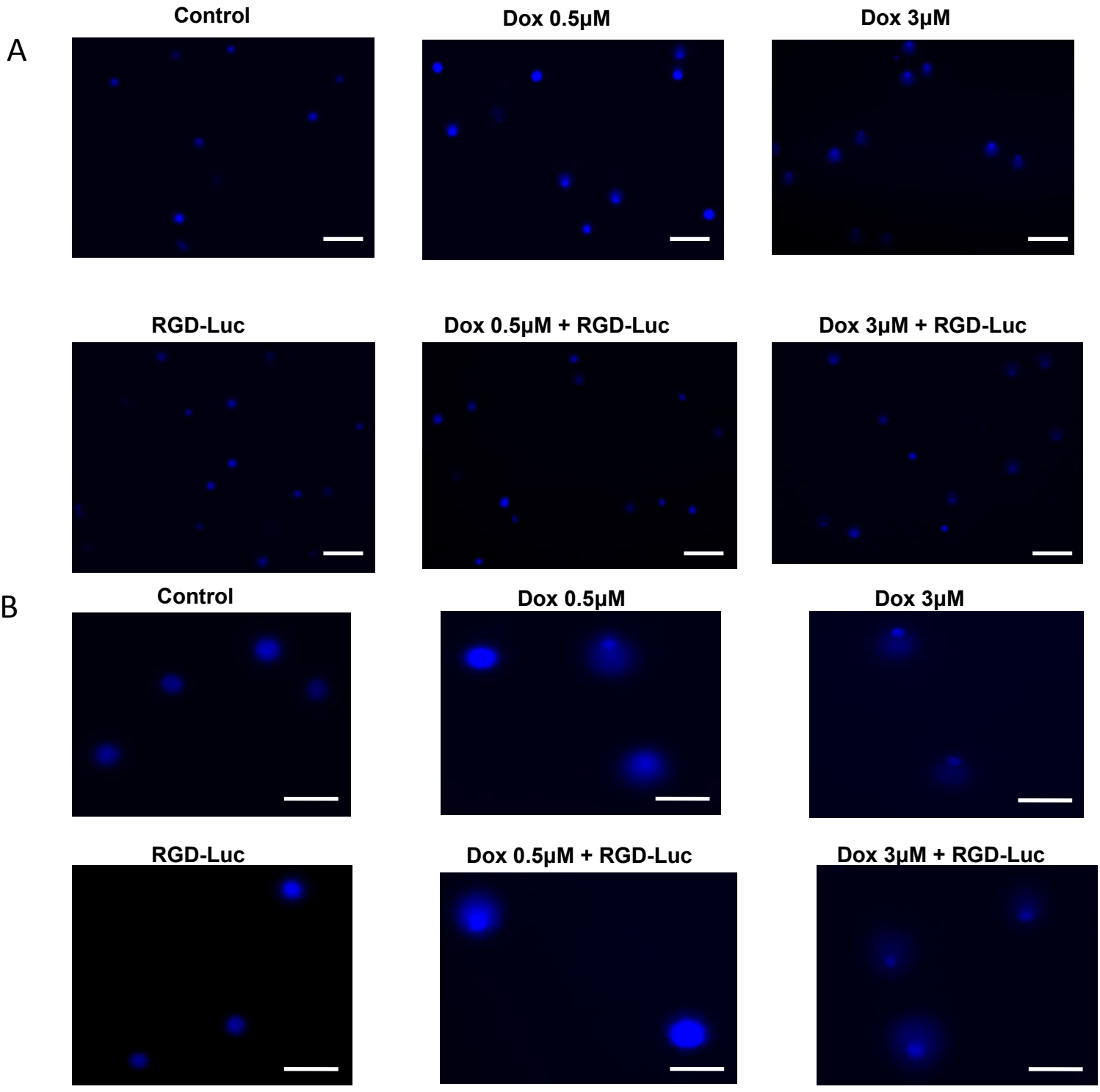

C

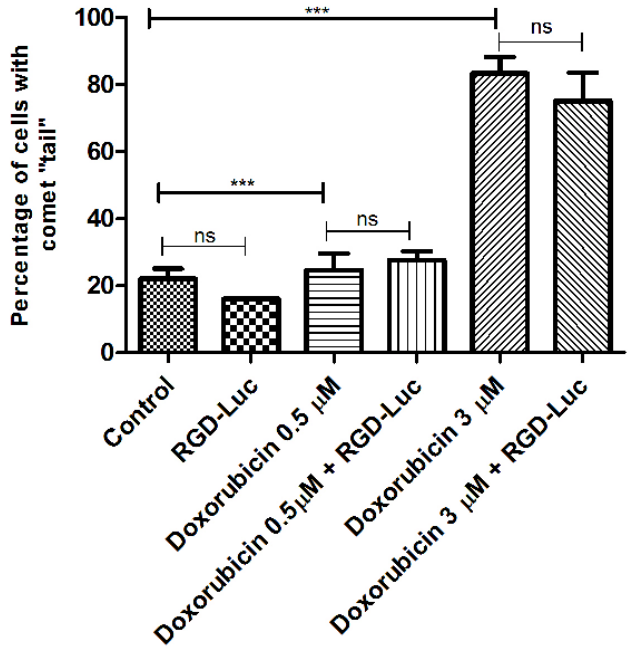

D

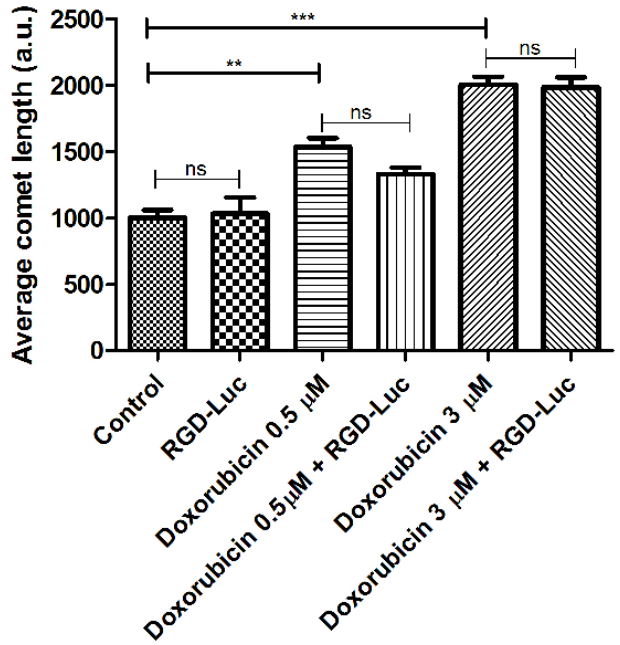

Figure 4.8 Comet assay. (A) Representatives images of 9L cells nuclei stained with DAPI taken by fluorescent microscope (10x). Scale bar=100 µM **(B)** Images of 9L cells nuclei stained with DAPI taken by fluorescent microscope (20x). Scale bar=10 µM **(C)** Graph showing the percentage of cell nuclei presenting comet ‘’tail’’. The percentage was measured in 5 representative fields for each condition and shown is the average. **(D)** Graph showing the average length of comet “tail”. The length was measured for 5 comets for each condition and shown is the average. Data represent the mean ± standard error of the mean (s.e.m.) of triplicate samples. P values were generated by one-way ANOVA and tukey’s post hoc tests. P values were considered significant when <0.05 and denoted as follows: n.s.-not significant, *p<0.05, **p<0.01, ***p<0.001.

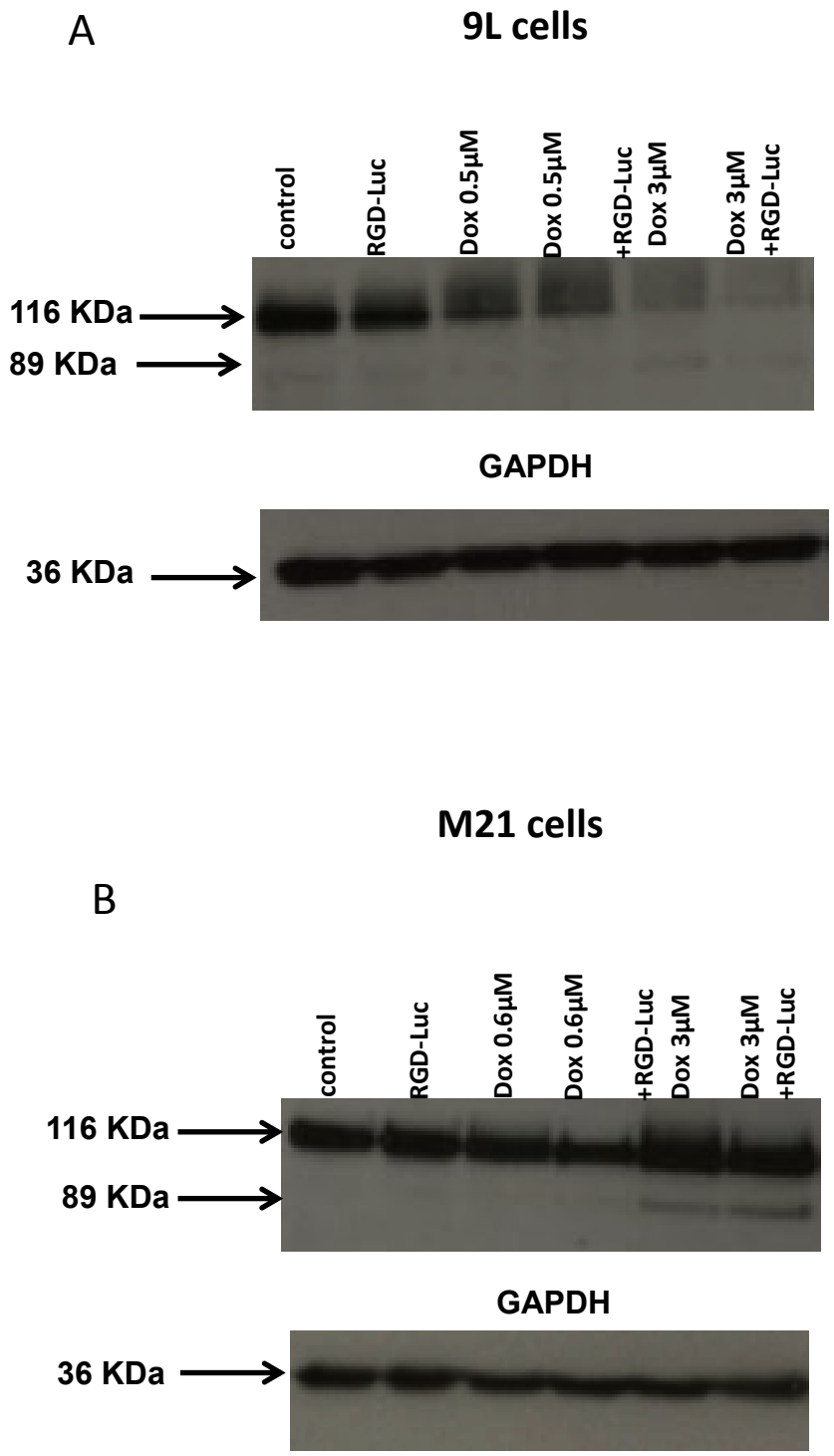

Figure 4.9 Western blot analysis of PARP-1 expression. 9L **(A)** and M21 **(B)** cells were transduced with targeted RGD-Luc vector in the presence or absence of doxorubicin. 24 hours post-transduction, cells were lysed and western blot was carried out using rabbit anti-PARP primary antibody and (HRP) conjugated anti-rabbit IgG secondary antibody. *GAPDH* expression was used to ensure equal amount of protein was loaded.

4.8 Doxorubicin enhances nuclear localisation of the RGD4C-AAVP vector genome.

Finally, we examined vector's genome accumulation in the nucleus to check whether doxorubicin treatment would result in enhanced nuclear localisation of vector's genome. Doxorubicin has already been reported to delay proper chromosome condensation and nuclear envelope formation during mitosis (Fasulo et al., 2012) which could result in increased transport through the nuclear pores. Thus, we evaluated the nuclear accumulation of the rAAV2 genome of AAVP, since gene expression by RGD4C-AAVP is mediated through its AAV2 transgene cassette. 9L cells were transduced with RGD-Luc or fd-Luc non-targeted vector in the presence or absence of doxorubicin, and harvested at day 4 post transduction. Next, the nuclei were extracted from the cells, followed by PCR using primers reading within the AAV2 ITR domain, as previously described (Aurnhammer et al., 2012), in order to semi-quantify the amount of vector genome in the nucleus (Figure 4.10). The data revealed a PCR product at the expected size, and electrophoresis gel analysis showed increased intensity of the ITR-derived PCR product when RGD4C-AAVP vector was used in combination with doxorubicin (Figure 4.10). Then product quantification of the band intensities using ImageJ software confirmed that combination of

doxorubicin with the targeted vector results in significant increase of vector DNA in the nucleus (Figure 4.10B).

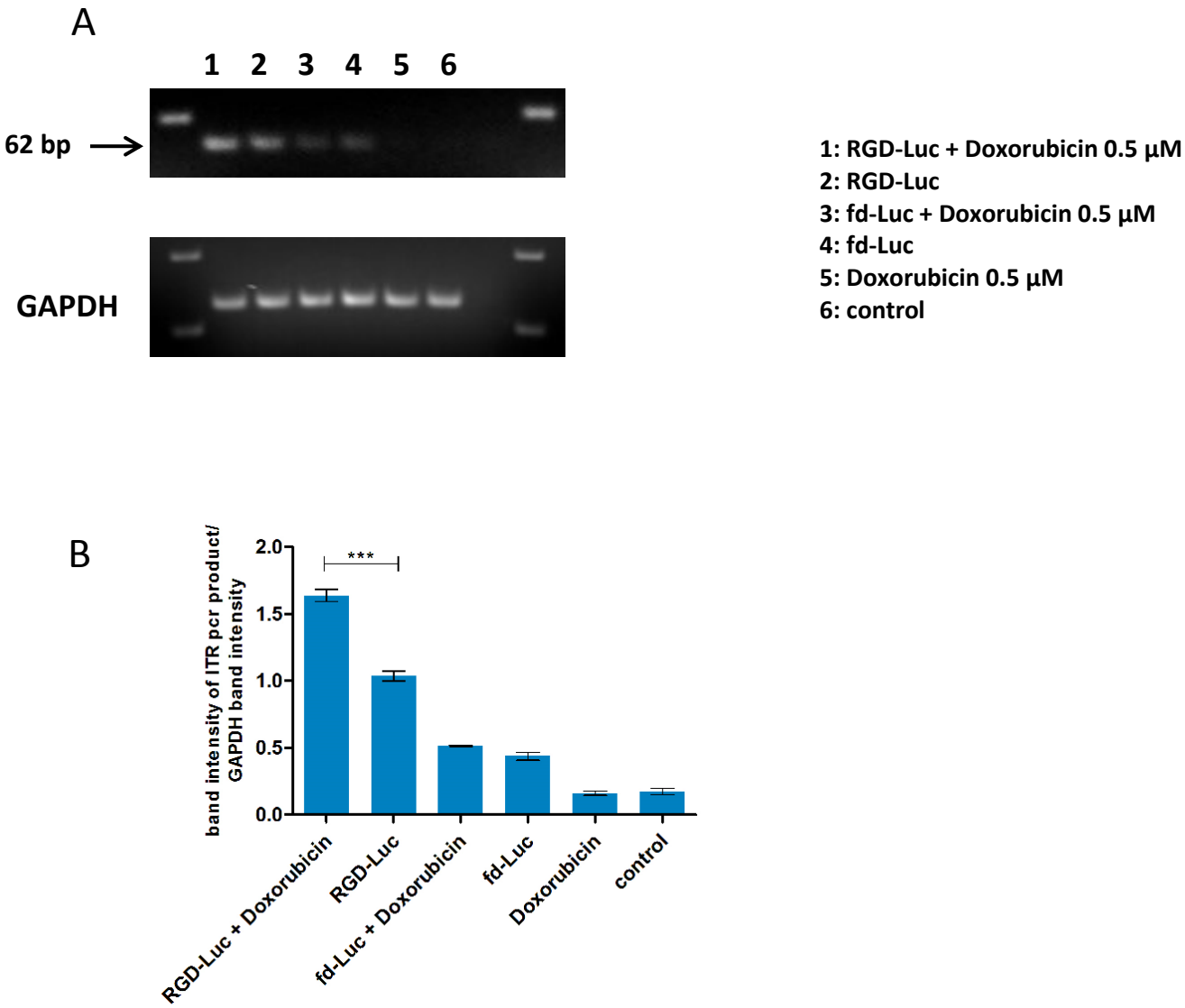

Figure 4.10 Mechanism of Doxorubicin. (A) 9L cells were plated on 48-well plates (70-80% confluent) and transduced with RGD-Luc targeted or fd-Luc control non-targeted vectors in the presence or absence of doxorubicin. On day 4 after transduction, cells were harvested and nuclei were extracted. Subsequently, DNA was extracted and used as template (10 ng of DNA) for PCR on the ITR domain of the vector in order to semi-quantify the amount of vector in the nucleus in the presence or absence of doxorubicin. The same amount of DNA (10 ng) was used as template for PCR in the *GAPDH* gene. **(B)** The band intensity of the ITR pcr product was quantified using ImageJ software and normalised to GAPDH. PCR of the ITR domain was repeated three times and shown is the mean ± standard error of the mean (s.e.m.) of triplicate samples. P values were generated by one-way ANOVA and tukey's post hoc tests. P values were considered significant when <0.05 and denoted as follows: *p<0.05, **p<0.01, ***p<0.001.

4.9 Evaluation of efficacy of doxorubicin and RGD4C-AAVP combination in a three-dimensional (3D) multicellular tumor spheroid model

After showing that doxorubicin dramatically increases the RGD4C-AAVP mediated targeted killing in tumor cells *in vitro*, we set up to assess the efficacy of this combination in a 3D tumor spheroid model that simulate the 3D tumors more accurately. The 3D tumor spheroids are considered valid models to recapitulate features of solid tumors *and* were used in this study to evaluate and confirm the efficacy of gene therapy by the targeted RGD4C-AAVP gene therapy in combination with doxorubicin. Since the increased tumor cell killing *in vitro* of the combination doxorubicin and RGD4C-AAVP was associated with the enhancing effect of doxorubicin on RGD4C-AAVP-mediated gene transfer, we first assessed the efficacy of gene transfer using phage carrying the *GFP* reporter gene to allow microscopic imaging of GFP expression within the 3D model of 9L and M21 tumor spheroids (Figure 4.11). The 9L and M21 tumor spheroids were transduced with RGD4C-AAVP-GFP (RGD-GFP) or control non-targeted fd-GFP vector in the presence or absence of doxorubicin. GFP expression was monitored with fluorescent microscopy over a period of 20 days to allow detectable gene expression by the RGD4C-AAVP in the spheroids. While the targeted RGD4C-AAVP showed minimal GFP expression in the spheroids at day 10 post-transduction, combination treatment (RGD-GFP +

doxorubicin) yielded dramatic increase in GFP expression compared to RGD-GFP treatment alone in both 9L and M21 spheroids (Figure 4.11).

Next, application of *HSVtk*/GCV suicide gene therapy on the rat 9L and human M21 tumors *in vitro* resulted in pronounced regression of the 9L (Figure 4.12) and M21 (Figure 4.13) spheroid volumes by combination of doxorubicin with the targeted RGD4C-AAVP-HSVtk (RGD-HSVtk) upon GCV treatment, compared to individual treatments with vector or doxorubicin alone. Subsequently, in 9L spheroids measurement of cell viability showed that the combination of doxorubicin plus RGD4C-AAVP achieved higher tumor cell killing ~97%, than the targeted RGD4C-AAVP vector or doxorubicin alone that induced ~92% and ~65% cancer cell killing, respectively (Figure 4.12 B). In M21 spheroids measurement of cell viability showed that combination of doxorubicin plus RGD4C-AAVP achieved higher tumor cell killing ~91%, than the targeted RGD4C-AAVP or doxorubicin alone that induced ~47% and ~82% cancer cell killing, respectively (Figure 4.13B). These findings establish that combination of doxorubicin with RGD4C-AAVP-mediated gene therapy greatly increases its potential as a gene therapy vector.

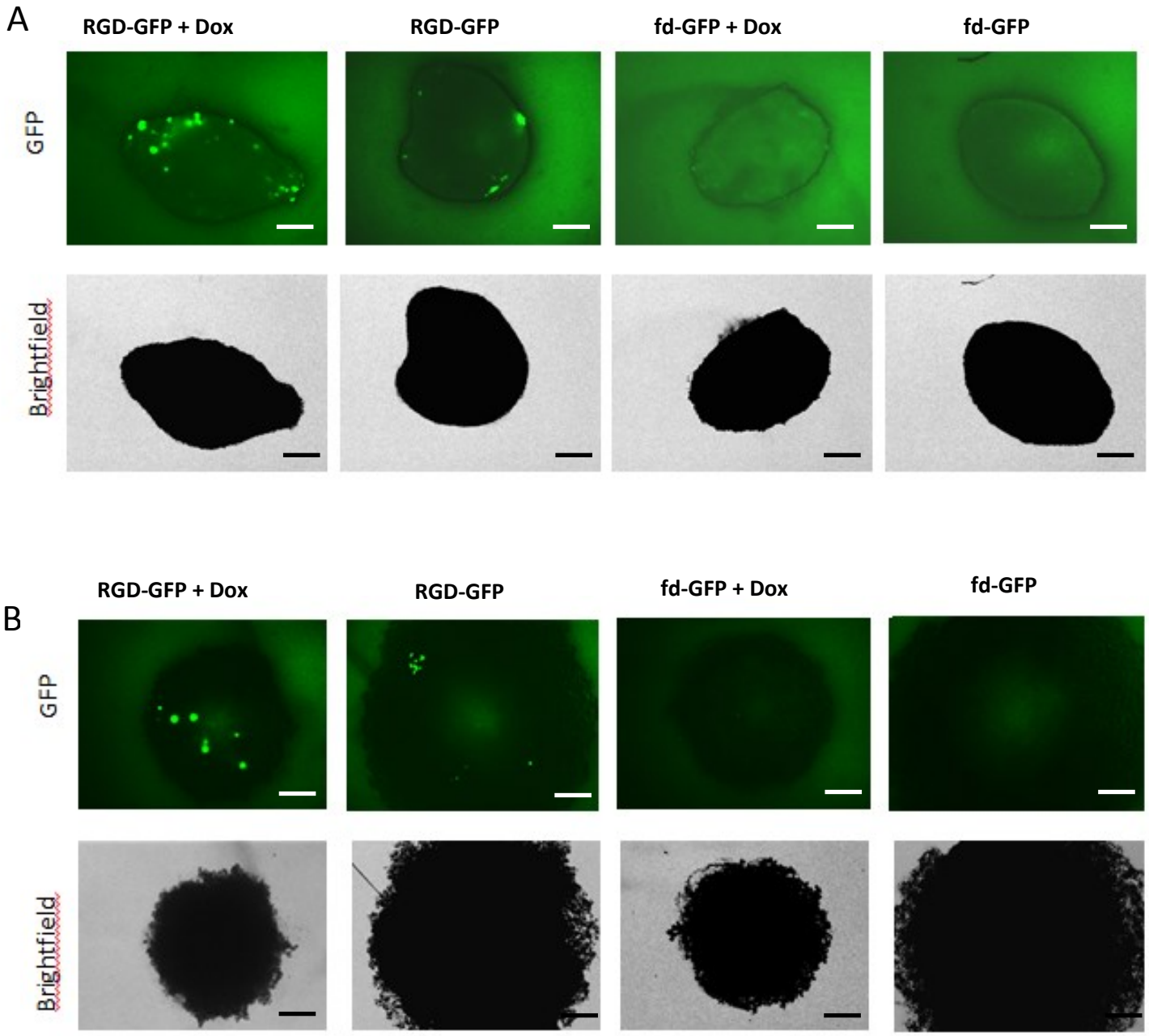

Figure 4.11 Doxorubicin increased the transduction efficiency in 9L and M21 spheroids. 9L **(A)** and M21 **(B)** cells (5 x 10^3) were seeded into a 96-well ultra-low attachment surface plate in 200µL complete medium. After 48 hours of incubation, a spheroid was formed in each well. Spheroids were then transduced with targeted RGD-GFP or fd-GFP control non-targeted vectors in the presence or absence of doxorubicin. GFP expression was evaluated with fluorescent microscopy at day 10 post-transduction. Scale bar= 0.5 mm

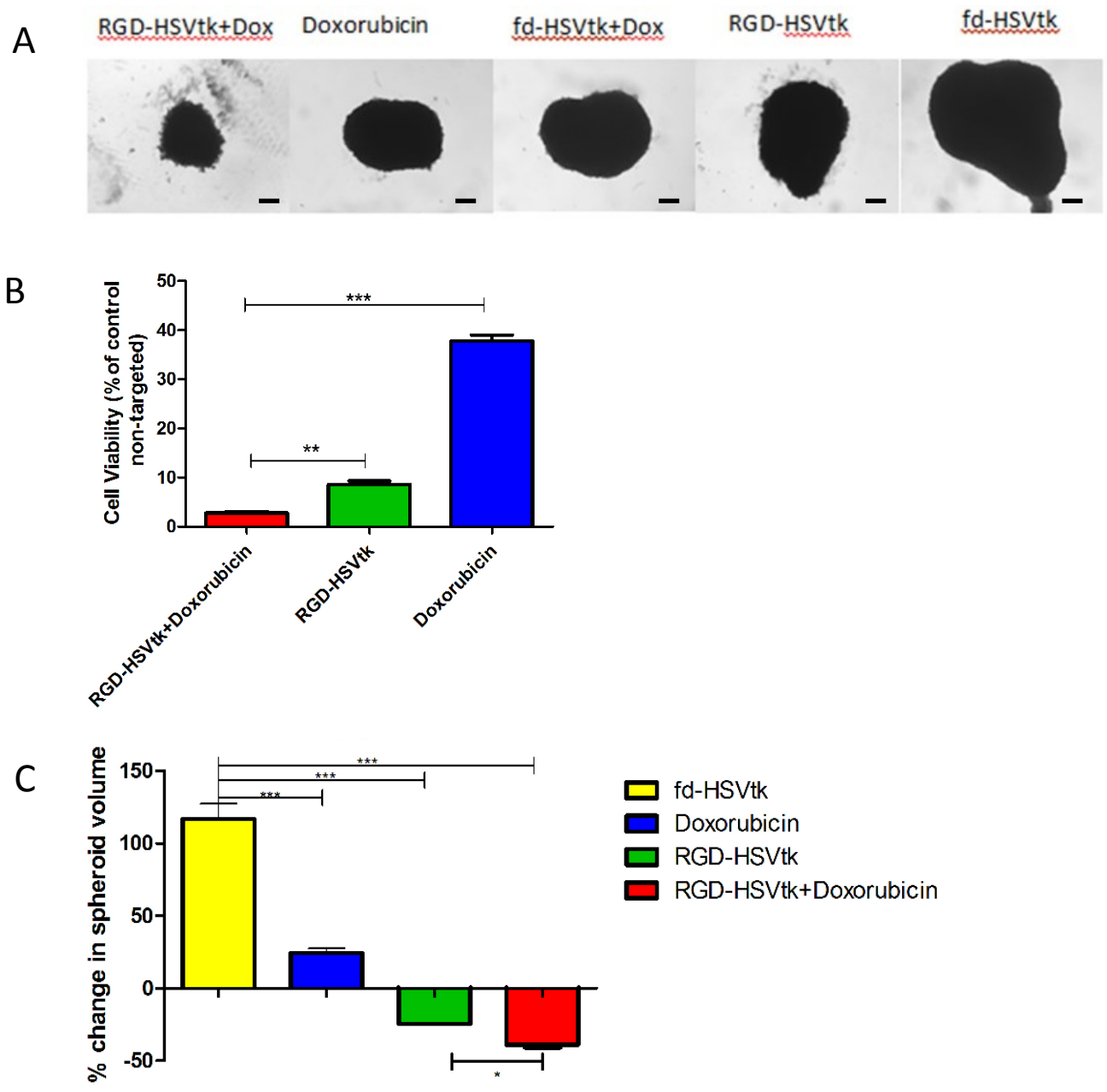

Figure 4.12 Doxorubicin increased cell death in 9L spheroids upon transduction with RGD-HSVtk (+GCV).

(A) Brightfield images showing the size of 9L tumor spheroids following transduction with RGD-HSVtk targeted vector or control non-targeted fd-HSVtk in the presence or absence of doxorubicin. GCV was added to the spheroids at day 5 post vector transduction and renewed every 2 days. Images were taken at day 5 post GCV treatment. Scale bar= 0.5 mm

(B) Evaluation of cell viability in 9L spheroids at day 5 post GCV treatment by using the CellTiter-Glo cell viability assay.

(C) Measurement of 9L spheroid volumes at days 0 and 5 post GCV treatment. The graph shows the % change of the average spheroid volumes. Data represent the mean ± standard error of the mean (s.e.m.) of triplicate samples. P values were generated by one-way ANOVA and tukey's post hoc tests. P values were considered significant when <0.05 and denoted as follows: n.s.-not significant, *p<0.05, **p<0.01, ***p<0.001.

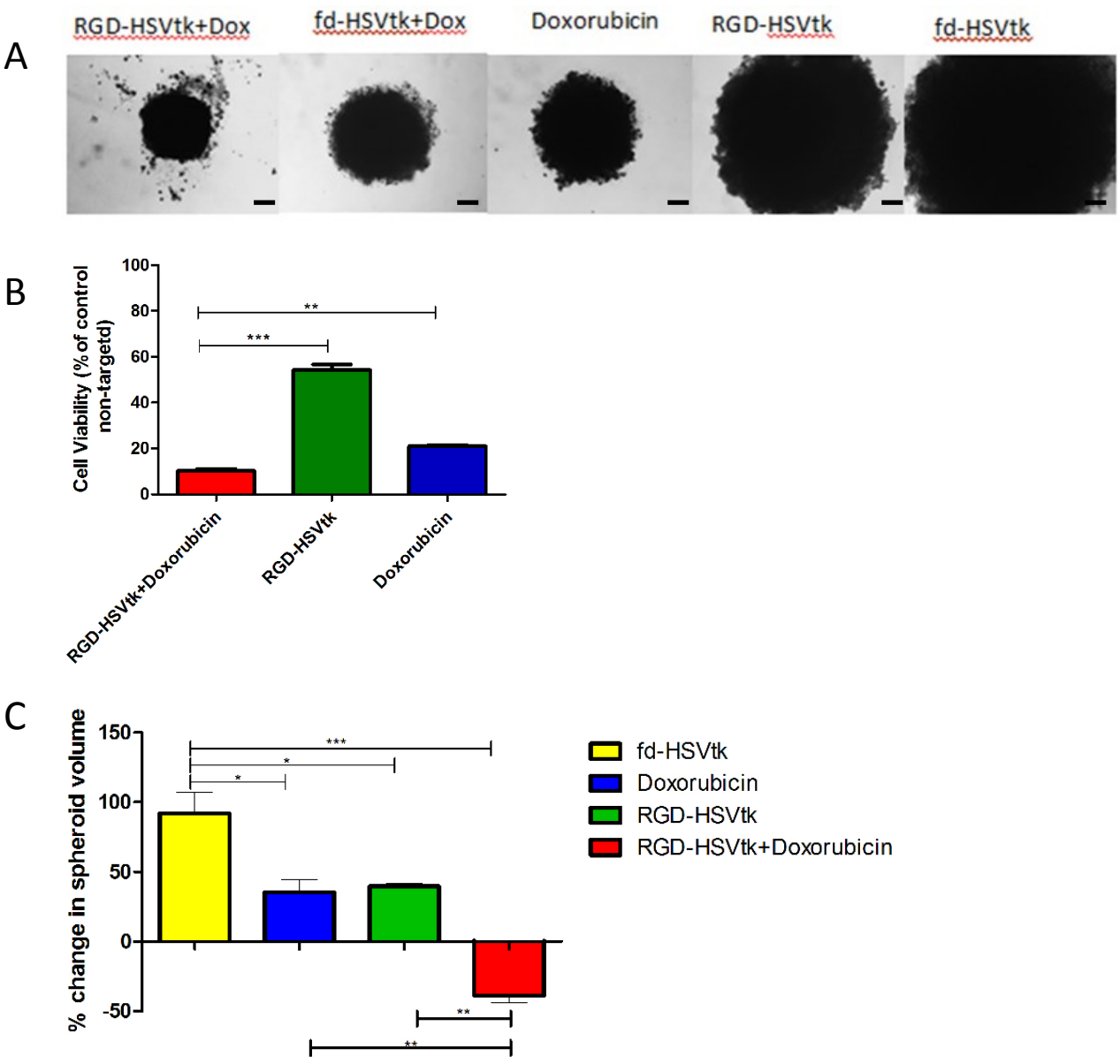

Figure 4.13 Doxorubicin increased cell death in M21 spheroids after transduction with RGD-HSVtk (+GCV).

(A) Brightfield images showing the size of M21 tumor spheroids following transduction with targeted RGD-HSVtk vector or control non-targeted fd-HSVtk in the presence or absence of doxorubicin. GCV was added to the spheroids at day 5 post vector transduction and renewed every 2 days. Images were taken at day 7 post GCV treatment. Scale bar= 0.5 mm

(B) Evaluation of cell viability in M21 spheroids at day 7 post GCV treatment by using the CellTiter-Glo cell viability assay.

(C) Measurement of M21 spheroid volumes at days 0 and 7 post GCV treatment. The graph shows the % change of the average spheroid volumes. Data represent the mean ± standard error of the mean (s.e.m.) of triplicate samples. P values were generated by one-way ANOVA and tukey's post hoc tests. P values were considered significant when <0.05 and denoted as follows: n.s.-not significant, *p<0.05, **p<0.01, ***p<0.001.

4.10 Discussion

Our results show that doxorubicin treatment of 9L and M21 cancer cell lines resulted in increased targeted AAVP-mediated gene delivery *in vitro*. First, we confirmed that treatment with doxorubicin increased reporter *GFP* and *Luc* transgene expression in 9L and M21 cancer cells. Moreover, doxorubicin treatment enhanced tumor cell killing by targeted AAVP-HSVtk plus GCV both in 2D cell cultures and 3D tumor spheroids.

These data are consistent with previous studies supporting that doxorubicin augments AAV transduction efficiency in airway cell lines (Yan et al., 2004). Doxorubicin was also reported to increase rAAV-2 transduction in rat neuronal cell lines (Zhang et al., 2009). According to (Zhang et al., 2009), the suggested mechanism was that doxorubicin increased transduction efficiency by enhancing nuclear translocation of rAAV-2. In addition, topoisomerase II inhibitors, such as doxorubicin, have already been reported to delay proper chromosome condensation and nuclear envelope formation during mitosis (Fasulo et al., 2012). Our data are consistent with these studies as we found increased ITR PCR product in the nuclear fraction of 9L cells treated with both doxorubicin and targeted AAVP vector compared to 9L cells treated with targeted AAVP only. Taking into account that combination of targeted AAVP with doxorubicin doesn't affect the internalisation nor the cell attachment of

the vector, our data indicate that doxorubicin facilitates the nuclear translocation of AAVP genome thus enhancing the transduction efficiency.

It has also been shown that genotoxic stress can increase AAV-mediated transduction efficiency (Ferrari et al., 1996) by facilitating the conversion of single-stranded DNA to double-stranded DNA. So, another possible mechanism is that doxorubicin-increased transduction efficiency of AAVP vector could be that low-dose doxorubicin caused moderate DNA damage (Tacar et al., 2013) that activated DNA repair enzymes. According to our hypothesis DNA repair enzymes can facilitate the conversion of single-stranded vector DNA to double-stranded thus increasing the transgene expression and the transduction efficiency of AAVP vector. Our comet assay results are in accordance with this hypothesis as we found that the low-dose doxorubicin that increased transduction efficiency of our vector causes moderate DNA damage. In addition, PARP-1 expression was upregulated in M21 cells treated with the low-dose doxorubicin compared to control untreated cells which indicates that the DNA repair mechanism was activated. In 9L cells PARP-1 expression was slightly down-regulated after low-dose doxorubicin treatment compared to control untreated cells but still indicates that there is DNA repair. This difference between the two cell lines can be attributed to the increased sensitivity of 9L cells to doxorubicin compared to M21 cells (as was shown in

MTT assay, Figure 4.2). Other possible mechanisms can be associated with doxorubicin effect in 9L cells.

In conclusion, in our study we proved that combining targeted AAVP with doxorubicin results in higher transduction efficiency by AAVP and better killing of cancer cells than either therapy alone. In addition, we elucidated possible mechanisms of doxorubicin-increased AAVP gene delivery. The next preclinical step will be to assess the efficacy of this combination treatment *in vivo* in tumor-bearing mice.

Chapter 5

Conclusion and General discussion

5.1 Conclusion

Hypothesis 1: Combination of genistein with our targeted AAVP vector could increase the AAVP-mediated transduction efficiency resulting in higher AAVP-guided cancer cell killing by delivering therapeutic genes.

- This hypothesis was proved by using genistein in combination with RGD4C-AAVP vector carrying reporter genes (*GFP*, firefly *luciferase* reporter genes) or RGD4C-AAVP carrying the *HSVtk* gene which kills cells in combination with ganciclovir. This hypothesis was investigated in 9L and M21 cell lines (2D model) and also in 9L and M21 tumor spheroid models (3D model). We found that treatment with genistein increased RGD4C-AAVP mediated transduction efficiency resulting in increased reporter gene expression and enhanced tumor cell killing.

Hypothesis 2: Treatment with genistein can inhibit proteasome-mediated degradation of AAVP particles resulting in increased gene expression from AAVP.

- In order to investigate this hypothesis we searched whether genistein increases polyubiquitination of AAVP phage coat proteins. 9L tumor cells

were transduced with RGD-AAVP vector alone or following pretreatment with genistein. Then, we performed immunostaining using antibodies against ubiquitin and phage coat proteins. Confocal microscopic analyses showed strong co-localization of ubiquitin and AAVP coat proteins in cells treated with combination of vector and genistein. These data show that one possible mechanism is that genistein can increase the transduction efficiency by inhibiting proteasome-mediated degradation of AAVP particles. Our data showing that genistein increased ITR PCR product in the nuclear fraction of cells treated with RGD4C-AAVP further support this hypothesis. The increased nuclear accumulation of AAVP genome, upon genistein pre-treatment, provides an additional mechanism that could further explain the improved AAVP-mediated transduction efficiency by genistein. One explanation is that pretreatment with genistein enhances the size of the nuclear pores, as genistein was reported to induce G2/M cell cycle arrest, during which nuclear localisation of gene therapy vectors can be enhanced (Cui et al., 2014, Han et al., 2013, Ouyang et al., 2009). However, in order to prove this additional mechanism we should have shown that the dose of genistein used in our experiments caused G2/M cell cycle arrest. One possible method to investigate if genistein causes cell cycle arrest is

using propidium iodide-FACS. Propidium iodide is an intercalating agent and can be used in flow cytometry to quantitatively assess the DNA content in cell cycle analysis (Cui et al., 2014).

Hypothesis 3: Combination of low-dose doxorubicin with our targeted AAVP vector could increase the AAVP-mediated transduction efficiency resulting in higher AAVP-mediated cancer cell killing.

- This hypothesis was proved by using low-dose doxorubicin in combination with RGD4C-AAVP vector carrying reporter genes (*GFP*, firefly *luciferase* reporter genes) or RGD4C-AAVP carrying the *HSVtk* gene which kills cells in combination with ganciclovir. This hypothesis was investigated in 9L and M21 cell lines (2D model) and also in 9L and M21 tumor spheroid models (3D model). We found that treatment with doxorubicin increased RGD4C-AAVP mediated transduction efficiency resulting in increased reporter gene expression and enhanced tumor cell killing. This result is consistent with the increased AAV2 ITR PCR product in the nuclear fraction of cells treated with combination of doxorubicin and RGD4C-AAVP vector compared to the cells treated with the targeted

vector only showing that doxorubicin increased the nuclear localization of our vector's genome.

Hypothesis 4: Treatment with low-dose doxorubicin can cause moderate DNA damage and trigger DNA repair mechanisms. DNA repair enzymes can facilitate the conversion from single-stranded DNA to double-stranded DNA necessary for gene expression to occur from AAVP.

- In order to investigate this hypothesis we performed comet assay and found that the low-dose doxorubicin that increased the transduction efficiency causes moderate DNA damage. Then, we performed western blot analysis in order to investigate the expression of PARP-1 repair enzyme in 9L and M21 cells after treatment with low-dose and high-dose doxorubicin. We found that in both cell lines there is PARP-1 expression in cells treated with the low-dose doxorubicin which indicates that the DNA repair mechanism is still active. According to the literature genotoxic stress can increase AAV-mediated transduction efficiency by activating DNA repair enzymes that can facilitate AAV second-strand synthesis which has been shown to be one of the rate-limiting steps that significantly impacts upon transduction efficiency by AAV (Ferrari et al., 1996, Qing et al., 1997). This is an indirect evidence that DNA repair may be one possible mechanism of how doxorubicin

increased AAVP-mediated gene delivery. In order to prove this hypothesis Southern blot is required showing the increase in double-stranded DNA compared to single-stranded DNA after treatment with doxorubicin. The increased ITR PCR product in the nuclear fraction of cells treated with the combination treatment compared to the cells treated with the targeted vector only, supports our hypothesis; however, it does not prove that the increase in ITR PCR product derives from the conversion of single-stranded to double-stranded DNA.

Hypothesis 5: Doxorubicin facilitates the nuclear translocation of vector's genome by delaying the chromosome condensation and proper envelope formation during mitosis. Therefore, combination of doxorubicin with our targeted AAVP vector could result in increased nuclear accumulation of vector and subsequently in enhanced AAVP-mediated gene expression efficiency.

- In order to investigate our vector's genome accumulation in the nucleus we performed PCR targeting the AAV2 ITR domain. We found increased ITR PCR product in the nuclear fraction of cells treated with doxorubicin compared to the cells treated with the targeted vector only. This shows that another possible mechanism of how doxorubicin increased AAVP-mediated gene delivery is that doxorubicin facilitates the nuclear localization of our vector's genome. However, in order to prove our

hypothesis we should have shown that doxorubicin delayed the chromosome condensation and nuclear envelope formation during mitosis. We can show this performing time-course confocal microscopic analysis in cells bearing histone-GFP construct and fluorescently labelled tubulin (Fasulo et al., 2012).

The present work reports an *in vitro* proof-of-concept investigation of combination treatment with drugs (genistein, doxorubicin) and RGD4C-AAVP. We do not make any specific claims or speculate regarding the in vivo potential. We have used a three-dimensional (3D) tumor spheroid models to recapitulate features of tumor microregions. These 3D models, representing the in vivo situation more accurately and imitating the avascular tumor regions, revealed increased transduction capacity by the targeted AAVP in combination with genistein or doxorubicin. These data point out towards promising efficacy of this combination treatment in tumor-bearing animals. Complete *in vivo* characterisation in tumor-bearing animals would fit in a separate investigation. Indeed, future preclinical studies will be conducted to determine what is the optimal drug dose *in vivo* and also in what tumor types this combination treatment can be applied. Thus, while we used fixed parameters in vivo in the past (Hajitou, Trepel et al. 2006, Hajitou, Rangel et al.

2007, Hajitou, Lev et al. 2008, Kia, Przystal et al. 2012, Przystal, Umukoro et al. 2013), further determination of drug/AAVP optimal doses and timeframes will apply on a case-by-case basis and will have to be carefully designed. In addition to transduction efficiency, whole body imaging in living animals will be important to investigate the spatio-temporal distribution of gene expression in combination with genistein and doxorubicin. Immunohistochemistry with an anti-phage antibody will be necessary to assess i) distribution of the targeted phage particles in the tumors versus healthy tissues, ii) cell type transduced by the targeted phage within the tumors in tumor-bearing mice treated with the combination treatment compared to mice treated with the targeted vector only. Toxicity studies and gene therapy in both immunodeficient and immunocompetent mice will be necessary to perform an accurate and complete *in vivo* evaluation.

5.2 General discussion

Cancer is a major cause of mortality and morbidity worldwide despite progress in the conventional therapies and despite the fact that several mechanisms of oncogenesis are now understood. Developing efficient systemic therapies would play a major advance in cancer treatment. Indeed, most cancer patients die of metastases and systemic chemotherapy is the most widely used treatment for cancer. The major obstacle to the success of chemotherapy in cancer treatment is the development of tumor drug resistance. In addition, chemotherapy is not specific and the dose of the drug that reaches the tumor may be as little as 5%–10% of the total dose as it accumulates in normal organs (Bosslet et al., 1998).

Cancer gene therapy is a promising approach for cancer treatment. Gene therapy was initially conceived as a treatment for inherited diseases, but today up to 70% of clinical trials of gene therapy are designed to treat cancer. Gene therapy uses carriers called vectors to deliver the therapeutic gene to the patient's target cells. Currently, the most common vectors are eukaryotic viruses because they can enter cells as part of the natural infection process. Eukaryotic viruses are, unquestionably, superior vectors for gene transfer, but have had limited success in systemic gene therapy as they are taken up by the

liver and reticulo-endothelial system, they have broad tropism for healthy tissues and they may lose efficacy due to the presence of neutralising antibodies (Waehler et al., 2007). A local vector delivery through intratumoral injection can be used to show proof of efficacy, but in practice clinical benefit for cancer treatment can only be achieved following systemic administration.

Bacteriophage is a new gene therapy vector with potential advantages over eukaryotic viral vectors that are commonly used for gene delivery and gene therapy. Phage has no native tropism for mammalian cells, but can be engineered to display tissue-specific ligands on the coat proteins to bind to specific mammalian cell receptors without disruption of the virus structure. Despite its advantageous natural characteristics, bacteriophage viruses are still considered poor vectors for gene delivery due to their low transduction efficiency compared to eukaryotic vectors, as they have evolved to infect bacteria only, and have no optimised strategies to transduce mammalian cells. The AAVP vector, created by incorporation of the mammalian transgene cassette from recombinant rAAV2 into the phage genome, was reported as an improved version of phage-based gene vectors to achieve enhanced gene delivery compared to conventional phage-derived vectors. Although, AAVP vectors are promising, they still have limitations inherent to bacteriophage. In

this study we proved that combining targeted RGD4C-AAVP with genistein results in higher tumor cell transduction efficiency by AAVP and more efficient killing of cancer cells than either therapy alone. We also proved that combining targeted RGD4C-AAVP with doxorubicin results in higher transduction efficiency by AAVP and more efficient killing of cancer cells than either therapy alone. In addition, we elucidated possible mechanisms of how these drugs increased AAVP-mediated gene delivery. The next preclinical step will be to assess the efficacy of these drugs combined with AAVP *in vivo* in tumor-bearing mice. Given that genistein and AAVP have been demonstrated to cross the blood-brain barrier (Malinowska et al., 2010, Staquicini et al., 2011), this combination treatment could be also applied *in vivo* for the treatment of brain tumors. Our study indicates that combining the RGD4C-AAVP with genistein or doxorubicin is a promising strategy than can be considered for future clinical applications of targeted systemic gene therapy with RGD4C-AAVP in cancer patients. The present study forms the foundation for future extensive preclinical studies that could pave the way towards clinical trials in cancer patients.

Publications

The natural dietary genistein boosts bacteriophage-mediated cancer cell killing by improving phage-targeted tumor cell transduction

Effrosyni Tsafa[1], Mariam Al-Bahrani[1], Justyna Przystal[1], Keittisak Suwan[1] and Amin Hajitou[1]

[1]Phage Therapy Group, Department of Medicine, Imperial College London, Hammersmith Hospital Campus, Burlington Danes Building, London W12 0NN, United Kingdom

Correspondence to: Amin Hajitou, email: a.hajitou@imperial.ac.uk

Accepted in Oncotarget with minor revision.

Chemovirotherapy with doxorubicin and phage-guided cancer gene therapy induces synergistic tumor cell killing

Effrosyni Tsafa[1], Keittisak Suwan[1] Nabil Hajji[2] and Amin Hajitou[1]

[1]Phage Therapy Group, Department of Medicine, Imperial College London, Hammersmith Hospital Campus, Burlington Danes Building, London W12 0NN, United Kingdom

[2]Division of Experimental Medicine, Department of Medicine, Imperial College London, Hammersmith Hospital Campus, Burlington Danes Building, London W12 0NN, United Kingdom

Correspondence to: Amin Hajitou, email: a.hajitou@imperial.ac.uk

To be submitted to Clinical Cancer Research

References

ADAM, V., EKBLAD, M., SWEENEY, K., MULLER, H., BUSCH, K. H., JOHNSEN, C. T., KANG, N. R., LEMOINE, N. R. & HALLDEN, G. 2012. Synergistic and Selective Cancer Cell Killing Mediated by the Oncolytic Adenoviral Mutant AdDeltaDelta and Dietary Phytochemicals in Prostate Cancer Models. *Hum Gene Ther,* 23**,** 1003-15.

AGHI, M., HOCHBERG, F. & BREAKEFIELD, X. O. 2000. Prodrug activation enzymes in cancer gene therapy. *J Gene Med,* 2**,** 148-64.

AN, D. S., WERSTO, R. P., AGRICOLA, B. A., METZGER, M. E., LU, S., AMADO, R. G., CHEN, I. S. & DONAHUE, R. E. 2000. Marking and gene expression by a lentivirus vector in transplanted human and nonhuman primate CD34(+) cells. *J Virol,* 74**,** 1286-95.

ARAP, M. A. 2005. Phage display technology: applications and innovations. *Genetics and Molecular Biology, Review*.

AURNHAMMER, C., HAASE, M., MUETHER, N., HAUSL, M., RAUSCHHUBER, C., HUBER, I., NITSCHKO, H., BUSCH, U., SING, A., EHRHARDT, A. & BAIKER, A. 2012. Universal real-time PCR for the detection and quantification of adeno-associated virus serotype 2-derived inverted terminal repeat sequences. *Hum Gene Ther Methods,* 23**,** 18-28.

BANERJEE, S., LI, Y., WANG, Z. & SARKAR, F. H. 2008. Multi-targeted therapy of cancer by genistein. *Cancer Lett,* 269**,** 226-42.

BARAJAS, M., MAZZOLINI, G., GENOVE, G., BILBAO, R., NARVAIZA, I., SCHMITZ, V., SANGRO, B., MELERO, I., QIAN, C. & PRIETO, J. 2001. Gene therapy of orthotopic hepatocellular carcinoma in rats using adenovirus coding for interleukin 12. *Hepatology,* 33**,** 52-61.

BARBAS C.F., B. D. R., SCOTT J.K., SILVERMANN G.J. 2001. *Phage Display: A laboratory manual,* New York.

BLACK, M. E., KOKORIS, M. S. & SABO, P. 2001. Herpes simplex virus-1 thymidine kinase mutants created by semi-random sequence mutagenesis improve prodrug-mediated tumor cell killing. *Cancer Res,* 61**,** 3022-6.

BLAESE, R. M., CULVER, K. W., MILLER, A. D., CARTER, C. S., FLEISHER, T., CLERICI, M., SHEARER, G., CHANG, L., CHIANG, Y., TOLSTOSHEV, P., GREENBLATT, J. J., ROSENBERG, S. A., KLEIN, H., BERGER, M., MULLEN, C. A., RAMSEY, W. J., MUUL, L., MORGAN, R. A. & ANDERSON, W. F. 1995. T lymphocyte-directed gene therapy for ADA- SCID: initial trial results after 4 years. *Science,* 270**,** 475-80.

BOSSLET, K., STRAUB, R., BLUMRICH, M., CZECH, J., GERKEN, M., SPERKER, B., KROEMER, H. K., GESSON, J. P., KOCH, M. & MONNERET, C. 1998. Elucidation of the mechanism enabling tumor selective prodrug monotherapy. *Cancer Res,* 58**,** 1195-201.

BURTON, E. A., GLORIOSO, J. C. & FINK, D. J. 2003. Gene therapy progress and prospects: Parkinson's disease. *Gene Ther,* 10**,** 1721-7.

CERVELLI, T., PALACIOS, J. A., ZENTILIN, L., MANO, M., SCHWARTZ, R. A., WEITZMAN, M. D. & GIACCA, M. 2008. Processing of recombinant AAV genomes occurs in specific nuclear structures that overlap with foci of DNA-damage-response proteins. *J Cell Sci,* 121**,** 349-57.

CONKLIN, C. M., BECHBERGER, J. F., MACFABE, D., GUTHRIE, N., KUROWSKA, E. M. & NAUS, C. C. 2007. Genistein and quercetin increase connexin43 and suppress growth of breast cancer cells. *Carcinogenesis,* 28**,** 93-100.

COURA RDOS, S. & NARDI, N. B. 2007. The state of the art of adeno-associated virus-based vectors in gene therapy. *Virol J,* 4**,** 99.

CUI, S., WIENHOEFER, N. & BILITEWSKI, U. 2014. Genistein induces morphology change and G2/M cell cycle arrest by inducing p38 MAPK activation in macrophages. *Int Immunopharmacol,* 18**,** 142-50.

DASH, P. R., READ, M. L., BARRETT, L. B., WOLFERT, M. A. & SEYMOUR, L. W. 1999. Factors affecting blood clearance and in vivo distribution of polyelectrolyte complexes for gene delivery. *Gene Ther,* 6**,** 643-50.

DOLIVET, G., MERLIN, J. L., BARBERI-HEYOB, M., RAMACCI, C., ERBACHER, P., PARACHE, R. M., BEHR, J. P. & GUILLEMIN, F. 2002. In vivo growth inhibitory effect of iterative wild-type p53 gene transfer in human head and neck carcinoma xenografts using glucosylated polyethylenimine nonviral vector. *Cancer Gene Ther,* 9**,** 708-14.

DZAU, V. J., BEATT, K., POMPILIO, G. & SMITH, K. 2003. Current perceptions of cardiovascular gene therapy. *Am J Cardiol,* 92**,** 18n-23n.

EL-ANEED, A. 2004. Current strategies in cancer gene therapy. *Eur J Pharmacol,* 498**,** 1-8.

FANECA, H., SIMOES, S. & DE LIMA, M. C. 2002. Evaluation of lipid-based reagents to mediate intracellular gene delivery. *Biochim Biophys Acta,* 1567**,** 23-33.

FASULO, B., KOYAMA, C., YU, K. R., HOMOLA, E. M., HSIEH, T. S., CAMPBELL, S. D. & SULLIVAN, W. 2012. Chk1 and Wee1 kinases coordinate DNA replication, chromosome condensation, and anaphase entry. *Mol Biol Cell,* 23**,** 1047-57.

FERRARI, F. K., SAMULSKI, T., SHENK, T. & SAMULSKI, R. J. 1996. Second-strand synthesis is a rate-limiting step for efficient transduction by recombinant adeno-associated virus vectors. *J Virol,* 70**,** 3227-34.

FEUER, W. J., SCHIFFMAN, J. C., DAVIS, J. L., PORCIATTI, V., GONZALEZ, P., KOILKONDA, R. D., YUAN, H., LALWANI, A., LAM, B. L. & GUY, J. 2015. Gene Therapy for Leber Hereditary Optic Neuropathy: Initial Results. *Ophthalmology*.

GRAHAM, F. L. & VAN DER EB, A. J. 1973. Transformation of rat cells by DNA of human adenovirus 5. *Virology,* 54**,** 536-9.

GREENSTEIN, D. & BESMOND, C. 2001. Preparing and using M13-derived vectors. *Curr Protoc Mol Biol,* Chapter 1**,** Unit1.15.

HAJITOU, A., RANGEL, R., TREPEL, M., SOGHOMONYAN, S., GELOVANI, J. G., ALAUDDIN, M. M., PASQUALINI, R. & ARAP, W. 2007. Design and construction of targeted AAVP vectors for mammalian cell transduction. *Nat Protoc,* 2**,** 523-31.

HAJITOU, A., TREPEL, M., LILLEY, C. E., SOGHOMONYAN, S., ALAUDDIN, M. M., MARINI, F. C., 3RD, RESTEL, B. H., OZAWA, M. G., MOYA, C. A., RANGEL, R., SUN, Y., ZAOUI, K., SCHMIDT, M., VON KALLE, C., WEITZMAN, M. D., GELOVANI, J. G., PASQUALINI, R. & ARAP, W. 2006. A hybrid vector for ligand-directed tumor targeting and molecular imaging. *Cell,* 125**,** 385-98.

HAN, J., KURITA, Y. & ISODA, H. 2013. Genistein-induced G2/M cell cycle arrest of human intestinal colon cancer Caco-2 cells is associated with Cyclin B1 and Chk2 down-regulation. *Cytotechnology,* 65**,** 973-8.

HASTIE, E. & SAMULSKI, R. J. 2015. Adeno-associated virus at 50: a golden anniversary of discovery, research, and gene therapy success--a personal perspective. *Hum Gene Ther,* 26**,** 257-65.

HEISE, C. & KIRN, D. H. 2000. Replication-selective adenoviruses as oncolytic agents. *J Clin Invest,* 105**,** 847-51.

HELENE, C., THUONG, N. T. & HAREL-BELLAN, A. 1992. Control of gene expression by triple helix-forming oligonucleotides. The antigene strategy. *Ann N Y Acad Sci,* 660**,** 27-36.

JENNINGS, K., MIYAMAE, T., TRAISTER, R., MARINOV, A., KATAKURA, S., SOWDERS, D., TRAPNELL, B., WILSON, J. M., GAO, G. & HIRSCH, R. 2005. Proteasome inhibition enhances AAV-mediated transgene expression in human synoviocytes in vitro and in vivo. *Mol Ther,* 11**,** 600-7.

KAY, M. A., GLORIOSO, J. C. & NALDINI, L. 2001. Viral vectors for gene therapy: the art of turning infectious agents into vehicles of therapeutics. *Nat Med,* 7**,** 33-40.

KAZI, A., DANIEL, K. G., SMITH, D. M., KUMAR, N. B. & DOU, Q. P. 2003. Inhibition of the proteasome activity, a novel mechanism associated with the tumor cell apoptosis-inducing ability of genistein. *Biochem Pharmacol,* 66**,** 965-76.

KIA, A., PRZYSTAL, J. M., NIANIARIS, N., MAZARAKIS, N. D., MINTZ, P. J. & HAJITOU, A. 2012. Dual systemic tumor targeting with ligand-directed phage and Grp78 promoter induces tumor regression. *Mol Cancer Ther,* 11**,** 2566-77.

KORDOWER, J. H., BLOCH, J., MA, S. Y., CHU, Y., PALFI, S., ROITBERG, B. Z., EMBORG, M., HANTRAYE, P., DEGLON, N. & AEBISCHER, P. 1999. Lentiviral gene transfer to the nonhuman primate brain. *Exp Neurol,* 160**,** 1-16.

KOTIN, R. M., SINISCALCO, M., SAMULSKI, R. J., ZHU, X. D., HUNTER, L., LAUGHLIN, C. A., MCLAUGHLIN, S., MUZYCZKA, N., ROCCHI, M. & BERNS, K. I. 1990. Site-specific integration by adeno-associated virus. *Proc Natl Acad Sci U S A,* 87**,** 2211-5.

KU, C. A. & PENNESI, M. E. 2015. Retinal Gene Therapy: Current Progress and Future Prospects. *Expert Rev Ophthalmol,* 10**,** 281-299.

KUIPER, G. G., LEMMEN, J. G., CARLSSON, B., CORTON, J. C., SAFE, S. H., VAN DER SAAG, P. T., VAN DER BURG, B. & GUSTAFSSON, J. A. 1998. Interaction of estrogenic chemicals and phytoestrogens with estrogen receptor beta. *Endocrinology,* 139**,** 4252-63.

LANG, L. H. 2006. FDA approves use of bacteriophages to be added to meat and poultry products. *Gastroenterology,* 131**,** 1370.

LAROCCA, D., WITTE, A., JOHNSON, W., PIERCE, G. F. & BAIRD, A. 1998. Targeting bacteriophage to mammalian cell surface receptors for gene delivery. *Hum Gene Ther,* 9**,** 2393-9.

LI, C. F., WU, W. J., WU, W. R., LIAO, Y. J., CHEN, L. R., HUANG, C. N., LI, C. C., LI, W. M., HUANG, H. Y., CHEN, Y. L., LIANG, S. S., CHOW, N. H. & SHIUE, Y. L. 2015. The cAMP responsive element binding protein 1 transactivates epithelial membrane protein 2, a potential tumor suppressor in the urinary bladder urothelial carcinoma. *Oncotarget,* 6**,** 9220-39.

LINDEN, R. M., WARD, P., GIRAUD, C., WINOCOUR, E. & BERNS, K. I. 1996. Site-specific integration by adeno-associated virus. *Proc Natl Acad Sci U S A,* 93**,** 11288-94.

MAH, C., QING, K., KHUNTIRAT, B., PONNAZHAGAN, S., WANG, X. S., KUBE, D. M., YODER, M. C. & SRIVASTAVA, A. 1998. Adeno-associated virus type 2-mediated gene transfer: role of epidermal growth factor receptor protein tyrosine kinase in transgene expression. *J Virol,* 72**,** 9835-43.

MALINOWSKA, M., WILKINSON, F. L., LANGFORD-SMITH, K. J., LANGFORD-SMITH, A., BROWN, J. R., CRAWFORD, B. E., VANIER, M. T., GRYNKIEWICZ, G., WYNN, R. F., WRAITH, J. E., WEGRZYN, G. & BIGGER, B. W. 2010. Genistein improves neuropathology and corrects behaviour in a mouse model of neurodegenerative metabolic disease. *PLoS One,* 5**,** e14192.

MOSKOT, M., MONTEFUSCO, S., JAKOBKIEWICZ-BANECKA, J., MOZOLEWSKI, P., WEGRZYN, A., DI BERNARDO, D., WEGRZYN, G., MEDINA, D. L., BALLABIO, A. & GABIG-CIMINSKA, M. 2014. The phytoestrogen genistein modulates lysosomal metabolism and transcription factor EB (TFEB) activation. *J Biol Chem,* 289**,** 17054-69.

NALDINI, L. 2015. Gene therapy returns to centre stage. *Nature,* 526**,** 351-60.

NALDINI, L., BLOMER, U., GAGE, F. H., TRONO, D. & VERMA, I. M. 1996. Efficient transfer, integration, and sustained long-term expression of the transgene in adult rat brains injected with a lentiviral vector. *Proc Natl Acad Sci U S A,* 93**,** 11382-8.

NEUMANN, M., MACKENZIE, I. R., CAIRNS, N. J., BOYER, P. J., MARKESBERY, W. R., SMITH, C. D., TAYLOR, J. P., KRETZSCHMAR, H. A., KIMONIS, V. E. & FORMAN, M. S. 2007. TDP-43 in the ubiquitin pathology of frontotemporal dementia with VCP gene mutations. *J Neuropathol Exp Neurol,* 66**,** 152-7.

NISHIKAWA, M. & HUANG, L. 2001. Nonviral vectors in the new millennium: delivery barriers in gene transfer. *Hum Gene Ther,* 12**,** 861-70.

OUYANG, G., YAO, L., RUAN, K., SONG, G., MAO, Y. & BAO, S. 2009. Genistein induces G2/M cell cycle arrest and apoptosis of human ovarian cancer cells via activation of DNA damage checkpoint pathways. *Cell Biol Int,* 33**,** 1237-44.

PACK, D. W., HOFFMAN, A. S., PUN, S. & STAYTON, P. S. 2005. Design and development of polymers for gene delivery. *Nat Rev Drug Discov,* 4**,** 581-93.

PAOLONI, M. C., TANDLE, A., MAZCKO, C., HANNA, E., KACHALA, S., LEBLANC, A., NEWMAN, S., VAIL, D., HENRY, C., THAMM, D., SORENMO, K., HAJITOU, A., PASQUALINI, R., ARAP, W., KHANNA, C. & LIBUTTI, S. K. 2009. Launching a novel preclinical infrastructure: comparative oncology trials consortium directed therapeutic targeting of TNFalpha to cancer vasculature. *PLoS One,* 4**,** e4972.

PILLAY, S., MEYER, N. L., PUSCHNIK, A. S., DAVULCU, O., DIEP, J., ISHIKAWA, Y., JAE, L. T., WOSEN, J. E., NAGAMINE, C. M., CHAPMAN, M. S. & CARETTE, J. E. 2016. An essential receptor for adeno-associated virus infection. *Nature,* 530**,** 108-12.

PONDER, K. P. 2001. *An Introduction to Molecular Medicine and Gene Therapy*, Wiley-Liss.

PRANJOL, M. Z. & HAJITOU, A. 2015. Bacteriophage-derived vectors for targeted cancer gene therapy. *Viruses,* 7**,** 268-84.

PRZYSTAL, J. M., UMUKORO, E., STONEHAM, C. A., YATA, T., O'NEILL, K., SYED, N. & HAJITOU, A. 2013. Proteasome inhibition in cancer is associated with enhanced tumor targeting by the adeno-associated virus/phage. *Mol Oncol,* 7**,** 55-66.

QING, K., WANG, X. S., KUBE, D. M., PONNAZHAGAN, S., BAJPAI, A. & SRIVASTAVA, A. 1997. Role of tyrosine phosphorylation of a cellular protein in adeno-associated virus 2-mediated transgene expression. *Proc Natl Acad Sci U S A,* 94**,** 10879-84.

ROSENBERG, S. A., BLAESE, R. M., BRENNER, M. K., DEISSEROTH, A. B., LEDLEY, F. D., LOTZE, M. T., WILSON, J. M., NABEL, G. J., CORNETTA, K., ECONOMOU, J. S., FREEMAN, S. M., RIDDELL, S. R., BRENNER, M., OLDFIELD, E., GANSBACHER, B., DUNBAR, C., WALKER, R. E., SCHUENING, F. G., ROTH, J. A., CRYSTAL, R. G., WELSH, M. J., CULVER, K., HESLOP, H. E., SIMONS, J., WILMOTT, R. W., BOUCHER, R. C., SIEGLER, H. F., BARRANGER, J. A., KARLSSON, S., KOHN, D., GALPIN, J. E., RAFFEL, C., HESDORFFER, C., ILAN, J., CASSILETH, P., O'SHAUGHNESSY, J., KUN, L. E., DAS, T. K., WONG-STAAL, F., SOBOL, R. E., HAUBRICH, R., SZNOL, M., RUBIN, J., SORCHER, E. J., ROSENBLATT, J., WALKER, R., BRIGHAM, K., VOGELZANG, N., HERSH, E. & ECK, S. L. 2000. Human gene marker/therapy clinical protocols. *Hum Gene Ther,* 11**,** 919-79.

ROY, I., HOLLE, L., SONG, W., HOLLE, E., WAGNER, T. & YU, X. 2002. Efficient translocation and apoptosis induction by adenovirus encoded VP22-p53 fusion protein in human tumor cells in vitro. *Anticancer Res,* 22**,** 3185-9.

SANTONI DE SIO, F. R., GRITTI, A., CASCIO, P., NERI, M., SAMPAOLESI, M., GALLI, C., LUBAN, J. & NALDINI, L. 2008. Lentiviral vector gene transfer is limited by the proteasome at postentry steps in various types of stem cells. *Stem Cells,* 26**,** 2142-52.

SCHAMBACH, A., ZYCHLINSKI, D., EHRNSTROEM, B. & BAUM, C. 2013. Biosafety features of lentiviral vectors. *Hum Gene Ther,* 24**,** 132-42.

SHEN, M., CHAN, T. H. & DOU, Q. P. 2012. Targeting tumor ubiquitin-proteasome pathway with polyphenols for chemosensitization. *Anticancer Agents Med Chem,* 12**,** 891-901.

SHERIDAN, C. 2011. Gene therapy finds its niche. *Nat Biotechnol,* 29**,** 121-8.

SHI, F., RAKHMILEVICH, A. L., HEISE, C. P., OSHIKAWA, K., SONDEL, P. M., YANG, N. S. & MAHVI, D. M. 2002. Intratumoral injection of interleukin-12 plasmid DNA, either naked or in complex with cationic lipid, results in similar tumor regression in a murine model. *Mol Cancer Ther,* 1**,** 949-57.

SPAGNUOLO, C., RUSSO, G. L., ORHAN, I. E., HABTEMARIAM, S., DAGLIA, M., SUREDA, A., NABAVI, S. F., DEVI, K. P., LOIZZO, M. R., TUNDIS, R. & NABAVI, S. M. 2015. Genistein and cancer: current status, challenges, and future directions. *Adv Nutr,* 6**,** 408-19.

STAQUICINI, F. I., OZAWA, M. G., MOYA, C. A., DRIESSEN, W. H., BARBU, E. M., NISHIMORI, H., SOGHOMONYAN, S., FLORES, L. G., 2ND, LIANG, X., PAOLILLO, V., ALAUDDIN, M. M., BASILION, J. P., FURNARI, F. B., BOGLER, O., LANG, F. F., ALDAPE, K. D., FULLER, G. N., HOOK, M., GELOVANI, J. G., SIDMAN, R. L., CAVENEE, W. K., PASQUALINI, R. & ARAP, W. 2011. Systemic combinatorial peptide selection yields a non-canonical iron-mimicry mechanism for targeting tumors in a mouse model of human glioblastoma. *J Clin Invest,* 121**,** 161-73.

STONEHAM, C. A., HOLLINSHEAD, M. & HAJITOU, A. 2012. Clathrin-mediated endocytosis and subsequent endo-lysosomal trafficking of adeno-associated virus/phage. *J Biol Chem,* 287**,** 35849-59.

TACAR, O., SRIAMORNSAK, P. & DASS, C. R. 2013. Doxorubicin: an update on anticancer molecular action, toxicity and novel drug delivery systems. *J Pharm Pharmacol,* 65**,** 157-70.

TREPEL, M., STONEHAM, C. A., ELEFTHEROHORINOU, H., MAZARAKIS, N. D., PASQUALINI, R., ARAP, W. & HAJITOU, A. 2009. A heterotypic bystander effect for tumor cell killing after adeno-associated virus/phage-mediated, vascular-targeted suicide gene transfer. *Mol Cancer Ther,* 8**,** 2383-91.

VALDMANIS, P. N., LISOWSKI, L. & KAY, M. A. 2012. rAAV-mediated tumorigenesis: still unresolved after an AAV assault. *Mol Ther,* 20**,** 2014-7.

VOLLMER, C. M., JR., EILBER, F. C., BUTTERFIELD, L. H., RIBAS, A., DISSETTE, V. B., KOH, A., MONTEJO, L. D., LEE, M. C., ANDREWS, K. J., MCBRIDE, W. H., GLASPY, J. A. & ECONOMOU, J. S. 1999. Alpha-fetoprotein-specific genetic immunotherapy for hepatocellular carcinoma. *Cancer Res,* 59**,** 3064-7.

WAEHLER, R., RUSSELL, S. J. & CURIEL, D. T. 2007. Engineering targeted viral vectors for gene therapy. *Nat Rev Genet,* 8**,** 573-87.

WIETHOFF, C. M. & MIDDAUGH, C. R. 2003. Barriers to nonviral gene delivery. *J Pharm Sci,* 92**,** 203-17.

XIAO, X., LIU, Z., WANG, R., WANG, J., ZHANG, S., CAI, X., WU, K., BERGAN, R. C., XU, L. & FAN, D. 2015. Genistein suppresses FLT4 and inhibits human colorectal cancer metastasis. *Oncotarget,* 6**,** 3225-39.

YAN, Z., ZAK, R., ZHANG, Y., DING, W., GODWIN, S., MUNSON, K., PELUSO, R. & ENGELHARDT, J. F. 2004. Distinct classes of proteasome-modulating agents cooperatively augment recombinant adeno-associated virus type 2 and type 5-mediated transduction from the apical surfaces of human airway epithelia. *J Virol,* 78**,** 2863-74.

YANG, H., ZONDER, J. A. & DOU, Q. P. 2009. Clinical development of novel proteasome inhibitors for cancer treatment. *Expert Opin Investig Drugs,* 18**,** 957-71.

YATA, T., LEE, E. L., SUWAN, K., SYED, N., ASAVARUT, P. & HAJITOU, A. 2015. Modulation of extracellular matrix in cancer is associated with enhanced tumor cell targeting by bacteriophage vectors. *Mol Cancer,* 14**,** 110.

YATA, T., LEE, K. Y., DHARAKUL, T., SONGSIVILAI, S., BISMARCK, A., MINTZ, P. J. & HAJITOU, A. 2014. Hybrid Nanomaterial Complexes for Advanced Phage-guided Gene Delivery. *Mol Ther Nucleic Acids,* 3**,** e185.

YIN, H., KANASTY, R. L., ELTOUKHY, A. A., VEGAS, A. J., DORKIN, J. R. & ANDERSON, D. G. 2014. Non-viral vectors for gene-based therapy. *Nat Rev Genet,* 15**,** 541-55.

ZHANG, T., HU, J., DING, W. & WANG, X. 2009. Doxorubicin augments rAAV-2 transduction in rat neuronal cells. *Neurochem Int,* 55**,** 521-8.

ZHU, Q., WANI, G., WANG, Q. E., EL-MAHDY, M., SNAPKA, R. M. & WANI, A. A. 2005. Deubiquitination by proteasome is coordinated with substrate translocation for proteolysis in vivo. *Exp Cell Res,* 307**,** 436-51.

ZINCARELLI, C., SOLTYS, S., RENGO, G. & RABINOWITZ, J. E. 2008. Analysis of AAV serotypes 1-9 mediated gene expression and tropism in mice after systemic injection. *Mol Ther,* 16**,** 1073-80.